

**FINAL REPORT**

**FORECASTING BEAUFORT SEA WIND WAVES  
BY MOMENTUM BALANCE METHOD -  
FURTHER HINDCAST STUDIES**

DSS FILE NO. 02SE.KM191-6-6396  
OUR FILE NO. 58010

Prepared for:

**Forecast Research Division  
Meteorological Services Research Branch  
Atmospheric Environment Services  
4805 Dufferin Street  
Downsview Ontario  
M3H 5T4**

Prepared by:

**MacLaren Plansearch Limited  
Suite 701, Purdy's Wharf Tower  
1959 Upper Water Street  
Halifax, Nova Scotia  
B3J 3N2**

June, 1987

MacLaren Plansearch

58010

MacLAREN PLANSEARCH LIMITED

SUITE 701, PURDY'S WHARF TOWER, 1959 UPPER WADER STREET, HALIFAX

NOVA SCOTIA CANADA B3J 3N2

TELEPHONE (902) 421-3200 TELEX: 019-22718 CABLE: LAVALIN HPX

12 August 1987

Forecast Research Division  
Meteorological Services Research Branch  
Atmospheric Environment Service  
4805 Dufferin Street  
Downsview, Ontario  
M3H 5T4

Attention: Dr. S. Clodman

Dear Dr. Clodman:

**RE: FINAL REPORT, FORECASTING BEAUFORT SEA WIND WAVES BY  
MOMENTUM BALANCE METHOD - FURTHER HINDCAST STUDIES.  
DSS File No. 02SE.KM191-G-6396**

MacLaren Plansearch Limited is pleased to provide the final report for the above referenced study. Your comments and suggestions were incorporated in this report. A magnetic tape contains all data used in this study and the model software will be sent separately.

We trust you will find this report satisfactory and we would be pleased to answer any further questions you may have. We would like to take this opportunity to thank you for your support throughout the course of this study.

Yours very truly.

**MacLAREN PLANSEARCH LIMITED**

Bassem M. Eid, Ph.D., P.Eng.  
Senior Oceanographer

BME/cag

Lavalin

TABLE OF CONTENTSPAGE

LIST OF FIGURES

LIST OF TABLES

1.0 INTRODUCTION

2.0 BEAUFORT SEA WAVE MODEL DESCRIPTION

2.1 Background

2.2 The Wave Model

2.2.1 Numerical Procedure

2.2.2 Model Algorithms

2.3 Model Logic

3.0 MODEL SET-UP AND DATA PROCESSING

3.1 Model Domain

3.2 Model Bathymetry

3.3 Ice-Edge Data

3.4 Wind Data

3.4.1 Input Data Processing

3.4.2 Model Processing

3.5 Wave Data

3.6 Data Availability

4.0 MODEL TESTING AND SENSITIVITY ANALYSIS

4.1 Introduction

4.2 Evaluation Techniques

4.2.1 Time Series Plots of Hindcast vs.

Observed Variable

4.2.2 Statistical Analysis

4.3 Model Performance, Sensitivity and Preliminary Testing

4.3.1 Controlled Tests

4.3.2 Beaufort Sea Test

4.4 Wave Data Evaluation

4.5 BSWM vs BSWM

5.0 MODEL EVALUATION

5.1 1981 Field year Evaluations

5.1.1 Open Water Season

5.1.2 1981 Storm Events

5.2 1982 Storm Events

5.3 1986 Storm Events

6.0 CONCLUSIONS AND RECOMMENDATIONS

7.0 REFERENCES

Appendix A: Description of Model Software

Appendix B: Input Data Format

Appendix C: Output Data Format

Appendix D: Master Data File Format

Appendix E: Ice Boundary Charts

LIST OF FIGURESFIGURE

- 2.1 Relationship Between Time Steps Used in Model
- 3.1 BSWM2 Model Grid
- 3.2 Computer Printout of Effective Shoreline
- 3.3 Site Locations for Years 1981 , 1982 and 1986
- 4.1 Model Domain for Controlled Tests
- 4.2a Evolution of Wave Field with Ice Cover Site 1
- 4.2b Evolution of Wave Field with Ice Cover Site 2
- 4.3 Cross-Section of Wave Heights
- 4.4 Evolution of Wave Field After Rapid Wind Shift
- 4.5 Wave direction, Adjustment to Wind Shift
- 4.6 Time Series Comparison of Model Versions, Sensitivity
- 4.7 Wave Data Comparison, Site 3
- 4.8 BSWM2 vs BSWM Model Comparison
- 5.1 Data Coverage, 1981 Open Water Season
- 5.2 Time Series of 1981 Field Year Simulations
- 5.3 Wave Height Scatter Plots, Dome vs BSWM2 1981
- 5.4 Wave Height Scatter Plots, Waverider vs BSWM2, 1981
- 5.5 Time Series; Storm 5
- 5.6 Scatter Plots, Storm 5
- 5.7 Time Series; Storm 6
- 5.8 Scatter Plots, Storm 6
- 5.9 Time Series, Storm 7
- 5.10 Scatter Plots; Storm 7
- 5.11 Time Series, Storm 8
- 5.12 Scatter Plots; Storm 8
- 5.13 Time Series; Storm 9
- 5.14 Time Series; Storm 10
- 5.15 Time Series; Storm 11

LIST OF TABLESTABLE

- 2.1 Planetary Boundary Layer Wind Reduction
- 2.2 Smoothing Weights
- 3.1 Data Availability for Years 1981 , 1982 and 1986
- 4.1 Comparison of BSWM2 With SMB Formulae
- 4.2 Correlations Between Model Versions, sensitivity
- 4.3 Wave Data Correlations
- 5.1 Evaluation Statistics; 1981 Open Water Season
- 5.2 Evaluation Statistics; Storm 1
- 5.3 Evaluation Statistics; Storm 2
- 5.4 Evaluation Statistics; Storm 3
- 5.5 Evaluation Statistics; Storm 4
- 5.6 Evaluation Statistics; Storm 5
- 5.7 Evaluation Statistics; Storm 6
- 5.8 Evaluation Statistics; Storm 7
- 5.9 Evaluation Statistics; Storm 8

## 1.0 INTRODUCTION

The ability to forecast waves accurately provides invaluable support for those who depend on the sea for their livelihood. Perhaps the most important reason for developing such a model is to provide accurate information such that safe operational procedures can be adopted at sea. In particular, the operation of vessels and drill rigs depends largely on wave climate.

This report describes the development of a practical wave forecast model for the Beaufort Sea. The reliability of any forecasting procedure depends on the validity of the model and the suitability of the input to the model. The validity of the model depends on whether or not the relevant physics of the problem at hand have been properly represented. Validity can be determined by testing the model in hindcast mode, where appropriate input data is usually available. Once the models' validity in hindcast mode is established its suitability for forecasting relies heavily on the accuracy of the inputs to the model. In fact in any modelling exercise it is the adequacy of inputs that can dictate the degree of success or failure of the model.

In this report, the numerical wave model developed by Schwab et al. (1984). Great Lakes Environmental Research Laboratory (GLERL), for the Great Lakes is adapted for use in the Beaufort Sea. The GLERL model is a refined version of a lake wave model originally formulated by Donelan (1977) and Hodson and Donelan (1978). The model is based on a simple parametric representation of momentum balance and is solved numerically by a finite difference scheme. The theory and assumptions from which the model is derived is outlined in the references cited previously. The present model, Beaufort Sea Wave Model, Version 2 defined (BSWM2), has been refined and adapted for use in the Beaufort Sea based on a previous version developed by MacLaren Plansearch Limited (1986) which is referred to as BSWM. BSWM was also adapted from a lake wave model and is based on the Donelan (1977) formulation. Therefore, the conversion procedure for the GLERL model will effectively be identical to that used in developing BSWM as outlined in MacLaren Plansearch Limited (1986). Although both models, BSWM and BSWM2, are based on essentially the same physics, there are significant differences between them, and these will be explained briefly later.

The suitability of utilizing Donelan's formulation for the Great Lakes has been demonstrated by Schwab et al, (1986). Schwab et al. (1984) and Donelan (1977). Extensive testing of Donelan's model has been carried out by Clodman (1983, 1983a). Model BSWM

has been shown to perform satisfactorily in the Beaufort Sea context, MacLaren Plansearch Limited (1986). Model BSWM2, which includes several improvements over the previous model should then also perform well in the Beaufort Sea.

This report describes the transformation of the latest GLERL model into BSWM2, for specific application in the Beaufort Sea, and provide extensive model evaluation. The report comprises the following sections. Section 2 briefly describes the background and theoretical basis for the model and outlines the algorithms and numerical techniques utilized in the model. Section 3 describes the Beaufort Sea domain and data availability and processing. Section 4 provides a discussion on model evaluation, sensitivity analysis and defines suitable model parameters. The results of extensive testing will follow in Section 5 including statistical evaluation of model performance. The model is evaluated in terms of accuracy in hindcasting long periods (1981 open-water season) as well as short periods of storm events (in 1981, 1982 and 1986). Finally a summary of major conclusions and recommendations is outlined in Section 6 .

## 2.0 BEAUFORT SEA WAVE MODEL

### 2.1 BACKGROUND

In 1986, MacLaren Plansearch Limited (MPL) was contracted by the Atmospheric Environment Service (AES) to set up and test a wave model for application in the Beaufort Sea. The resulting model, BSWM, (described in MPL (1986)) had its roots in the Donelan (1977) Parametric wave model. Since then refinements to the Donelan model have been made by Schwab and his colleagues at the Great Lakes Environmental Research Laboratory (GLERL) in Ann Arbor, Michigan. The refined model denoted GLERL, has been presented by Schwab et al. (1986) and is currently being tested by Clodman (personal communication) at AES, Downsview. Improvements made to the earlier Donelan model included refinements in specifying the wind field and allowance for a variable integrating time step. In particular the model has the capability to account for the planetary boundary layer physics including the effects of atmospheric stability when processing the wind inputs. A linear interpolation in time is performed on the wind inputs to provide for a relatively smooth transition of the wind field. Also a procedure to allow for a spatially variable wind was developed. Further details of these features are presented in this report.

Another fundamental difference between GLERL and older versions of the Donelan model is that the "fossil" wave formulation is removed from GLERL model. The "fossil" wave was an attempt to represent the effects of swell. It was suspected that the deletion of the fossil wave calculation would lead to significant savings in computer time while not surrendering any accuracy. Schwab et al. (1986) found this to be the case for model tests for Lake Erie. To determine whether this is true for the much larger Beaufort Sea domain rests in comparison of BSWM and BSWM2, which is based on the GLERL version, for actual test cases which will be described later.

The procedure that was used to develop BSWM (detailed in MPL (1986)) was also followed in transforming the GLERL model into BSWM2. Briefly, modifications were necessary due to two considerations: i) environmental adjustment and ii) input/output compatibility. Adapting GLERL to Beaufort Sea conditions required simply providing for appropriate bathymetry and allowing for a dynamic ice field. Accounting for a dynamic ice field effectively allows the boundaries of the model to change in time. The input requirements of the model are basically specification of control parameters and the wind data to provide the forcing. The model, as it stands at present, can accommodate and process several wind

'options' depending on the type of data supplied. The options available deal with the planetary boundary layer and also the spatial distribution of the winds. Some other modifications were implemented such as including a spatial smoothing function, for stability reasons, and reformulating the energy spreading function. These features are described in the following sections. In general, the logic and integrity of the GLERL model was not altered.

## 2.2 THE WAVE MODEL

The theoretical framework upon which the model is based, as well as the results of some model testing and evaluation can be found in the previously cited references. The basic procedure for converting the model has also already been documented in MPL (1986). This section describes the program in its final state, including a description of the model algorithms and numerical technique. An outline of the modifications made to the program during the course of the study is presented along with a discussion of their physical relevance. A summary of model options and parameter choices is also presented.

The prediction method developed by Donelan (1978) is based on the solution of the equation for the conservation of momentum of the waves given as:

$$\frac{\partial M_i}{\partial t} + \frac{\partial}{\partial x} (V_x M_i) + \frac{\partial}{\partial y} (V_y M_i) + \frac{\tau_i}{\rho_w g} \quad \text{for } i=x,y \quad (2.1)$$

Where

- $i$  = x, y are the two space coordinates;
- $t$  = time;
- $M_i$  = momentum of the wave field in the  $i$  direction;
- $V_i$  = average group velocity in the  $i$  direction;
- $\rho_w$  = density of water;
- $g$  = acceleration of gravity;
- $\tau_i$  = effective wind stress acting in the  $i$  direction; that affects the wave field.

The first term on the left hand side is simply the time rate of change of momentum. The second term represents a divergence of the wave momentum flux. The right hand side represents the input of momentum due to the wind field.

The solution of (2.1) requires, first of all, a suitable representation for the terms in the equation and also an appropriate numerical procedure. A brief discussion of both follows.

### 2.2.1 Numerical Procedure

#### Finite Difference Method

The solution of (2.1) is accomplished numerically by representing the space and time derivatives by suitable finite differences. In the model, equation (2.1) is then numerically represented by:

$$\frac{M_i(t+\Delta t) - M_i(t)}{\Delta t} + \frac{V_x M_i(x) - V_x M_i(x+\Delta x)}{\Delta x} + \frac{V_y M_i(y) - V_y M_i(y+\Delta y)}{\Delta y} = \frac{(\tau_i)}{\rho_w g}, \quad \text{for } i = x, y \quad (2.2)$$

The difference equation (2.2) can be easily rearranged to provide a solution for the momentum at the new time  $t+\Delta t$ .

Several points worth noting in the manner in which this representation is solved in the program are:

- i) the wind stress must be specified for each integration period for each grid location;
- ii) the time step of integration ( $\Delta t$ ) is limited by numerical stability considerations;
- iii) the spatial differences are determined dependent on the momentum flux.

#### i) Temporal Resolution of Wind

One of the concerns raised in a previous evaluation of the Donelan-type model was the manner in which the waves responded to a changing wind direction, Clodman (1983). Inherent in this consideration are how rapidly the wind changes direction and how frequently wind data is supplied to the model. The evolution of the wind field is completely independent of modelling considerations, however, the modeler can have some control over the frequency of data input. Unfortunately, the availability of data may not be suitable. The GLERL (BSWM2) model, however, provides the user with the ability to interpolate the wind values, linearly, between available observation times. This provides for a more gradual adjustment of the wind field. Previously, the wind data was updated at specific intervals determined by data availability, in a step-like manner. In GLERL (BSWM2) the user controls the increment at which the wind is to be updated and adjustment occurs in a series of smaller step-like changes. The use of this interpolation scheme is a definite improvement over the previous model versions. The time interval (DT) between interpolated wind values is a parameter which can be varied.

## ii) Integration Time Step

The integration between model time  $t$  and  $t+DT$ , when the wind data is updated, occurs in steps of  $\Delta t$ . The integration time step is based on stability considerations depending on the wind speed supplied at time  $t$ . The relationship between the times of data availability, model time ( $t$ ), interpolation time ( $DT$ ) and integration time ( $\Delta t$ ) is illustrated in Figure 2.1 .

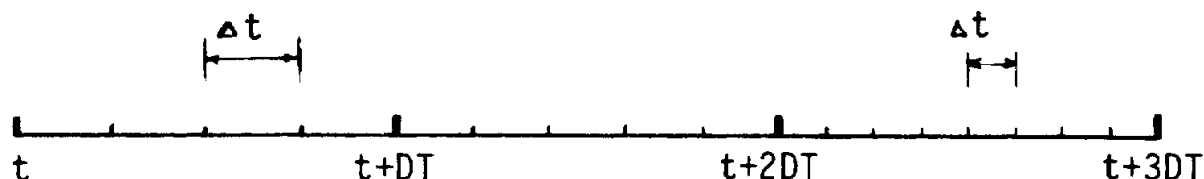


Figure 2.1 Relationship between the time steps used in BSWM2

The smaller  $DT$  is, the finer the interpolation. Older versions of the model could only update the winds when new information became available. This procedure does not require the wind data to be available at regularly spaced intervals. In fact, gaps in the record are effectively filled by this procedure.

## iii) Spatial differences

The spatial finite differences in the model are calculated in a backward sense. At each grid point  $(x,y)$  the point at which a difference is to be calculated (i.e.  $x\pm\Delta x$ ,  $y\pm\Delta y$ ) is selected to be that point from which the momentum flux is arriving. This flexible finite difference representation, allowing  $\Delta x$ ,  $\Delta y$  to be positive or negative, depends on the wave momentum field.

Further details of aspects of the numerical procedure are described in Hodson and Donelan (1978).

### 2.2.2 Model Algorithms

The solution of the momentum conservation equation (2.2) is carried out by suitably representing the divergence of wave momentum flux terms and wind stress as described below.

#### **Divergence of Wave Momentum Flux**

The determination of the momentum flux terms is based on several assumptions, one of which deals with the lateral spread of energy as the waves propagate. The formulation of the flux terms in the GLERL model is based on the derivation illustrated in Schwab et

al. (1984). The directional spectrum,  $F(f, \Theta)$ , is represented as a product of the frequency spectrum and a term to represent directional distribution of energy such that

$$F(f, \Theta) = E(f) D(\Theta) \quad (2.3)$$

where  $E(f)$  is the frequency spectrum;  
 $D(\Theta)$  parameterizes the directional distribution of energy;  
 $f$  is the frequency;  
 $\Theta$  is the direction of propagation.

In that work the spreading  $D$  took the form  $(2/\pi) \cos^2(\Theta - \Theta_0)$  restricting spreading to a swath of  $\pm 90^\circ$  from the mean angle of propagation ( $\Theta_0$ ) and also independent of frequency. The terms  $T_{xx}$ ,  $T_{xy}$ ,  $T_{yy}$  of Schwab et al. (1984) (representing  $V_x M_x$ ,  $V_x M_y$  ( $V_y M_x$ ) and  $V_y M_y$  in equation (2.1)) represent the momentum flux terms using this form for the spreading.

Recently Clodman (personal communication) has expressed some concern over the amount of lateral spreading and has rederived the momentum flux terms based on a variable spreading factor. In the formulation suggested by Clodman (personal communication) the  $\cos^2$  form is retained but in the form:  $D(\Theta) = (4/\pi) \cos^2(2(\Theta - \Theta_0))$ . The terms become:

$$\begin{aligned} V_x M_x &= T_{xx} = \frac{1}{2} g \sigma^2 [(1-S) \cos^2 \Theta_0 + \frac{1}{2} S] \\ V_x M_y &= V_y M_x = T_{xy} = T_{yx} = \frac{1}{2} g \sigma^2 (1-S) \sin \Theta_0 \cos \Theta_0 \\ V_y M_y &= T_{yy} = \frac{1}{2} g \sigma^2 [(1-S) \cos^2 \Theta_0 + \frac{1}{2} S] \end{aligned} \quad (2.4)$$

where  $\sigma^2 = \text{variance of wave energy} = \int_0^\infty E(f) df,$

0

and  $S = 0.0$  represents no spreading ;  
 $0.1512$  spreading restricted to  $[\Theta - \Theta_0] \leq \pi/4$   
 $0.5$  spreading restricted to  $[\Theta - \Theta_0] \leq \pi/2$  identical to the GLERL version.

The spreading factor  $S$  effectively limits the amount of lateral spreading allowed. It is a parameter in the model which can be altered for testing model sensitivity.

### Wind Input of Momentum

The forcing for the model is provided by calculating a surface wind stress from the wind field data. Donelan's formulation

allows for the influence of the wave field on the roughness elements as well as accounting for the shearing velocity encountered. The formula for stress is quadratic and given as:

$$\frac{\underline{\tau}}{\rho_w g} = \gamma D_f |U - 0.83C_p| (U - 0.83C_p) \quad (2.5)$$

where  $\underline{\tau}$  is the wind stress vector;

$\rho_w g$

$U$  is the wind velocity at a given reference level (10m);  $0.83C_p$  defines the effective wave speed at full wave development;

$D_f$  is a drag coefficient accounting for form and skin drag, a function of sea state;

and  $\gamma$  is the empirical fraction of stress that is retained by the waves.

Further details on the derivation of this stress law are found in Donelan (1978), however, it is important to note that it was based on having the wind velocity at 10m. The factor  $\gamma$  (gamma) is present to account for the fraction of the wind stress that affects the wave field in terms of growth or decay. The remainder of the wind stress is used for driving currents, etc. The value for gamma is a parameter to be tested. Gamma ( $\gamma$ ) was taken to be 0.028 in Schwab et al. (1984).

In the calculation of the wind stress a suitable wind field must be prescribed. Atmosphere stability and the height at which the wind is measured (or prescribed) are potentially important considerations. The model has the capability to account for effects in the surface boundary layer utilizing the relationships developed by Businger et al. (1971) and Dyer (1968). If a measured wind speed at a given height  $Z$  is input to the model, the program can provide an estimate of the effective wind speed at any other height  $Z$ . For this study,  $Z$  is taken to be the standard height of 10 m above sea level. The procedure to do this is based on mixing length arguments which results in a logarithmic profile of the wind speed with height. Factors affecting the profile shape are the stability of the air and an effective roughness length of the surface. The procedure works well provided the condition:

$$-1 \leq \frac{z'}{L} \leq 1 \quad (2.6)$$

is met, where

$z'$  is the height of the wind observation (m)

L is the Monin - Obukhov length (m) approximated by

$$L = \frac{U^2 T_a}{g (T_a - T_w) n(\underline{Z})}$$

$Z_0$

and U is measured wind speed at height Z (m/s);

$T_a$ ,  $T_w$  are the air and water temperatures respectively ( $^{\circ}\text{K}$ );

$Z_0$  is a roughness length, given initially as  $.00459 (.04U)^2$ , based on Charnock's (1955) form of  $Z_0 = au^2/g$  (as described in subroutine UZL).

As an example of the transformation of winds due to this procedure, Table 2.1 illustrates effective 10 metre winds derived from various anemometer heights and atmospheric stability conditions ( $T_a - T_w$  is positive) the speeds are suppressed the most.

TABLE 2.1

Effective 10m wind speeds, as determined by the BUSINGER-DYER formulation, for various wind speeds and anemometer heights. Formulation and parameters are outlined in subroutines UZ and UZL of model BSWM2.

Anemometer Height (m)	Ta-Tw (°C)	Measured Wind Speed (kts)		
		20	40	60
80	-8	19.3	35.0	49.6
	-4	18.6	34.1	48.6
	0	16.6	32.1	46.9
	4	9.8	27.2	43.7
	8	8.5	22.8	40.7
60	-8	19.5	35.6	50.6
	-4	18.8	34.7	49.7
	0	17.0	33.0	48.2
	4	10.7	29.1	45.8
	8	9.2	26.4	43.3
40	-8	19.8	36.5	52.3
	-4	19.1	35.7	51.5
	0	17.6	34.3	50.4
	4	12.4	31.6	48.6
	8	10.2	29.0	46.9
20	-8	20.5	38.4	55.9
	-4	19.9	37.8	55.3
	0	18.7	36.8	54.6
	4	15.7	35.3	53.6
	8	13.1	33.9	52.6
10	-8	21.4	41.1	60.8
	-4	20.9	40.6	60.4
	0	20.0	40.0	60.0
	4	18.4	39.2	59.5
	8	16.8	38.4	58.9

Invoking this procedure requires the added information of air and sea temperatures, which in many cases is not available, and the height at which the wind data is available. In addition, the computation of the 10 m effective wind is only an approximation in the model and can be a source of errors in model predictions. The estimation of an effective 10 m wind speed is an option in the model which will be tested.

The above algorithms basically describe the computational portion of the program which was taken from the GLERL Coding. In the Beaufort Sea context the model (BSWM2) has been modified to account for other factors identified below.

### Ice Edge

The domain of the lake is allowed to change based on ice conditions. At present, the ice information is updated at weekly intervals by simply redefining the lake's boundaries. In terms of monitoring specific sites this results in variable fetch lengths based on both changing winds and ice position. The algorithm developed in the previous version (BSWM) was used in the present version of the model, see MPL (1986).

### Smoothing

When the shape of the 'lake' is allowed to change, there are circumstances when large spatial gradients in the wave field can occur. The spatial redistribution of energy is accounted for by the momentum flux terms which can include the effects of spreading as previously described. However, there is a potential for introducing artificially high gradients which will initiate oscillations in the wave field. If these oscillations are large enough they may contaminate the results. In an attempt to reduce the potential of contamination or oscillation by this mechanism, a 5-point spatial smoothing is utilized. This is accomplished by suitably averaging the wave field. The technique used is a simple spatial 5-point weighted average scheme denoted schematically as:

$$P(I,J) = (1-4\alpha) P(I,J) + \alpha[P(I-1,J) + P(I+1),J) + P(I,J-1) + P(I,J+1)] \quad (2.7)$$

where  $P(I,J)$  is the quantity to be smoothed,  
 $\alpha$  is the weighting term,  
 $I,J$  denote the location of the point on the grid.

The weighting term  $\alpha$ , can be varied according to the importance to be placed on each point. For example, for  $\alpha = .2$ , all values are of equal importance. The factor  $\alpha$  can itself be a function of computational time step and for this report is given by:

$$\alpha = (\text{SMTH}) \times \Delta t \quad (2.8)$$

where SMTH is a smoothing factor and  $\Delta t$  is the integration time step.

Letting  $\alpha$  be a function of the integration time allows the weights to change with time. For instance if the integrating step is large, then more weight is placed on the neighbouring points. This is a reasonable formulation since for a longer  $\Delta t$  more energy is exchanged between neighbours.

The degree to which smoothing is performed is also dependent on the factor SMTH. Typical weights,  $\alpha$ , for various integrating time steps,  $\Delta t$ , and a value of SMTH of 0.00002 is shown in Table 2.2 .

TABLE 2.2

Smoothing Weights (a) For Various Integrating Time Steps ( $\Delta t$ )

<u><math>\Delta t</math>(s)</u>	<u><math>\alpha</math></u>
120	.0024
300	.0060
600	.0120
1200	.0240
3600	.0720

The choice of a value for SMTH depends on the extent to which smoothing is desired. For our purposes, it is to reduce spurious oscillations. It is important then, not to oversmooth and alter the actual spatial structure of the field. After testing, a value of SMTH 0.00002 was found to provide a satisfactory result.

The smoothing was applied to the momentum fields immediately after the divergence of wave momentum flux contributions were calculated.

### Wave Variables

The transformation of wave momentum into significant wave height and period forms the basis for the parametric nature of this model. As outlined in Donelan (1977) and Schwab et al. (1984). The wave spectrum is assumed to be well represented by the JONSWAP formula (Hasselmann et al. 1973). The wave variables are determined from the wave variance ( $\sigma^2$ ) and the peak frequency ( $f_p$ ) which are related to the momentum field by:

$$\frac{\sigma^2}{M} = \frac{C_p}{g} \quad (2.9)$$

$$\sigma^2 = 0.30 \alpha g^2 (2\pi)^{-4} f_p^{-4} \quad (2.10)$$

with  $\alpha = 0.0097 (\frac{U}{C_p})^{2/3}$ , the Phillips equilibrium range parameter

$C_p = g/(2\pi f_p)$ , the wave phase speed;  
U is the 10m wind speed;  
 $f_p$  is the frequency of peak energy in the spectrum;  
and M is the magnitude of the wave momentum, vector ( $M_x$ ,  $M_y$ ).

The assumptions inherent in utilizing these relationships is well documented in the above references.

### 2.3 MODEL LOGIC

The discussion presented has illustrated the basic formulation of the model in terms of theoretical and numerical considerations. The program itself is highly modular and as such is relatively easy to document. A description of the software is provided in Appendix A to complement the previous discussion. The basic components in the model are:

- i) to initialize variables and parameters,
- ii) prescribe the model domain based on the ice field,
- iii) prescribe the windfield based on data type,
- iv) perform the integrations over the time steps, and
- v) repeat steps ii to iv until the end of the simulation period.

Although the procedure is fairly simple in character, there are numerous options and decision paths which the model can take, dependent mostly on processing the wind data. The basic Flow Chart logic of the model is outlined in Appendix A .

### **3.0 MODEL SET-UP AND DATA DATA PROCESSING**

The model relies heavily on data in order to provide forcing and for validation. The types of data available, their quality and the processing options available are outlined below. Further documentation of the data utilized in this report is provided in the companion report entitled 'Supplementary Data Base Report', see also MPL (1986).

#### **3.1 MODEL DOMAIN**

The model domain extends from 117°W to 150°W and from the coast to 74°N. The model grid is illustrated in Figure 3.1 . The origin of the model grid (1,1) is at 68°40' North Latitude and 150°00' West Longitude. The x-axis runs west to east and the y-axis runs south to north. The grid is comprised of 18.5 km square blocks giving an (x,y) matrix of grid points of size (67,33). This discretization is based on the fact that at this latitude the ratio of the distance defined by 1° of latitude to that defined by 1° of longitude is about 3 (i.e.  $\Delta x = 30'$  latitude,  $\Delta y = 10'$  longitude).

#### **3.2 MODEL BATHYMETRY**

The bathymetry corresponding to the model grid was obtained from the AES and is described in the accompanying Data Base Report. Since the model neglects shallow water effects the bathymetry then is used only to delineate the shoreline. A computer printout indicating those grid points located on land is shown in Figure 3.2 . As is apparent, the grid boundary points have been assigned as land points. This is necessary because the model has no provisions to deal with open boundaries. It should be noted however, that for most of the cases studied, open water did not extend to the domain boundaries because of sea ice cover. Sea ice cover is considered incapable of transmitting waves and therefore plays the same role as land. The situations when open water extended out of the domain occurred generally in a narrow band, and truncation of the fetch at the boundary was not considered to be a serious concern.

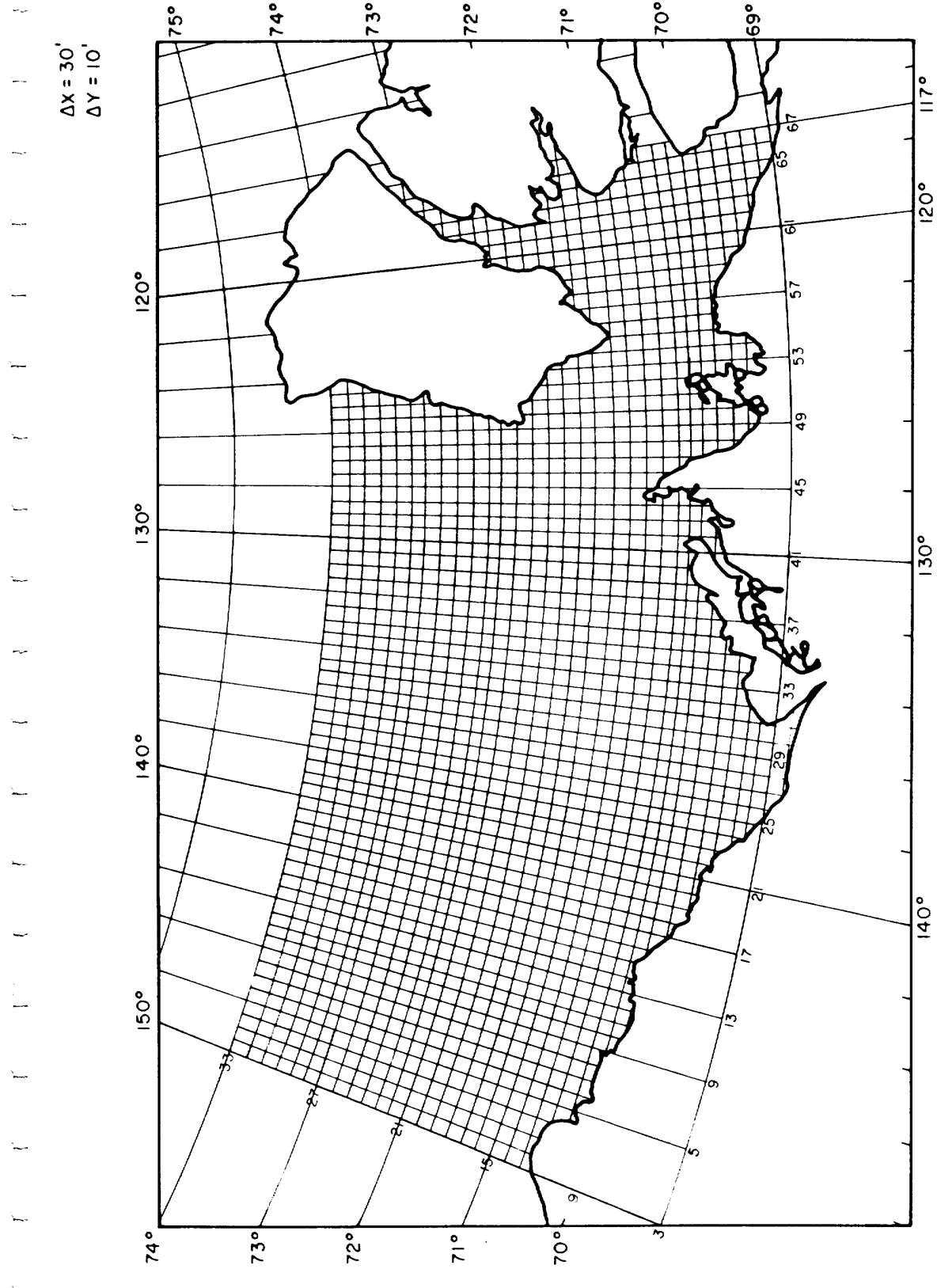


Figure 3.1: BSM2 Model1 Grid.



Figure 3.2 Computer Printout of Effective Shoreline

### 3.3 ICE-EDGE DATA

The location of the ice edge effectively delineates the boundary of the 'lake' domain. Weekly composite ice charts were obtained for the study periods of interest from Ice Centre, Environment Canada. The charts were digitized manually. The criteria used to delineate impermeable ice was subjective. Ice of any concentration was considered incapable of transmitting waves. Exceptions considered were ice islands and narrow outcroppings having low ( $\leq 2/10$ ) concentrations.

### 3.4 WIND DATA

The most important input to the model is the prescription of an appropriate wind field. Ideally, a suitable spatial distribution and temporal resolution of data representative of conditions over the 'lake' would be desirable. However, this is rarely achieved. For this study, 2 sources of wind information are available, measured winds at various locations and the Canadian Meteorological Centre (CMC) Weather prediction model winds. The information from both sources have positive and negative attributes associated with them. Measured winds provide good local information and as such provide accurate information about conditions occurring over the site. An array of measurements provides information on spatial variation and perhaps phase propagation of the wind field. They may, however, be subject to local topographic or small scale effects which may affect their validity for larger scale modelling. The CMC model winds, on the other hand are a product of a large scale numerical weather prediction scheme. The model is concerned with large scale phenomena and thus some smaller scale effects have been parameterized and some neglected.

An important difference between the wind sets is that with the measured data the effects of the planetary boundary layer can be estimated. Measurements can be related to a standard height in order for stresses to be estimated.

The obtained CMC winds (archived at the Canadian Meteorological Centre in Dorval, Quebec) are those determined for the 1000 mb level which does not necessarily correspond to a standard height. On the other hand the CMC model winds form part of an existing forecasting scheme. If the wave model is to be used in forecast mode a forecast wind is necessary. The CMC model has the capability to provide this information.

It is not the purpose of this study to evaluate which wind source is the most appropriate. However, given the data availability and the purposes that this model is being developed for, both data

types will be utilized with more emphasis on testing the model with measured winds as input. Only three case studies will be run using CMC winds as shown in Section 5 .

The model requires wind information at each time step and for each active grid point. This information is supplied to the model by processing the data according to data type, spatial and temporal availability of data, data quality and model requirements. The procedure is outlined below.

#### **3.4.1 Input Data Preprocessing**

Prior to running the model the following steps were taken:

##### A) Visual Inspection of Data

Wind data gathered for the project were visually inspected in order to make preliminary comparisons, identify gaps in the records and any obvious errors.

##### B) Data Selection

The records perceived to have high quality in terms of coverage, representing conditions over the area and completeness were selected for use.

##### C) Data Preparation

The selected records were then prepared by eliminating any obvious errors and filling gaps in the records of variables that the model (at present) does not provide an interpolation for. This step utilizes information at other sites and is basically subjective in nature in that the gaps are filled manually. It should be mentioned that the gaps were not large and that information from other sites provided good guidance. The data sets were then tabulated in a format required by the model.

#### **3.4.2 Model Processing**

The model processes the input data depending on the data type supplied. The important differences in processing occur in considering boundary layer effects and spatial data coverage. The options outlined below are accessed by supplying the program with the necessary information to select the processing option. The data required by each option is specific in terms of format. Some of the processing routines were formulated for the specific purposes of this project and the data availability. The types and format of the data required for each option is outlined in Appendix B .

A) Boundary Layer Effects (Input Wind Dome Observations)

As outlined previously, for observed winds given at different anemometer heights, an estimate of the effects of the planetary boundary layer is made in order to provide an effective wind speed at a standard height (10m). This process is optional and can be bypassed.

B) Spatial Distribution (Observed and CMC Winds)

From the array of selected wind data sites a decision is made as to the manner in which wind data for the remainder of the grid is to be assigned. The options in the model are:

i) Homogeneous field. In the event of poor spatial coverage of data a single 'representative' site is chosen and its wind is prescribed over the entire domain.

ii) Least Squares Plane Fit

For increased spatial coverage a least squares plane is fit to each wind component, and values at each grid determined by the plane equations. This requires a suitable number of data points for confidence purposes. Also good spatial coverage is necessary to avoid erroneous extrapolation resulting from a tight cluster of data points. This is physically more appealing than i), however it requires suitable data coverage and presumes a functional form for the wind field. For a large domain this functional form may be inadequate.

iii) Weighted average scheme

For an array of arbitrarily located data the wind components at each grid are formed by a weighted average of the available data, where weights depend on the distance from the point to the data site. This procedure performs a form of spatial averaging. Its suitability depends on reasonable spatial coverage.

iv) Subgrid Interpolation

This procedure (at present) presumes that data are available in a coarse Cartesian co-ordinate frame with data points available at equidistant steps. A bilinear interpolation is performed on this coarse data in a sequential fashion to estimate values for the subgrid points that lie within the coarse grid box. This procedure is dependent on such regularly spaced data being available.

The data format required to invoke any of these options is outlined in Appendix B .

### C) Temporal Resolution

The model requires wind information for all integration steps. As discussed previously the model winds are updated at user specified intervals,  $DT$ , based on a linear interpolation in time. This procedure allows for inputs with different sampling rates to be used and in the event of missing data the model can proceed without stopping. Linear interpolation in time is adequate for cases when data is not separated by long gaps, This procedure is accomplished after the spatial structure of the wind field has been determined for the present time and the time of the next available data. The interpolation is carried out for each grid point at intervals of  $DT$ . Note that the actual integration occurs over a finer time step ( $\Delta t$ ) depending on stability considerations as discussed previously.

The processing options are data dependent and some routines were written for the specific purposes of this project. Not all of these processing options were used in the model evaluation stage of the project. The number of options reflects the refinements and modifications made during the course of the project.

### 3.5 WAVE DATA

Two sources of wave data are available to compare with model output, measured wave information acquired from Dome Petroleum and waverider buoy data. Model output will be compared with both sets when available.

The Dome data consists of manual estimates of significant wave height and period. The waverider buoy information (i.e. significant wave height and peak period) were derived from wave spectra obtained from the recorded heave information. The only preprocessing of the wave data was to visually inspect it and, if necessary, eliminate any obvious errors.

### 3.6 DATA AVAILABILITY

The data available for model evaluation consists of both long time series and shorter storm specific events. The evaluation consists of two aspects, i) to evaluate long term model statistics and ii) to evaluate the model's ability to hindcast short period storm events. The data utilized in this study is comprised of information from the years 1981, 1982 and 1986. The 1981 data (July 25 - Oct, 5) was used for the long term statistical evaluation and sensitivity testing while data from large-wave generating events that occurred in 1981, 1982 and 1986 were selected for event hindcasting. Tables 3.1 illustrate the

availability of measured data for these periods. Figures 3.3 shows the site locations at which the information is available.

Further documentation of these data are provided in the supplementary data report.

Model Site Code	Grid Coord. (I, J)	Lat. (N)	Long. (W)	Site Name	Vessel Name	Operator	Water Depth (M)	Anemometer Height (M)	OBSERVATIONS			
									Winds		Waves	
									Dates (From-To) M/D/Hr - M/D/Hr	M/D/Hr - M/D/Hr	Manual M/D/Hr - M/D/Hr	Wave/Ider M/D/Hr - M/D/Hr
01	(42,14)	70°46'	129°21'	KILANNAK	EXP. IV	DOME	25	58	7/25/00 - 9/06/21	7/25/00 - 9/06/09	8/05/21 - 8/14/21	---
02	(31,11)	70°24'	135°12'	KOPANGAR	EXP. I	DOME	56	65	7/25/00 - 10/06/00	7/25/00 - 10/06/00	---	---
03	(32,9)	70°05'	134°26'	ISSUNGNAK	EXP. II	DOME	27	65	7/25/00 - 10/05/00	7/25/00 - 10/06/00	7/28/03 - 8/31/17	---
04	(33,12)	70°28'	134°06'	KOAKOAK	EXP. III	DOME	60	27	7/25/00 - 10/06/00	7/25/00 - 10/06/00	8/07/13 - 10/06/01	---
05	(28,11)	70°22'	136°32'	ORVILJUK	EXP. IV	DOME	59	58	9/07/00 - 9/19/21	9/07/21 - 9/19/21	---	---
06	(33,13)	70°42'	133°59'	KFNALOOAK	EXP. IV	DOME	64	58	9/21/00 - 9/26/21	9/21/00 - 9/26/21	---	---
07	(33,12)	70°35'	134°14'	IRKALUK	EXP. IV	DOME	60	58	9/27/00 - 10/06/00	9/27/00 - 10/06/00	---	---

TABLE 3.1a - DATA AVAILABILITY FOR 1981

Model Site Code	Grid Coord. (I,J)	Lat. (N)	Long. (W)	Site Name	Vessel Name	Operator	Water Depth (M)	Anemometer Height (M)	OBSERVATIONS			
									Winds Dates (From-To) M/D/Hr - M/D/Hr	Waves		Waverider M/D/Hr - M/D/Hr
										Manual M/D/Hr - M/D/Hr	Manual M/D/Hr - M/D/Hr	
01	(27,10)	70°22'	136°32'	ORVLIHIKO-3	EXP. III	DOME	48	27	9/18/07 - 10/25/06	9/18/07 - 10/25/06	9/01/00 - 9/29/15	
02	(29,9)	69°55'	135°55'	TARSIUT ISLAND	---	DOME	20	17	7/26/07 - 9/24/06	7/26/07 - 9/24/06	7/30/00 - 9/29/18	
03	(32,9)	69°57'	134°30'	KIGGAVIK H-32	EXP. I	DOME	21	65	7/26/07 - 9/24/06	7/26/07 - 9/24/06	7/30/00 - 9/29/18	
04	(33,12)	70°35'	134°14'	ITLYOK ISLAND	---	FSSO	14	--	---	---	8/03/00 - 9/25/18	
05	(33,13)	70°44'	133°50'	IRIALUK B-35	EXP. II	DOME	58	65	7/26/07 - 9/24/06	7/26/07 - 9/28/06	7/28/00 - 9/29/12	
06	(34,11)	70°24'	133°27'	KENALOOK J-94	EXP. IV	DOME	71	58	7/26/07 - 10/25/06	7/26/07 - 10/25/06	7/25/00 - 8/25/00	
07	(38,9)	69°58'	131°13'	NERLUPRK M-98	EXP. III	DOME	52	27	7/26/07 - 8/26/06	7/26/07 - 8/26/06	7/27/00 - 8/25/00	
				McKINLEY BAY	---	DOME	8	20	7/26/07 - 8/03/06	---	---	

TABLE 3.1 b - DATA AVAILABILITY FOR 1982

Model Site Code	Grid Coord. (I,J)	Lat. (N)	Long. (W)	Site Name	Vessel Name	Operator	Water Depth (M)	Anemometer Height (M)	OBSERVATIONS				
									Winds		Waves		Haverlinder
									Dates (From-To)	M/D/Hr	Manual	M/D/Hr	
01	(9,11)	70°22'	146°01'	HAMMERHEAD	EXP. II	DOME	34	65	9/19/08 - 10/11/11	9/19/08 - 10/11/11	---	---	
02	(12,11)	70°18'	144°45'	CORONA	EXP. II	DOME	34	65	7/27/04 - 9/18/23	7/27/04 - 9/18/23	---	---	
03	(28,7)	69°43'	130°28'	MIMIK I-53	---	ESSO	15	16	7/20/00 - 8/11/00	7/20/00 - 8/11/00	7/28/06 - 9/19/22	---	
04	(30,8)	69°53'	135°23'	KAUIRVIK I-43	---	ESSO	18	--	8/26/00 - 10/03/05	8/26/00 - 10/03/05	8/26/22 - 10/03/05	---	
05	(34,8)	69°46'	133°44'	ARNAK K-06	---	ESSO	7	13	7/03/00 - 8/23/06	7/03/00 - 8/23/06	8/07/18 - 9/10/18	---	
06	(39,11)	70°19'	131°12'	HAVIK	EXP. I	DOME	34	65	7/18/06 - 8/24/14	7/18/06 - 8/24/14	---	---	

TABLE 3.1 c - DATA AVAILABILITY FOR 1986

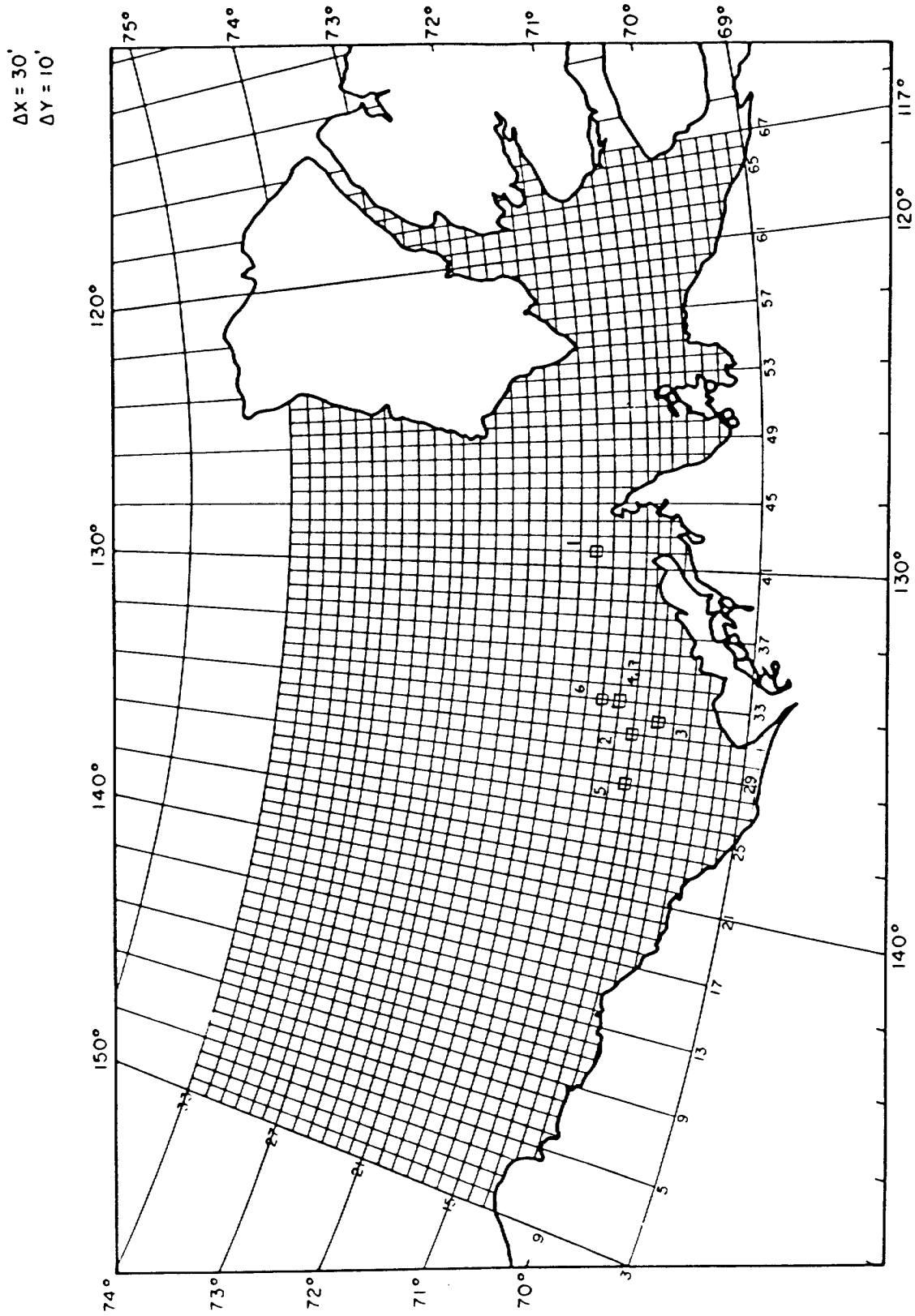


Figure 3.3a: Site Locations for 1981, Open Water Season.

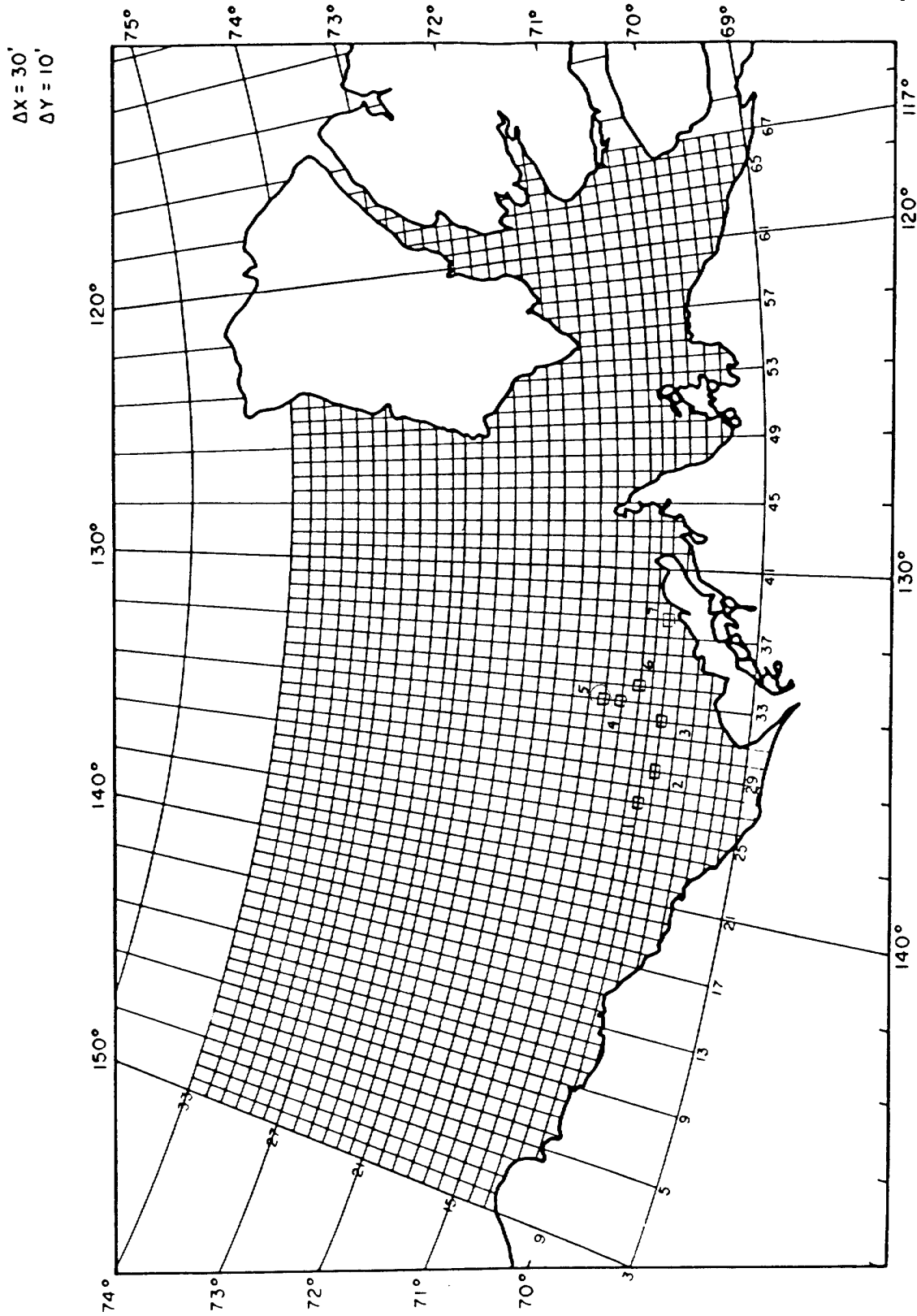


Figure 3.3b: Site Locations for 1982 Storm Simulations

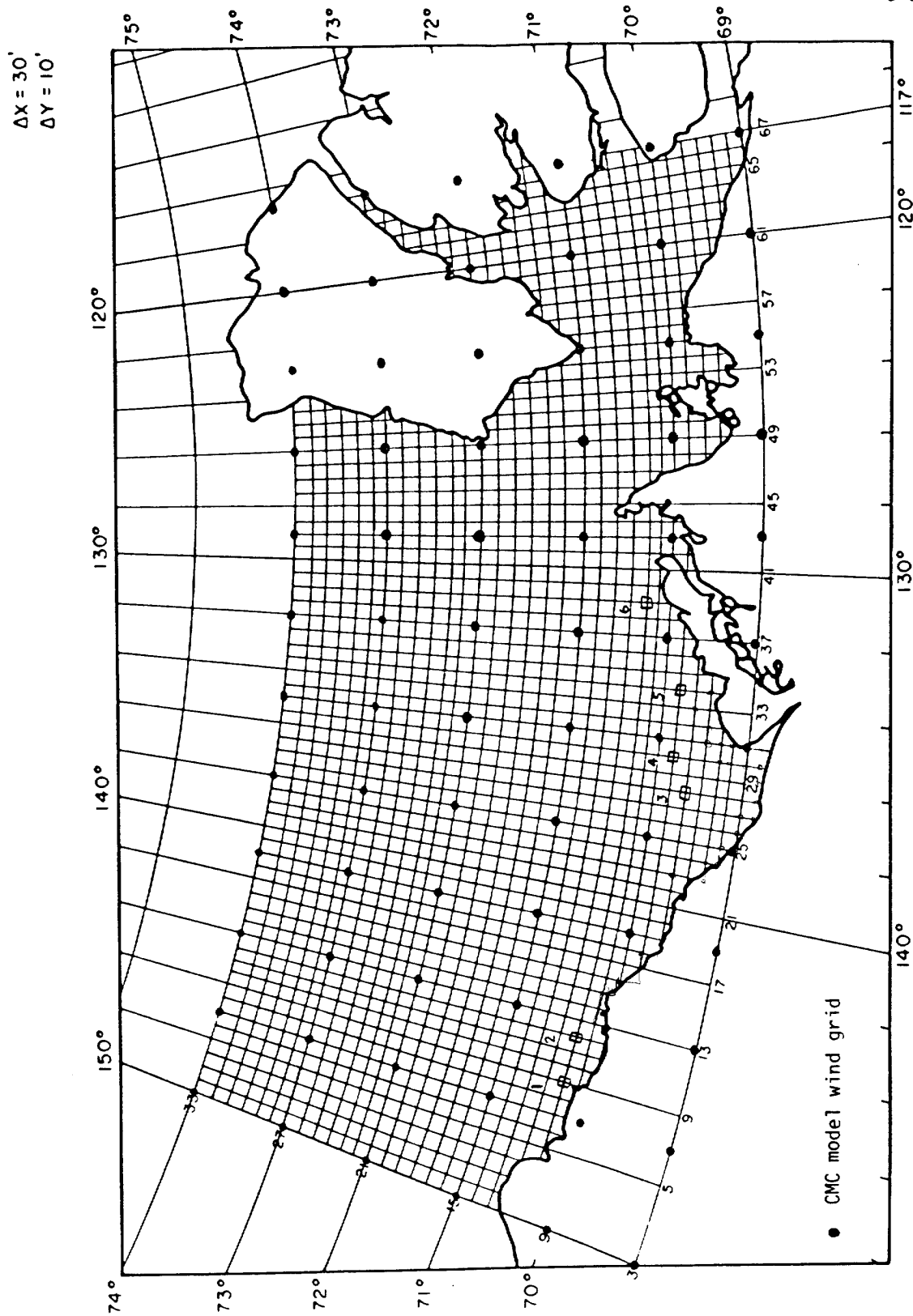


Figure 3.3c: Site Locations for 1986 Storm Simulations.

## **4.0 MODEL TESTING AND SENSITIVITY ANALYSIS**

### **4.1 INTRODUCTION**

The evaluation of a model is generally based on comparisons with reliable observations. The primary difficulty with such a procedure is that errors in the measured variables are usually not known, unless perhaps they are systematic in nature. As well errors in the input to a model will lead to a degradation of model results. Therefore it is important to be able to have reliable and accurate input and validation data. Donelan and Pierson (1983) have demonstrated that sampling variability alone can contribute errors up to 15% (at the 90% confidence level) in the wave height record determined from waverider buoy data. Larger errors can be expected in manual observations (e.g. ship reports and visual observations). Also there are assorted instrument, calibration and human errors that will undoubtedly arise. Obviously at this stage the modeler has very little control over the data quality. In this light with inherent uncertainties about data quality some subjective decisions are required. However in order to provide an objective framework on which to base the model's performance, the following comparison procedures are utilized.

### **4.2 EVALUATION TECHNIQUES**

#### **4.2.1 Time Series Plots of Hindcast vs. Observed Variables**

Time series of predicted significant wave height and period together with the forcing wind speed and direction will be presented at each evaluation site. When available, the observed variables will be plotted on the same figure for comparison.

#### **4.2.2 Statistical Analysis**

A quantitative statistical analysis is carried out to provide an overall evaluation basis for the model. The statistical parameters considered in this study are defined as follows.

At each station (j)

Let  $Y_i$  represent the modelled variable at time i  
 $X_i$  represent the observed variable at time i,

then we can define for each station the following quantities.

A) Cross Correlation Coefficient  $r_{xy}$

Obviously a high correlation between model result and reliable observations is desirable. For the purposes of this study the zero lag cross correlation coefficient between X and Y is calculated as follows:

$$r_{xy} = \frac{\sigma_{xy}^2}{(\sigma_x^2 \sigma_y^2)^{1/2}} \quad (4.1)$$

where  $\sigma_x^2$  is the variance of variable X;  
 $\sigma_y^2$  is the variance of variable Y;  
 $\sigma_{xy}^2$  is the covariance of variables X and Y;  
the above quantities are defined in the standard manner.

The cross-correlation can be generalized to allow for time lags and can be applied between any set of variables and between stations. However for this work the calculation was restricted to zero lag and like variables at the same station.

#### B) Linear Regression and Scatter Diagrams

Scatter diagrams between modelled and observed variables will be presented. Superimposed on these plots will be the least squares fitted line determined from the regression model of the form.

$$Y = a X + b \quad (4.2)$$

where X = observed variable;  
Y = model variable.

The least squares procedure minimizes the error in Y assuming the independent variable (X) to be accurate. This assumption, of course, is not strictly true as the observed wave field is subject to random measurement error. In particular, the manually observed wave data are only resolved to a half metre.

No error bars are determined for the parameters a and b although a measure of the goodness of fit can be determined from the correlation coefficient. The parameter a, the slope of the regression line, can be used for tuning the model. The y-intercept, b, is a measure of bias in the model. The adequacy of a linear model should be apparent from the scatter plots. A note of caution is Emphasized in the interpretation of the regression results. The coefficients are dependent on the manner in which the regression was performed. Had the model,  $X = cY + d$  been employed; there is no guarantee that the values of c and d would be equivalent to  $1/a$  and  $-b/a$  as a simple rearrangement of (4.2) would suggest.

Therefore, interpreting regression coefficients is critically dependent on the manner in which the regression was performed, and on the source, types and magnitude of errors associated with

the variables Y and, X. The regression line is determined only as a reference.

### C) Error Statistics

Other quantities produced for evaluation purposes are the mean error (Bias), Root Mean Square Error (RMSE) and Scatter Index (SI) defined as:

$$\text{Bias} = \frac{\sum_{i=1}^N (Y_i - X_i)}{N}$$

$$\text{RMSE} = \left[ \frac{\sum_{i=1}^N (Y_i - X_i)^2}{N} \right]^{1/2}$$

$$\text{SI} = \left( \frac{\text{RMSE}}{\bar{x}} \right) \times 100\%$$

$$\text{with } \bar{x} = \frac{\sum_{i=1}^N X_i}{N}$$

and N = number of data points.

These terms can be interpreted as follows. Positive (negative) bias indicates whether the model over (under)-estimates the value on average. The root mean square error is a measure of the deviation of the variable Y about variable X. The scatter index indicates the relative strength of the deviation of the Y variable about X.

The statistics themselves do not provide a definitive measure of the model's performance, however they can provide insight into model behaviour and perhaps point to areas in which improvement is necessary, such as parameter selection. As well, data suitability may be determined through this evaluation process.

It is again emphasized that care should be taken when utilizing the statistics. As mentioned previously the statistics calculated are restricted in scope since no allowance for possible time lags is made. Therefore interpretation of the results requires both a physical and statistical evaluation.

### 4.3 MODEL PERFORMANCE, SENSITIVITY AND PRELIMINARY TESTING

The evaluation procedures outlined previously will form the basis for model validation. However, prior to implementing statistical evaluations it is instructive to first study the model's performance under controlled conditions, and to test its sensitivity to different parameters. In this way the behaviour of

the model can be monitored and the influence of parameters may be judged.

#### 4.3.1 Controlled Tests

The model was set up to run with a rectangular domain (Figure 4.1 ) of grid size (29, 23) where the distance between grid points ( $\Delta x$ ) was 18.5 km. A number of tests were carried out under ideal conditions using different model parameters. The conditions for each test case will be listed. The conditions not changing in these ideal tests are:

PERIOD OF INTERPOLATION:	DT = 30 minutes
WIND STRESS FACTOR	: $\gamma = 0.1$
SPREADING FACTOR	: SPRD = 0.1512
INITIAL CONDITIONS	: Quiescent

The effect of varying the wind stress factor ( $\gamma$ ) is obvious. Spreading was tested during the development of the model, the value of 0.1512 was selected for physical reasons (Clodman, personal communication) and corresponds to spreading restricted to  $\pm 45^\circ$  from the mean wave direction. The period of interpolation determines how fine the wind information will be resolved. This period should be sufficient based on previous testing. The locations monitored in the tests are Site 1 (12,12) and Site 2 (23,12). The designations a) and b) will denote model runs with conditions indicated as shown below.

#### TEST 1 - MODEL SPIN-UP AND SMB COMPARISON

Purpose: Determine spin-up characteristics and steady state predictions versus the SMB empirical formulae (Bretschneider (1958)).

Ice: None

Smoothing: SMTH = 0.00002

Wind: Homogeneous in space, and constant in time with:  
a) 20 knots, westerly (along models X axis)  
b) 40 knots, westerly (along models X axis)

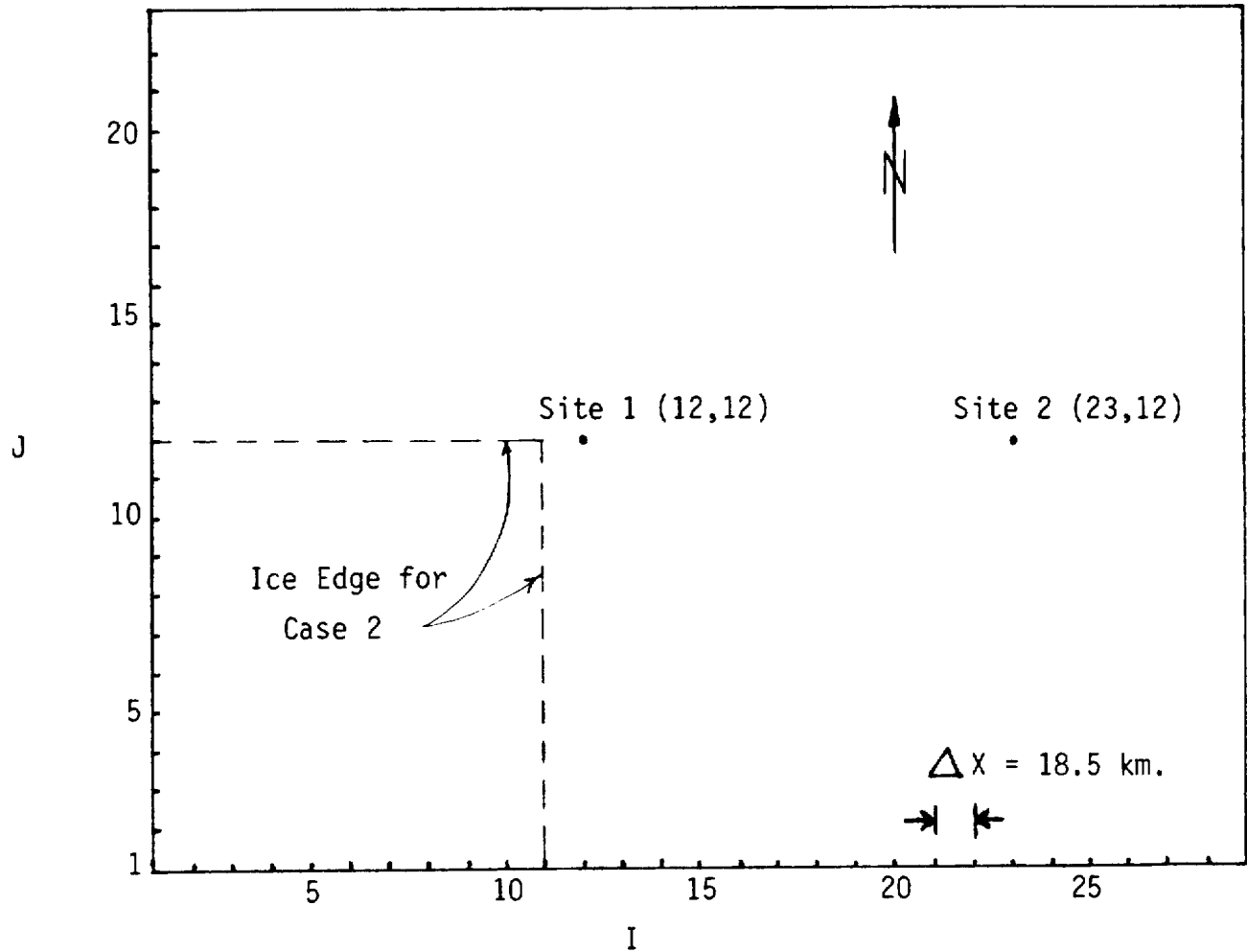


Figure 4.1 Model Domain for Controlled Tests

For both wind speeds the model spun-up in a stable, exponential fashion to its final steady state. The steady state conditions at the two locations are compared with the SMB formulae in Table 4.1 .

TABLE 4.1  
Comparison of BSWM2 with SMB formulae

Windspeed (knots)	20		40		
Fetch Length (km)	203.5	407	203.5	407	
Significant Height (m)	BSW2	2.3	2.6	7.8	9.2
	SMB	2.0	2.4	5.0	6.7
Significant Period (s)	BSWM2	6.5	7.0	11.9	13.2
	SMB	5.7	6.3	8.9	10.2
*Duration (hrs)	BSWM2	14	19	8	13
	SMB	15	27	11	18

\* Duration indicates elapsed time until fully developed sea is established.

The model yields higher values for both wave height and period than predicted by the SMB curves. Spin-up occurs quicker in the model.

#### TEST 2 - INTRODUCTION OF ICE BOUNDARIES

Purpose: To test the models behaviour when an ice edge is introduced suddenly into the domain.

Ice: Ice introduced at  $T = 24$  hrs into the run and covers the section  $I \leq 11$ ,  $J \leq 12$  (as shown in Figure 4.1 ).

Smoothing: a) SMTH = 0.00002  
b) SMTH = 00.0

Wind: Homogeneous and constant  
20 knots westerly.

The introduction of ice can cause large spatial gradients in the wave field to be set up. These can lead to oscillations being generated and propagated throughout the domain. To test this effect on model predictions, an ice edge is introduced suddenly. The smoothing function is tested to illustrate how it can dampen these oscillations.

Figures 4.2 a ,b show the evolution of the wave field in time at locations 1 and 2. For both locations smoothing has no effect on the results prior to the ice being introduced. The readjustment to steady state for the new fetch conditions imposed by the ice is rapid at site 1, closest to the ice edge while at site 2 the ice effects are less pronounced. Note that smoothing has altered the results. At site 1, the effect of smoothing is

felt rapidly. The disturbance or oscillation induced by the ice edge took same time to develop at site 2 and therefore the effect of smoothing the field is felt at a later time. The apparent discontinuities seen in the plots is due to roundoff error in the output. (i.e. resolution is in decimetres).

The purpose of the smoothing was to damp out oscillations and is best illustrated in Figure 4.3 . This shows a cross-section of the wave heights across the lake along the line I = 12, one grid block downwind of the ice, 12 hrs, after the introduction of the ice edge. In the no smoothing case a small oscillation persists. When smoothing is implemented the bump is eliminated. As shown in the time series of site 2 the oscillations appear to propagate through the domain. The model, however was stable for this test case. Further testing on the effects of these oscillations should be carried out since, in the Beaufort Sea context, the boundaries of the lake are dynamic and the domain is large. The effect of smoothing has an appreciable effect on the results in areas of spatial gradients of the wave field.

BEAUFORT WAVE MODEL COMPARISON

4-9

Site 1, Ice Edge Test

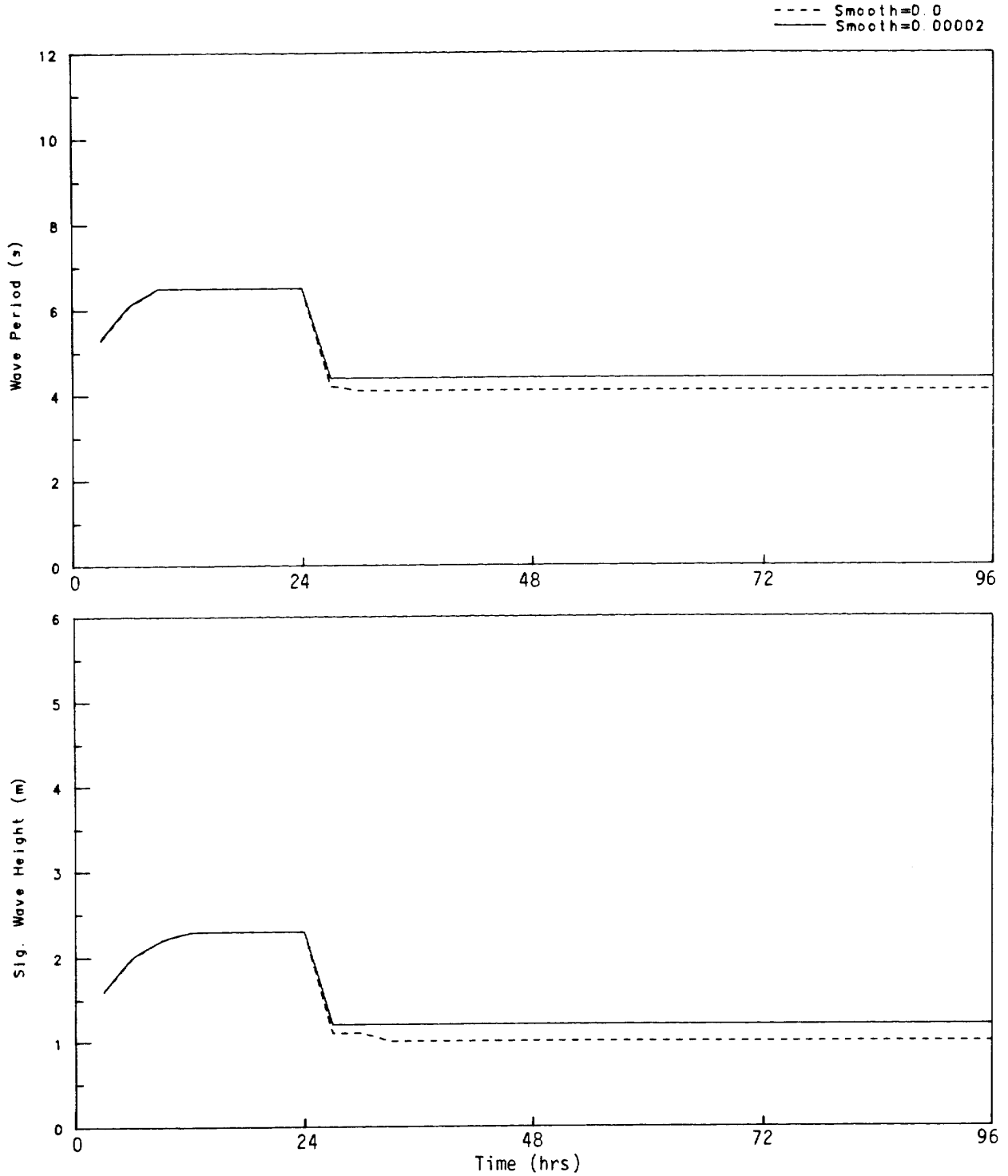


Figure 4.2a : Evolution of Wave Field With Ice Cover, Site 1.

BEAUFORT WAVE MODEL COMPARISON

4-10

Site 2, Ice Edge Test

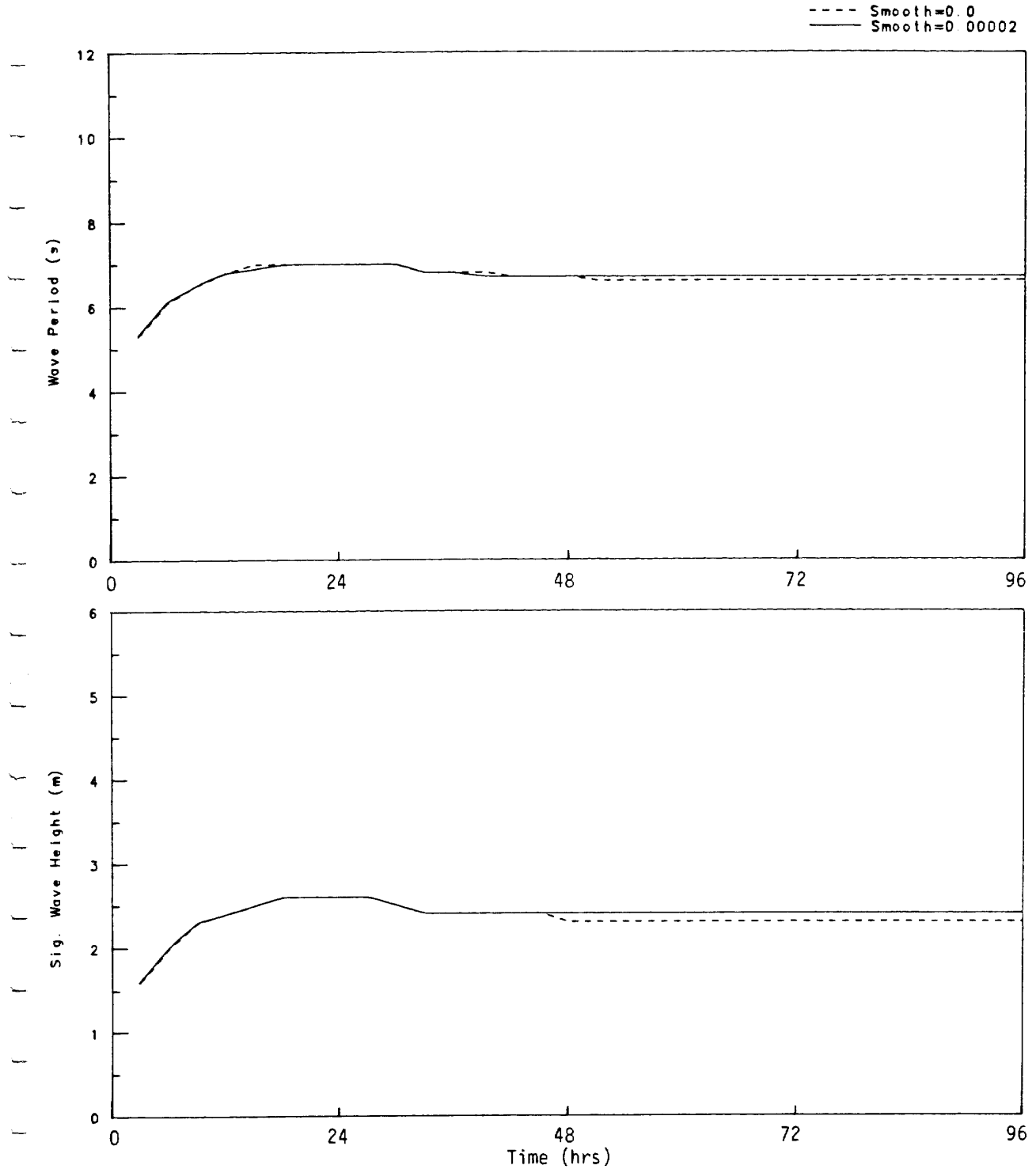


Figure 4.2b: Evolution of Wave Field with Ice Cover, Site 2.

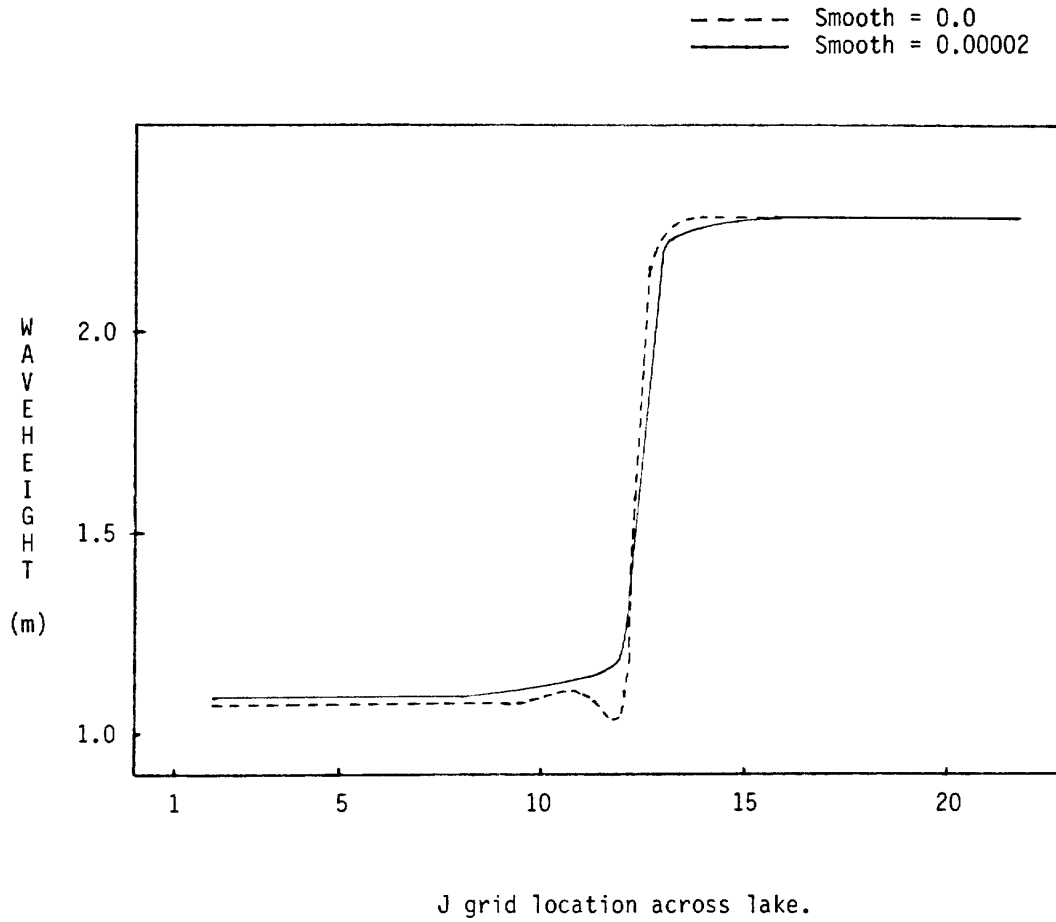


Figure 4,3: Cross-Section of Waveheights.

Again, the apparent discontinuities seen in the plots are simply due to roundoff errors.

#### TEST 3 - SHIFTING WIND

Purpose: How does the model respond to a sudden shift of 90° in wind direction.

Ice: None

Smoothing: SMTH = 0.00002

Wind: Homogeneous  
Constant speed at 20 kts, westerly for first 24 hours then southerly from 25, hrs until the end of the run.

Figure 4.4 illustrates the development of the wave field for both sites when a rapid wind shift is applied. The model readjusts to a steady state slightly longer than the spin-up time. This is due to the fact that an existing wave field was present. The final values for both sites is identical, as expected since they both have the same fetch length after the shift. The adjustment of the wave direction with time is illustrated in Figure 4.5 for both locations. The wave field requires about a day in order to become aligned with the wind field.

The above runs do not comprise a complete set however they do illustrate the models behaviour. Further testing is outside the scope of this report due to the large number of parameters and options that can be tested and the innumerable tests that can be performed. The previous tests illustrate that the model performs stably under ideal conditions.

#### **4.3.2 Beaufort Sea Test**

The final test performed utilizes actual Beaufort Sea data. Information from the first 3 weeks of the 1981 study period (July 25 August 14, 1981) is used. Site locations for this period are shown in Figure 3.3 . A comparison is made between the model in its final modified state with recommended parameter values and a "primitive" version using parameter values of the original GLERL model. Statistical analysis is performed as described below.

#### TEST 4 - BEAUFORT SEA DOMAIN

Purpose: Test BSWM2 in its refined state with actual data.

Configuration: Beaufort Sea Domain (67,33),  $\Delta x = 18.5$  km.

Time Step: DT = 30 minutes

Ice: Ice-edge updated on (month/day), 7/30, 8/6 and 8/13

BEAUFORT WAVE MODEL COMPARISON

4-13

Rapid Wind Shift

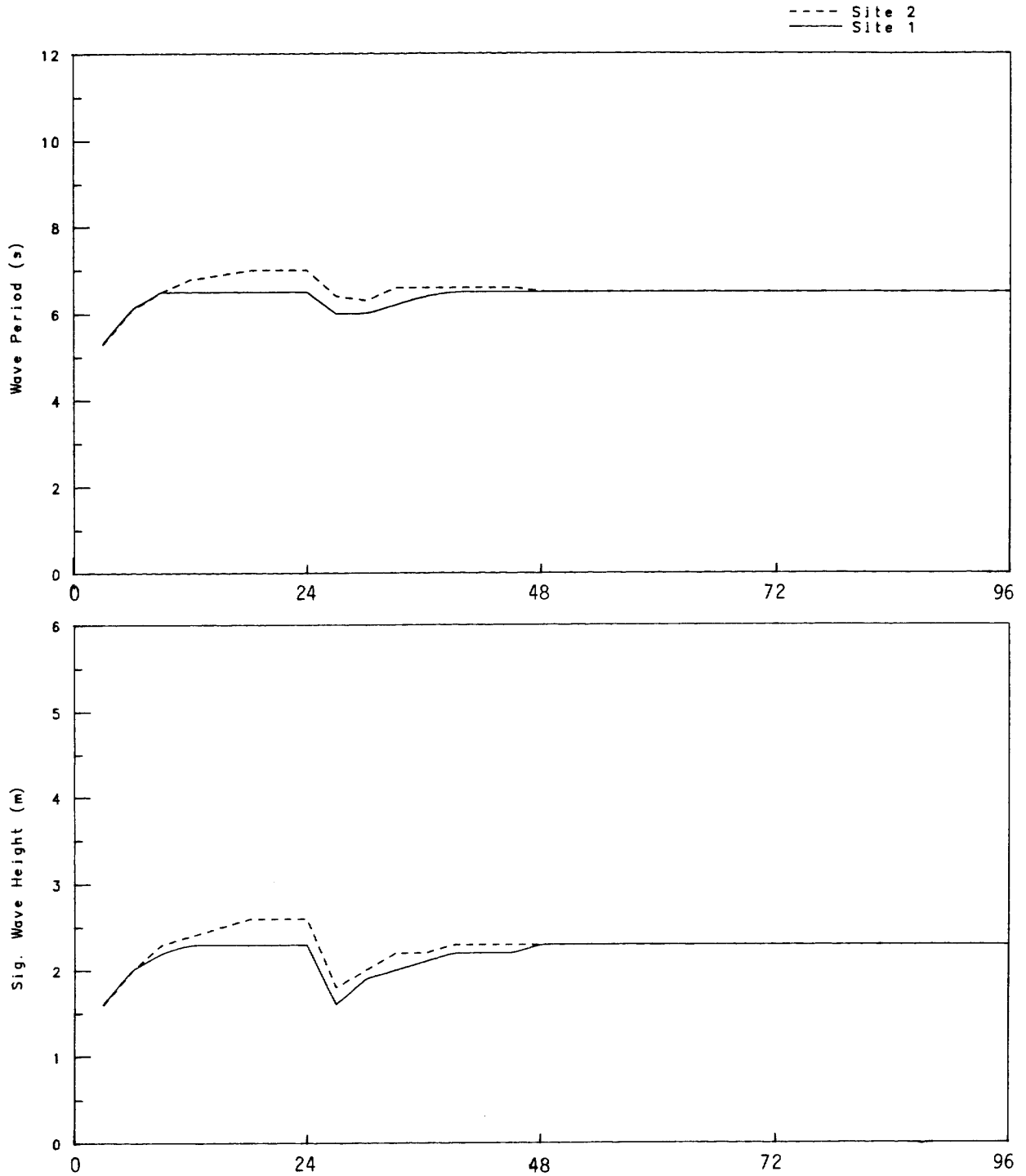


Figure 4.4: Evolution of Wave Field After Rapid Wind Shift.

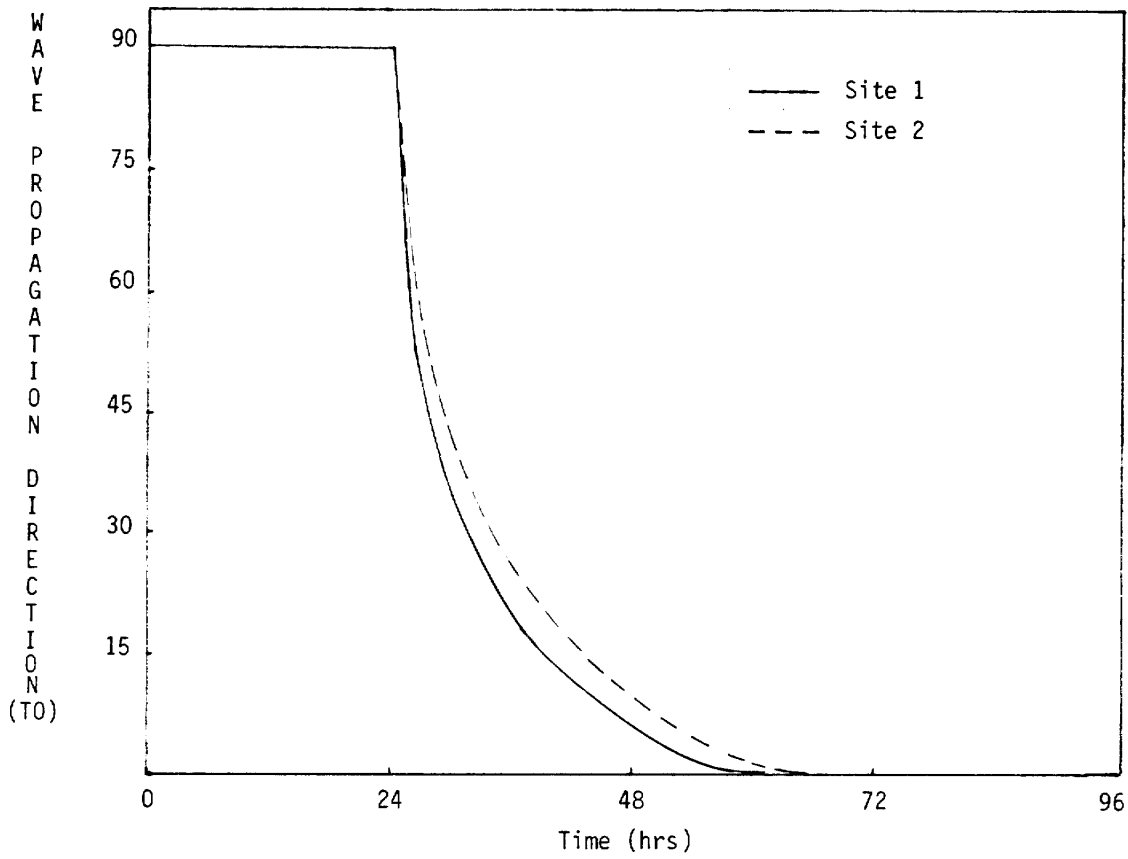


Figure 4.5: Wave Direction, Adjustment to Wind Shift.

Friction:	a) $\gamma = 0.28$ b) $\gamma = 0.10$
Spread:	a) SPRD = 0.5 b) SPRD = 0.1512
Smooth:	a) SMTH = 0.00000 b) SMTH = 0.00002
Wind:	Homogeneous Dome observed wind from site 2 (z = 65m) a) as observed (i.e. without modification to 10 m) b) neutral (at 10 m above MSL).

The parameter values used in run a) define the model in its primitive state, those used for run b) represent the model in its refined state. The results of both runs are illustrated in Figure 4.6 along with observations, for site 2. whose wind was used as input to the model. It is difficult to assess superior performance visually however some general comments can be made.

i) significant difference in wind speeds due to accounting for boundary layer effects, both models are dominated by wind forcing;

ii) interpolation of wind effectively fills in gaps of wind record;

iii) both refined and primitive versions of the model overestimate wave period consistently (this may be because the observed wave period represents the zero-crossing, or average, period whereas the model period represents the peak period, which is usually higher than observed).

iv) both models underestimate apparent high wave height events although this may be due to observational error;

A more quantitative evaluation of model performance is given by the correlations between model estimates and the observations. Table 4.2 presents these values for the different variables.

TABLE 4.2

Correlation coefficient between observations and model versions.

	PRIMITIVE	REFINED
WAVE HEIGHT	0.83	.91
WAVE PERIOD	0.62	.69
WIND SPEED	1.0	.94*

\*The correlation of .94 between observed and the neutrally stable winds indicates that there is a significant influence exerted by the boundary layer.

It is evident that the refined model performs better, on the basis of correlations with the Dome observed wave data. As was obvious from the time series plots, wave height is modelled well while wave period is only marginally accounted for. It appears that the refined model performs satisfactorily. Using recommended parameter values results in a substantial improvement in results.

BEAUFORT WAVE MODEL COMPARISON

4-17

Model Sensitivity Test  
July 25, 1981 to August 14, 1981

----- Primitive  
- - - - - Refined  
\_\_\_\_\_ Observed (Dome)

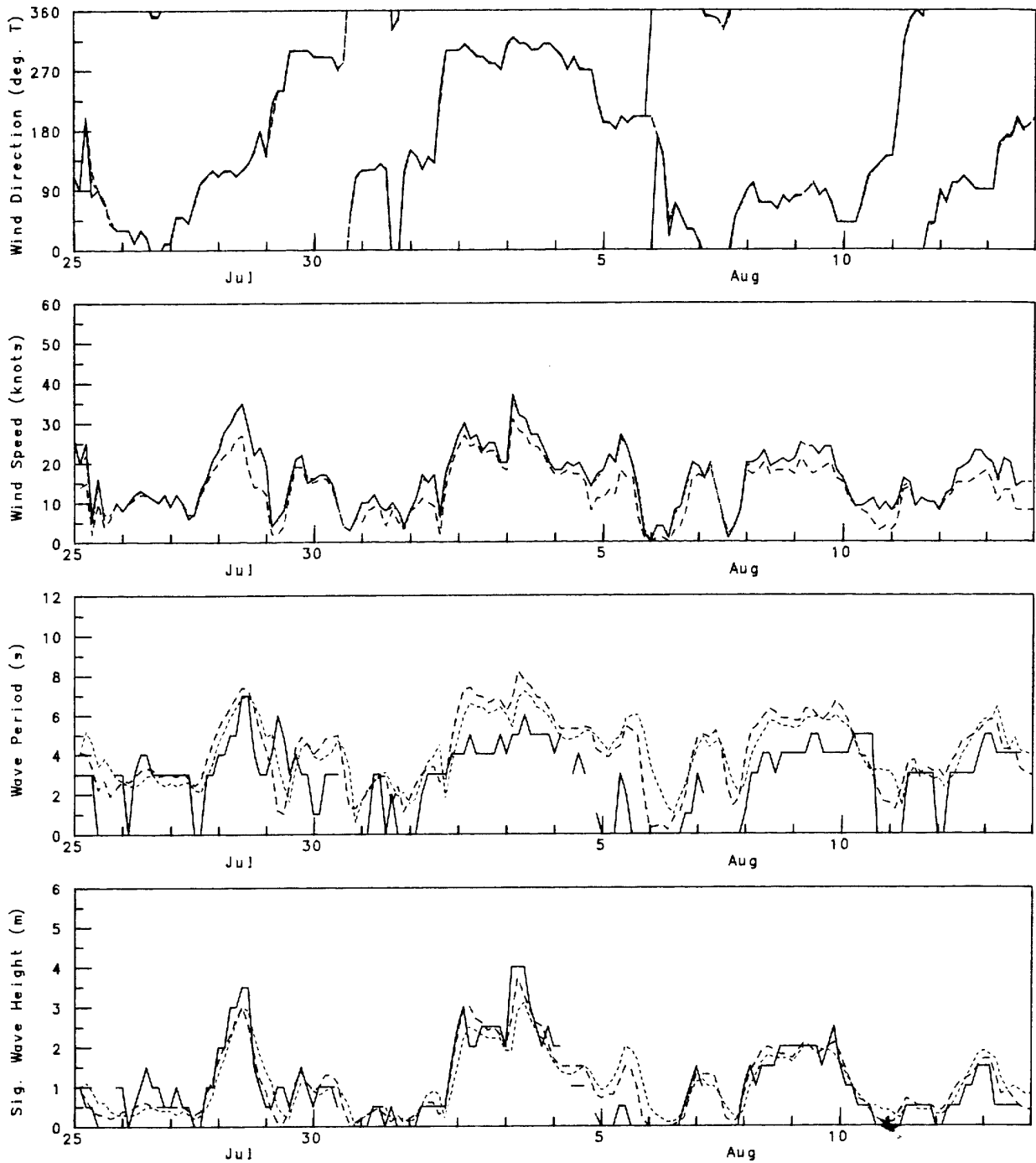


Figure 4.6: Model Sensitivity Test

#### 4.4 WAVE DATA EVALUATION

Another consideration is the quality of the Dome observations. Of prime concerns are the accuracy, consistency and resolvability. For example, the observed significant wave heights are generally recorded to the nearest half metre. This coarseness can lead to errors at low wave heights of up to 100% and for wave heights about 3m for example, errors on the order of 20%. As well, consistency between observers is not guaranteed while resolving the information visually is also a potential source of error. Also the observed wave periods are usually estimated as a zero crossing period and tend to be lower than the peak period defined by the spectrum.

Another source of data available for comparisons is waverider buoy records which were obtained from The Marine Environment Data Service (MEDS) . Unfortunately the spatial and temporal coverage of the buoys is sparse. For the test period, waverider data (MEDS) were available at site 3 which is located about 2 grid blocks away from site 2. A comparison of the model output (refined version of BSWM2) at Site 3 with the two data sources is shown in Figure 4.7 . The forcing wind, 10 m neutral wind from Site 2, is generally lower than the observed Site 3 winds, directions are virtually identical. Visual comparison indicates marginal agreement between wave period estimates and satisfactory agreement for wave heights. Correlation between estimates of the wave variables is shown in Table 4.3 for this period.

TABLE 4.3

Correlations Between Data Sets from Waverider Buoy and From Dome  
(Site 3)

	<u>WAVE HEIGHT</u>	<u>WAVE PERIOD</u>
MODEL - DOME	0.82	0.58
MODEL - WAVERIDER	0.89	0.58
DOMES - WAVERIDER	0.91	0.69

### BEAUFORT WAVE MODEL COMPARISON

Data Comparison - Site 3  
July 25, 1981 to August 14, 1981

----- Waverider  
- - - - - Model Estimates  
\_\_\_\_\_ Observed (Dome)

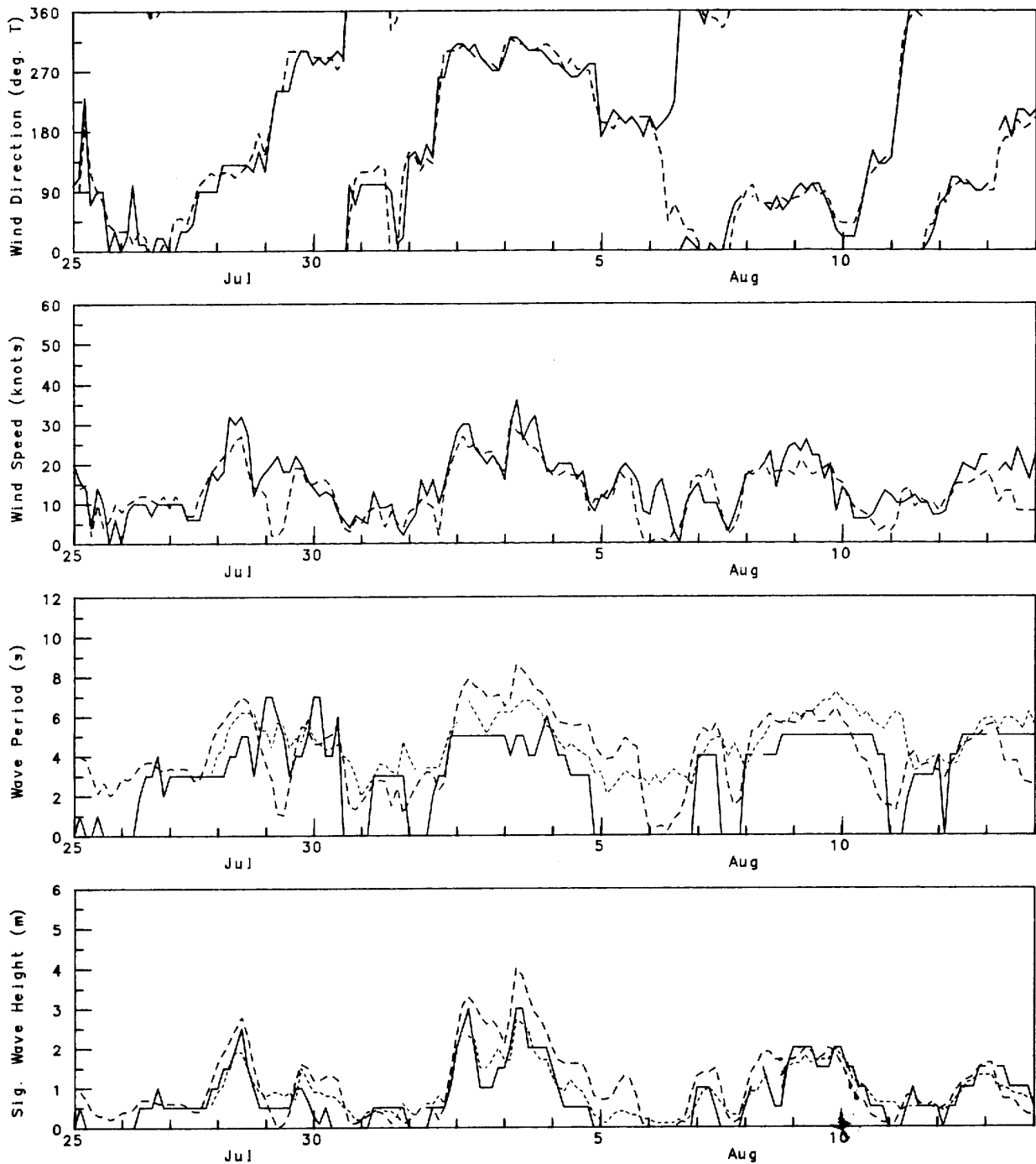


Figure 4.7: Wave Data Comparison, Site 3

The model appears to be slightly better correlated with the waverider data. Note, however, that the correlation between DOME and the waverider at this site is good for wave height but marginal for wave period. There is a significant difference between spectrally and manually derived wave data. Therefore, the choice of data to compare the model with and for use in evaluation purposes should be given increased priority, to ensure that an appropriate comparison is made. Indeed the comparability of data types rests largely on the manner with which they are derived. The model wave variables are based on the JONSWAP form for the spectrum as discussed previously. The waverider variables are derived from the measured spectrum, which may differ from the JONSWAP spectrum. The manual observations are based on visual estimates and accuracy depends heavily on the experience of the observer and the conditions under which the observations are made. There will undoubtedly be some margin of error amongst these realizations.

The above discussion focused on differences between data sets at the same location. Of course one must then expect that differences in observables will occur between sites. This is briefly discussed using sites 2 and 3, as an example. Based on their proximity to one another, one would expect similar wind and wave conditions at these two locations assuming that local effects are small. This will be investigated briefly here. The correlation between model output wave height at Sites 2 and 3 was .99 indicating that, in addition to identical wind forcing, the model considers that both sites are subject to identical conditions (e.g. fetch, energy flux). The correlation between DOME observations at these sites was round to be .83 for wave height. This might indicate a genuine and significant change in wave climate between the sites and/or the effects of measurement error. If the wave climate has changed over this short distance then it must be due to local changes in forcing and perhaps topographic effects or due to existence of transient ice patches not resolved in the ice charts. Indeed, although wind directions at both sites are almost identical, the correlation of the observed (i.e. non-neutral) wind speeds between sites was only 0.80. An explanation for the apparent change in wind speeds between sites is not obvious at this time. Both wind observations were made at the same anemometer height. If the change is real then this again emphasizes the importance of improving spatial resolution of the wind field.

With this amount of variability between observables, it is difficult to assess the accuracy of the data. Especially since the differences can be physically based, inherent error or a combination of both. Therefore, in the evaluation of the model,

which itself is subject to some error, one must expect sane margin of error.

At this point in time the model has been found to perform adequately in the refined state, although perhaps further improvements can be implemented. The major sources of discrepancy should not be solely attributed to the model alone. Indeed, observational error and also poor spatial resolution of the wind field have contributed to the discrepancies found in this testing procedure.

Of course one might argue that in order to optimize the model an extensive sensitivity analysis should be performed by varying only one parameter value at a time. However, with three parameters, several options as to the wind input to be used and uncertainty in the wave data upon which comparisons are based this task can be overwhelming in scope. The choice of parameter values and model options for the remainder of the evaluation process is based on providing the best possible information to the model from a physical standpoint. The parameters selected are:

```

FRICITION FACTOR:    $\gamma = 0.1$ 
SPREAD:             SPRD = 0.1512
SMOOTH:             SMTH = 0.00002
WIND:               Best Available

```

The wind selected will be described in more detail for each run.

#### 4.5 BSWM vs. BSWM2

Finally, to determine whether or not any significant improvements in hindcasting skill has been achieved by BSWM2, a comparison is made between it and the previous Beaufort Wave Model, BSWM. Figure 4.8 illustrates the results for Site 3 of a simulation covering the period July 25 to August 14, 1981. Identical wind inputs were supplied to each model. Visually, both models appear to perform equally as well. However, the statistics, based on the waverider data over this period, favour BSWM2. The correlations between the wave models and the waverider data for this period are:

	Significant Height	Period
BSWM2	0.89	0.58
BSWM	0.76	0.50

One obvious improvement is the inclusion of the boundary layer effects. Indeed, Donelans stress derivation was based on having

wind speeds at the 10 m height, BSWM2 not only provides a better estimation of the magnitudes of the wave variables, it also accounts for superior timing as evidenced by the improved correlations. In testing the GLERL model, Schwab et al (1986) found that, for the Great Lakes, the swell component was small. For the much larger Beaufort Sea domain, the inclusion of swell may be important. The time series plot of figure 4.8 indicates swell is a minor effect in comparison to the effect of wind reduction since the results in both models are wind dominated.

### BEAUFORT WAVE MODEL COMPARISON

BSWM2 vs. BSWM - Site 3  
July 25, 1981 to August 14, 1981

----- BSWM  
- - - - - BSWM2  
————— Waverider

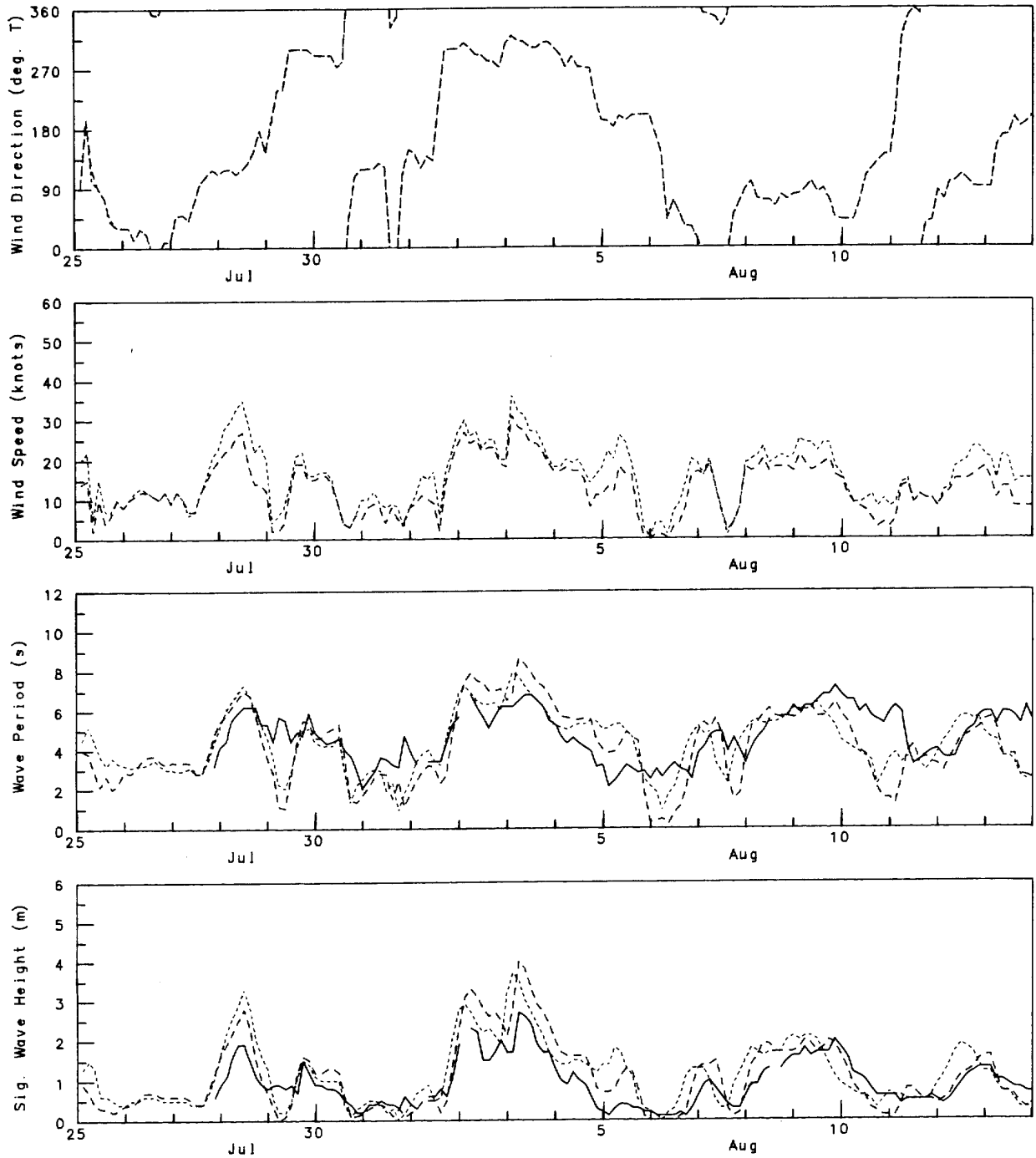


Figure 4.8: BSWM2 vs. BSWM Model Comparison

## 5.0 MODEL EVALUATION

The previous section outlined the sensitivity of the model to various parameter choices and provided a preliminary evaluation on model performance. Of course, those evaluations indicated the most important consideration is the adequacy of the wind input. In fact, the choice of parameters to use may be dependent on the type of wind information supplied to the model.

In this section a comprehensive evaluation of the Model BSWM2 is performed. Two sets of model runs were carried out: 1) the model was run for over a 2 month period to compile a statistical bases on which to assess overall model performance; 2) the model was run for several 5 to 7 day periods to evaluate how well storm events are modelled.

The evaluation was performed for the three years 1981, 1982 and 1986. The 1981 open water season provided sufficient in-formation to perform long term statistical evaluations, as well as 4 storm events. In 1982, another 4 storm events were analyzed while in 1986, 3 storm events were studied.

The type of wind available will dictate whether the boundary layer routines are used as well as the type of spatial processing of the wind information. The evaluation is thus performed for the above sets separately since the available information is different for these data sets. The actual data files used in these evaluations are further described in the Supplementary Data Base Report.

### 5.1 1981 FIELD YEAR

The data available for the 1981 season is illustrated in Table 3.1a with site locations shown in Figure 3.3a . A line chart of data coverage is illustrated in figure 5.1 . A homogeneous wind field was used as input to the model This choice of forcing field was necessary due to the limited spatial coverage of the observations.

The wind data from Site 2 (Dome observation) was selected. Some gaps in the temperature record of Site 2 were filled. The anemometer height of measurement was 65m. Boundary layer effects were taken into account and the neutral 10 m wind speeds were determined. New ice boundaries were introduced on the following dates, (month/day), 7/30, 8/6, 8/13, 8/20, 8/27, 9/3, 9/10, 9/17, 9/24 and 10/1. Figures illustrating the actual location of these ice-edges are given in Appendix E .

SITE	DATA SOURCE	JULY	AUGUST					SEPTEMBER					OCTOBER	
			5	10	15	20	25	31	5	10	15	20		25
1	WIND DOME	25	EXPLORER IV AT KILANNAK					5						
	WAVE DOME		-----						-----					
	MEDS		5	-----			14							
2	WIND DOME	25	EXPLORER I AT KOPANOAR										6	
	WAVE DOME		-----					-----						
	MEDS		-----					-----						
3	WIND DOME	25	EXPLORER II AT ISSUNGNAK										6	
	WAVE DOME		-----					-----						
	MEDS		28	-----			31							
4	WIND DOME	25	EXPLORER III AT KOAKOAK										6	
	WAVE DOME		-----					-----						
	MEDS		-----					7	-----					
5	WIND DOME						7	EXPLORER IV 19						
	WAVE DOME							ORVILUK						
	MEDS							-----						
6	WIND DOME							EXPLORER IV						
	WAVE DOME							21-----26						
	MEDS							-----						
7	WIND DOME										27	EXPLORER IV 6		
	WAVE DOME											IRKALUK		
	MEDS											-----		

Figure 5.1: Data Coverage 1981 Open Water Season.

A timing discrepancy was discovered in the Dome data. It was necessary to shift the waverider data (GMT) by six hours to coincide with the Dome observation data which was found to be given in local time. All information for 1981 is therefore referenced to local time.

### 5.1.1 Open Water Season

The model was run from July 25 to October 5, 1981 encompassing a major proportion of the open water season. The model results are plotted in Figures 5.2 a-g. for the seven sites, alone with available observed data. Before entering into a discussion on the statistical evaluation of the model, several points should be noted:

It is evident from some of the time series plots that an apparent time lag occurs between sets of variables. For instance at Site 1 the observed variables lag the model estimates by about 12 hours. This is easily seen in the wind direction time series. The model was forced by Site 2 winds, where Site 2 is located about 200 km west of Site 1. Figure 3.3a . The implication of the lag then, is that the wind field propagated to the east with an apparent phase speed of about 17 km/h and remained relatively unchanged in its passage. The observed wave field shows a similar lag behind model estimates suggesting that the waves are dominated by the local wind. Assuming spatial homogeneity in the wind field appears to be a poor approximation as significant horizontal variation in the wind field can be present within the model domain. If homogeneity is assumed, the propagation characteristics and spatial structure of the wind field should be monitored. The lags are not as large at sites close to Site 2 although they do exist. The presence of such lags can influence the statistical analysis and interpretation of the results should be made with caution. In fact, the evaluation of lagged correlations might prove to be a better indicator of model performance in this case.

A summary of the evaluation statistics for wave heights and periods is presented in Table 5.1 . Both observed and waverider data are utilized.

TABLE 5.1

Evaluation Statistics; 1981 Open Water Seasona) Significant Wave Heights

## Dome Observations vs. Model Estimates

Site	Error Statistics			Regression Parameters			# of Data Points	$\sigma_x$ (m)	$\sigma_y$ (m)
	Bias (m)	RMSE (m)	S.I. (%)	Slope	Intercept (m)	r			
1	0.24	0.79	80	0.66	0.58	0.63	274	0.85	0.90
2	0.09	0.76	68	0.58	0.57	0.68	533	0.99	0.85
3	0.34	0.65	71	0.77	0.55	0.83	494	0.97	0.90
4	-0.13	0.68	50	0.63	0.37	0.82	529	1.15	0.88
5	0.30	0.76	78	0.75	0.54	0.71	96	0.89	0.94
6	-0.27	0.45	35	0.29	0.63	0.43	48	0.38	0.26
7	-0.59	0.98	43	1.08	-0.77	0.79	63	0.94	1.28

## Waverider vs. Model Estimates

1	0.33	0.58	115	1.07	0.30	0.56	57	0.30	0.57
3	0.27	0.53	58	1.06	0.22	0.82	267	0.61	0.79
4	0.20	0.60	57	1.05	0.14	0.79	433	0.68	0.91

b) Wave Period

## Dome Observations vs Model Estimates

Site	Error Statistics			Regression Parameters			# of Data Points	$\sigma_x$ (s)	$\sigma_y$ (s)
	Bias (s)	RMSE (s)	S.I. (%)	Slope	Intercept (s)	r			
1	1.59	2.40	84	0.51	3.00	0.55	273	1.95	1.82
2	0.80	1.93	53	0.45	2.80	0.59	534	2.13	1.62
3	1.23	2.26	69	0.43	3.09	0.63	494	2.44	1.68
4	0.46	1.55	39	0.58	2.14	0.76	530	2.30	1.73
5	1.65	2.21	80	0.70	2.49	0.72	96	1.97	1.92
6	0.69	0.96	27	0.39	2.88	0.44	48	0.67	0.60
7	-0.75	1.56	26	1.43	-3.34	0.80	63	1.18	2.11

## Waverider vs. Model Estimates

1	-0.38	2.05	50	-0.06	3.97	-0.06	57	1.44	1.32
3	-0.39	1.34	28	0.68	1.15	0.64	267	1.46	1.55
4	-0.74	1.79	34	0.64	1.13	0.48	433	1.32	1.77

\*The above error statistics and regression parameters are defined in Section 4.2.2.

In general, the error statistics indicate that the model is reasonably correlated with the available data. It is interesting to note that the sites closest to Site 2 have the highest correlations, a consequence of using Site 2 winds to force the model. The reduced correlations at site 1 are partially a result of the time lag mentioned previously. Another interesting feature is that at Site 2, for the Dome observations, the correlations are lower than the neighboring sites. However, when using the waverider buoy data, site 2 exhibits the highest correlations. Of course, the discrepancies should not be attributed completely to the model since there is inherent error in the observables. Scatter plots of observed wave height and waverider wave height versus model predictions are shown in Figures 5.3 a-e. The scatter plots allow easier identification of outliers and perhaps erroneous points. For instance, for Site 29 there is a group of points clearly displaced from the main cluster. These points can be traced back to the time series on October 3, where the results diverge. The rise in the Dome observed wave heights are not coincident with the wind forcing. For Sites 3 and 4 at this time the rise in the observed wave field occurs about a day later, coincident with the model estimates based on the wind field. It is unlikely that this apparent time lag between observations is physically based if, representing propagation of swell, the apparent group speed is too low for waves of this size. If this portion of the record is removed, the correlation between observed wave height and model estimates for Site 2 increased from 0.68 to 0.78, a significant amount. The reason for this discrepancy cannot be explained since the model predictions of large events are usually very good.

The correlation between waverider and Dome observed significant heights for Stations 1, 3 and 4 are 0.86, 0.89, and 0.87, respectively. This suggests that between observables there is a significant amount of variability as previously discussed.

The long term error statistics, based on the conditions with which the model was run and the limited evaluation techniques employed, suggest that for the 1981 field year the following results may be noted.

- 1) A homogeneous wind field is inadequate for such a large domain, small scale variability exists, since the model results are dominated by the wind it is necessary to adequately represent the spatial structure of the wind field.
- 2) A better spatial observing network is required to resolve the wind field properly.

3) The validation data are subject to error which will degrade the evaluation process.

4) The model appears to perform adequately. The time series plots indicate that the variability in the wave field is well modelled, especially for storm events.

5) A more complete evaluation procedure, allowing for lagged correlations is required in order to properly assess model performance and perhaps identify relevant physical phenomena such as storm tracking.

The model, however, has shown definite improvements over the BSWM results outlined in MPL (1986) for this period. In fact the correlations improved for each site, except site 6. The choice of parameters and model options utilized in BSWM2 resulted in reduced error statistics as well. Therefore, not only is BSWM2 better correlated, it appears to be more accurate than BSWM.

### BEAUFORT WAVE MODEL COMPARISON

Site 1 - Kilannak (Explorer IV)  
July 25, 1981 to August 30, 1981

----- Waverider  
- - - - - Model Estimates  
\_\_\_\_\_ Observed (Dome)

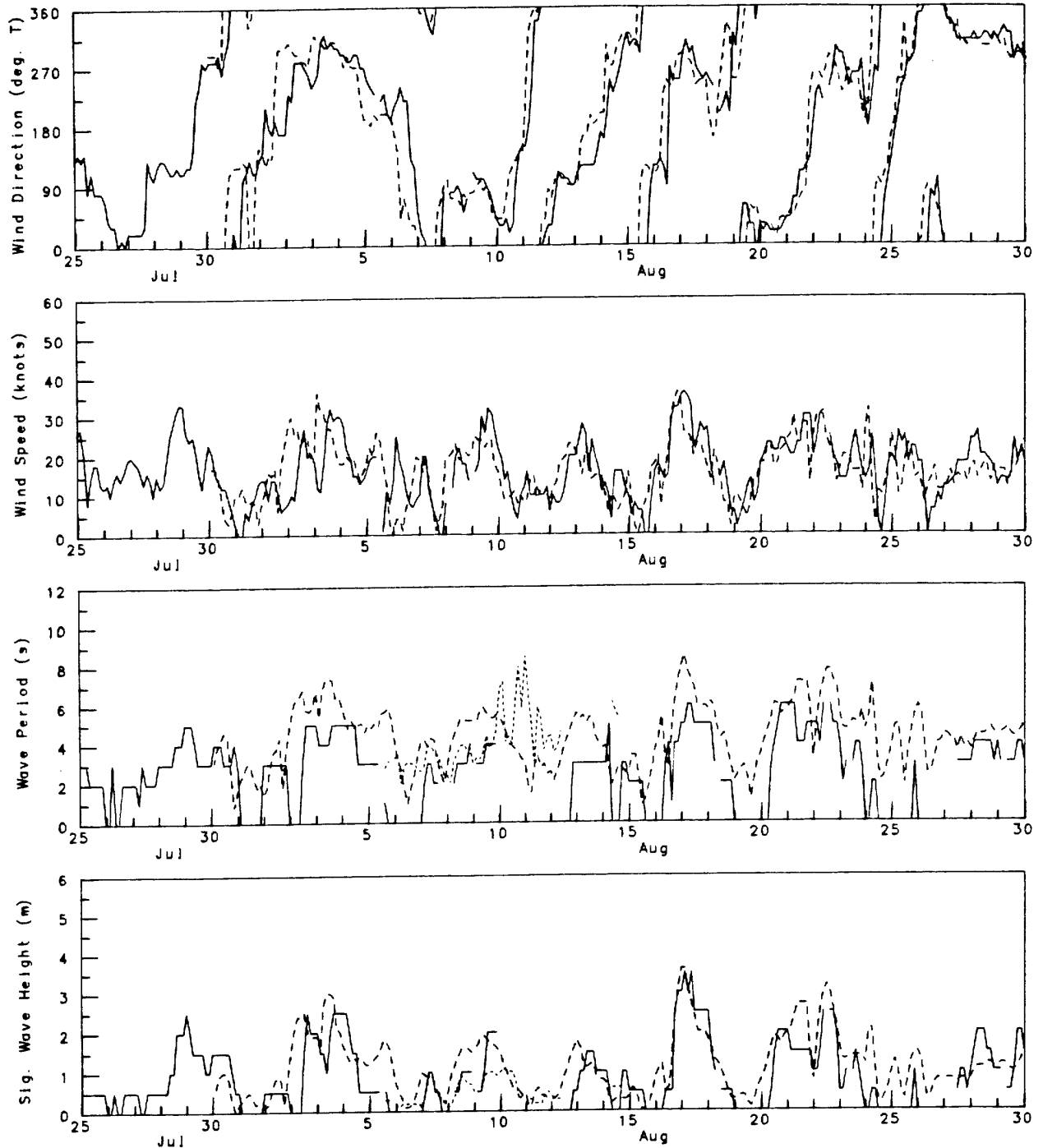


Figure 5.2a: Site 1

### BEAUFORT WAVE MODEL COMPARISON

Site 1 - Kilannak (Explorer IV)  
August 30, 1981 to October 5, 1981

..... Waverider  
- - - - - Model Estimates  
————— Observed (Dome)

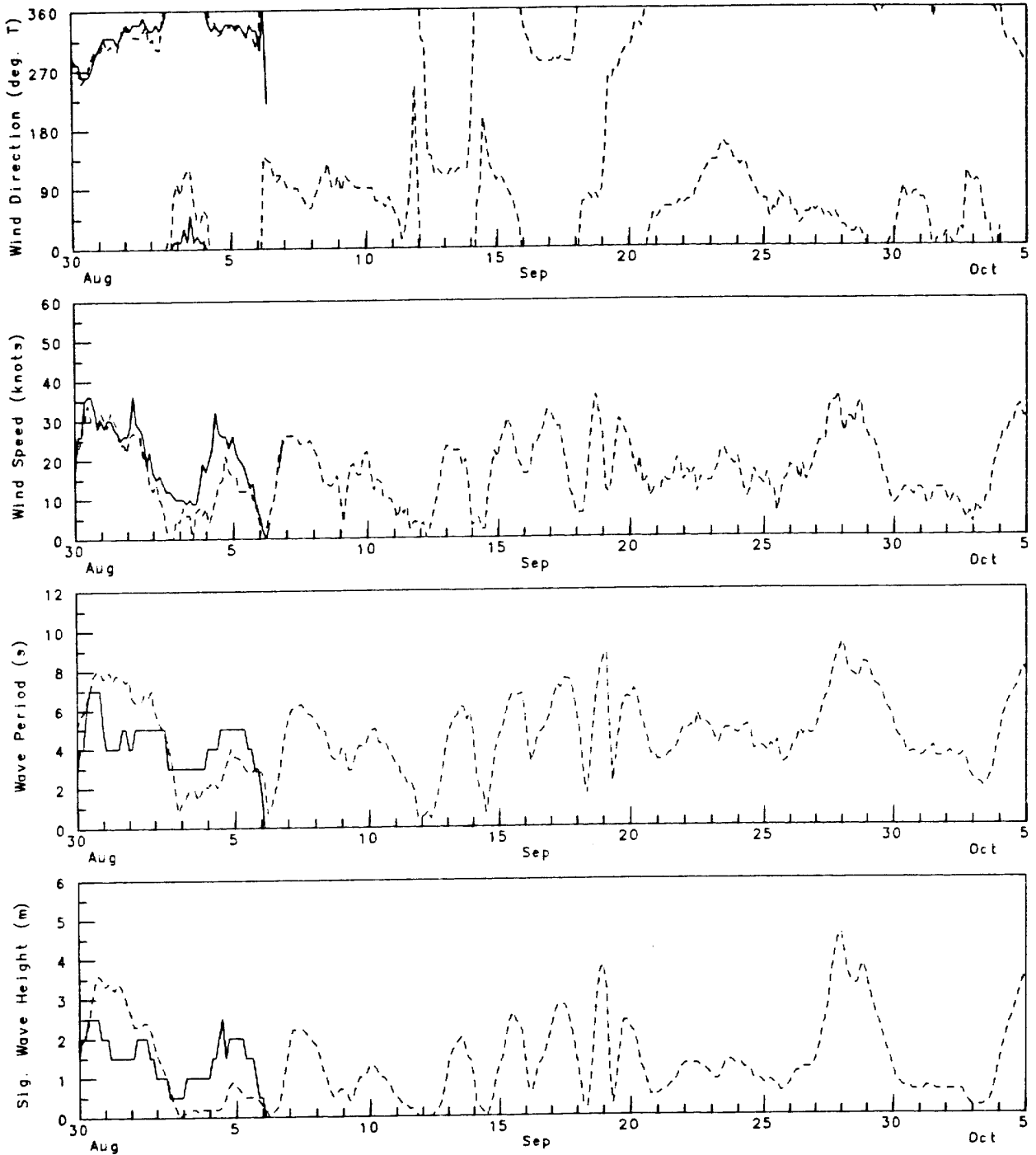


Figure 5.2a (continued)

BEAUFORT WAVE MODEL COMPARISON

5-9

Site 2 - Kopanoar (Explorer I)  
 July 25, 1981 to August 30, 1981

----- Waverider  
 - - - - - Model Estimates  
 \_\_\_\_\_ Observed (Dome)

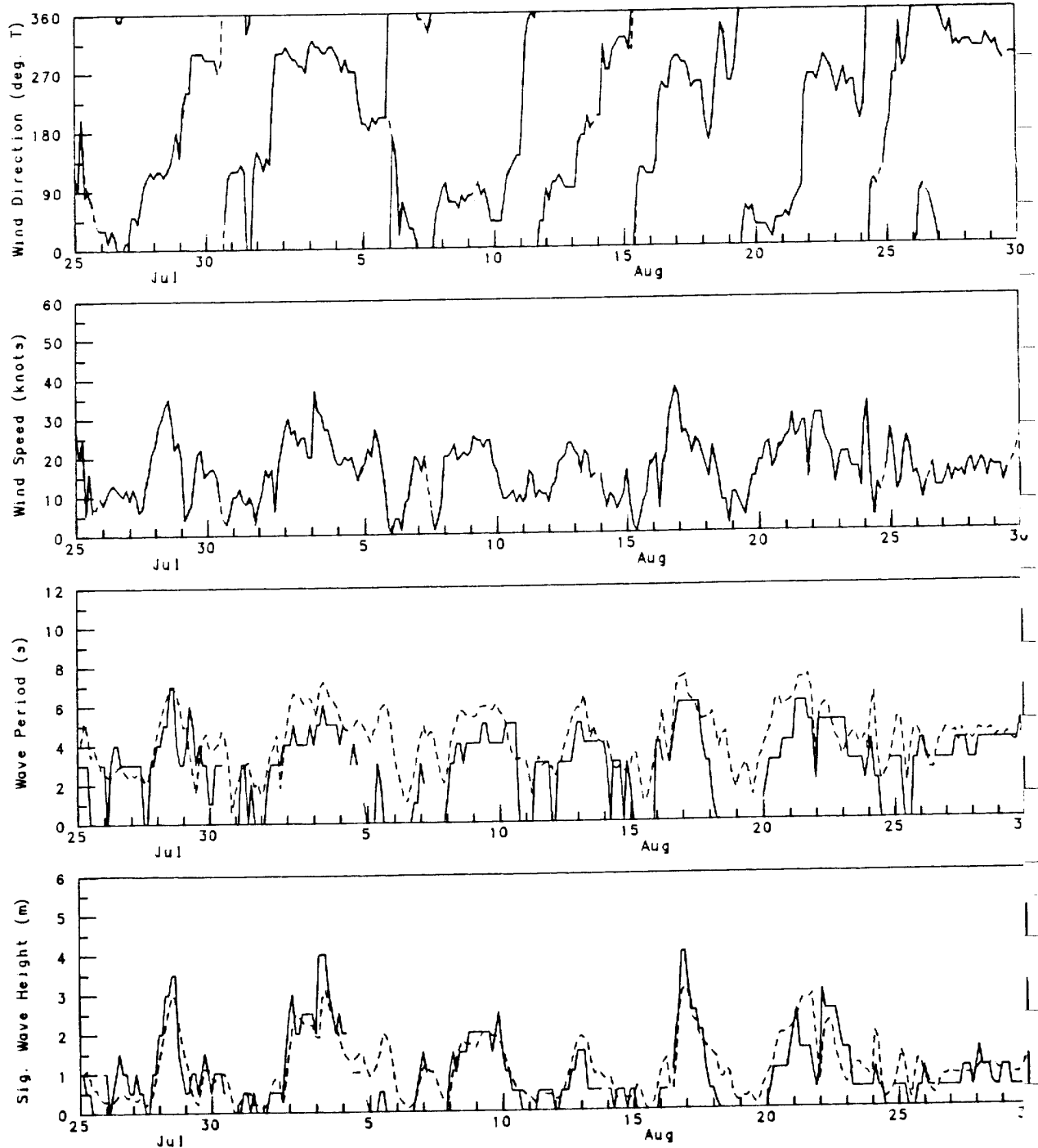


Figure 5.2b: Site 2

### BEAUFORT WAVE MODEL COMPARISON

Site 2 - Kopanoar (Explorer I)  
August 30, 1981 to October 5, 1981

----- Waverider  
- - - - - Model Estimates  
\_\_\_\_\_ Observed (Dome)

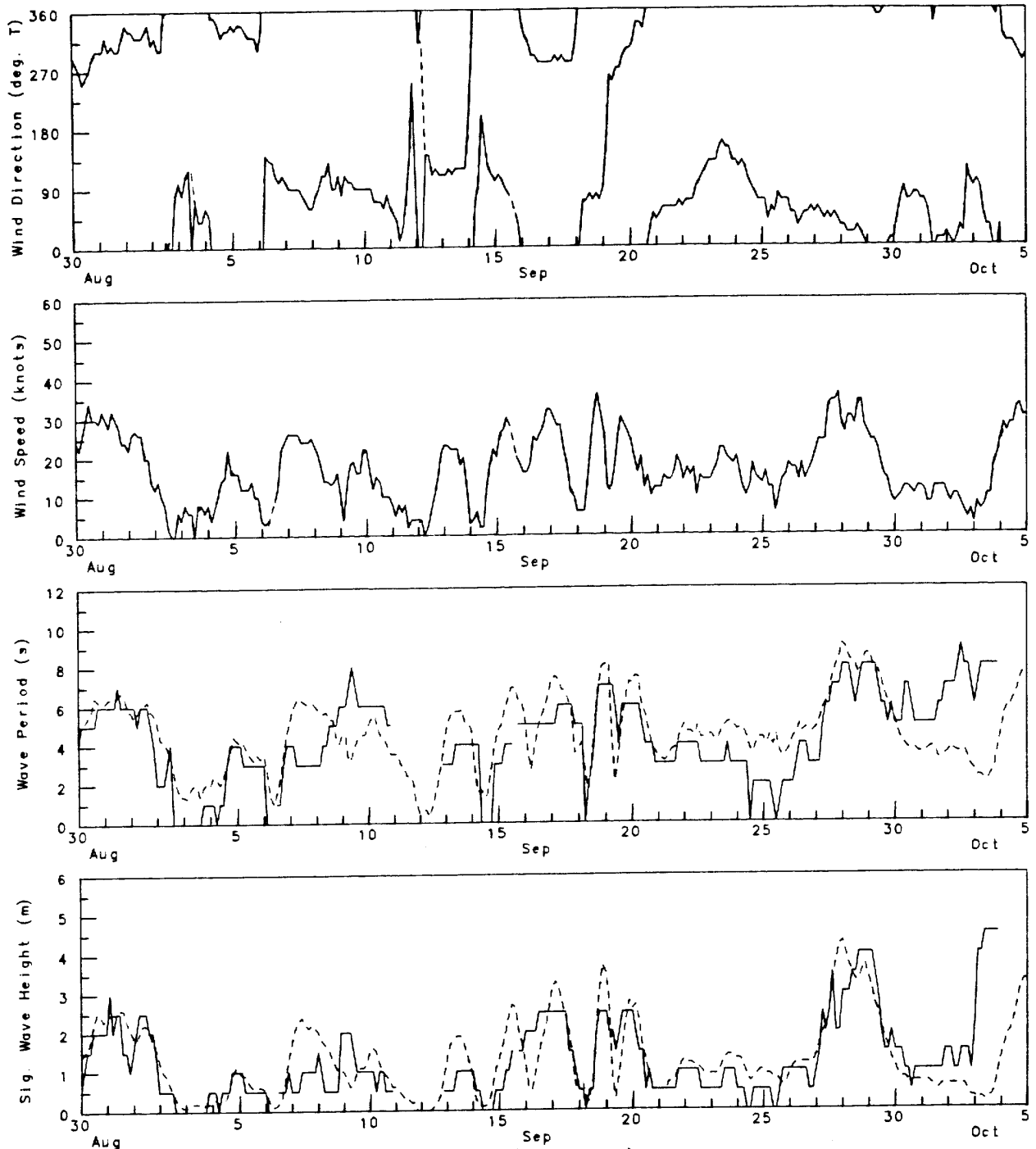


Figure 5.2b (continued)

BEAUFORT WAVE MODEL COMPARISON

Site 3 - Issungnak (Explorer II)  
 July 25, 1981 to August 30, 1981

..... Waverider  
 - - - - - Model Estimates  
 \_\_\_\_\_ Observed (Dome)

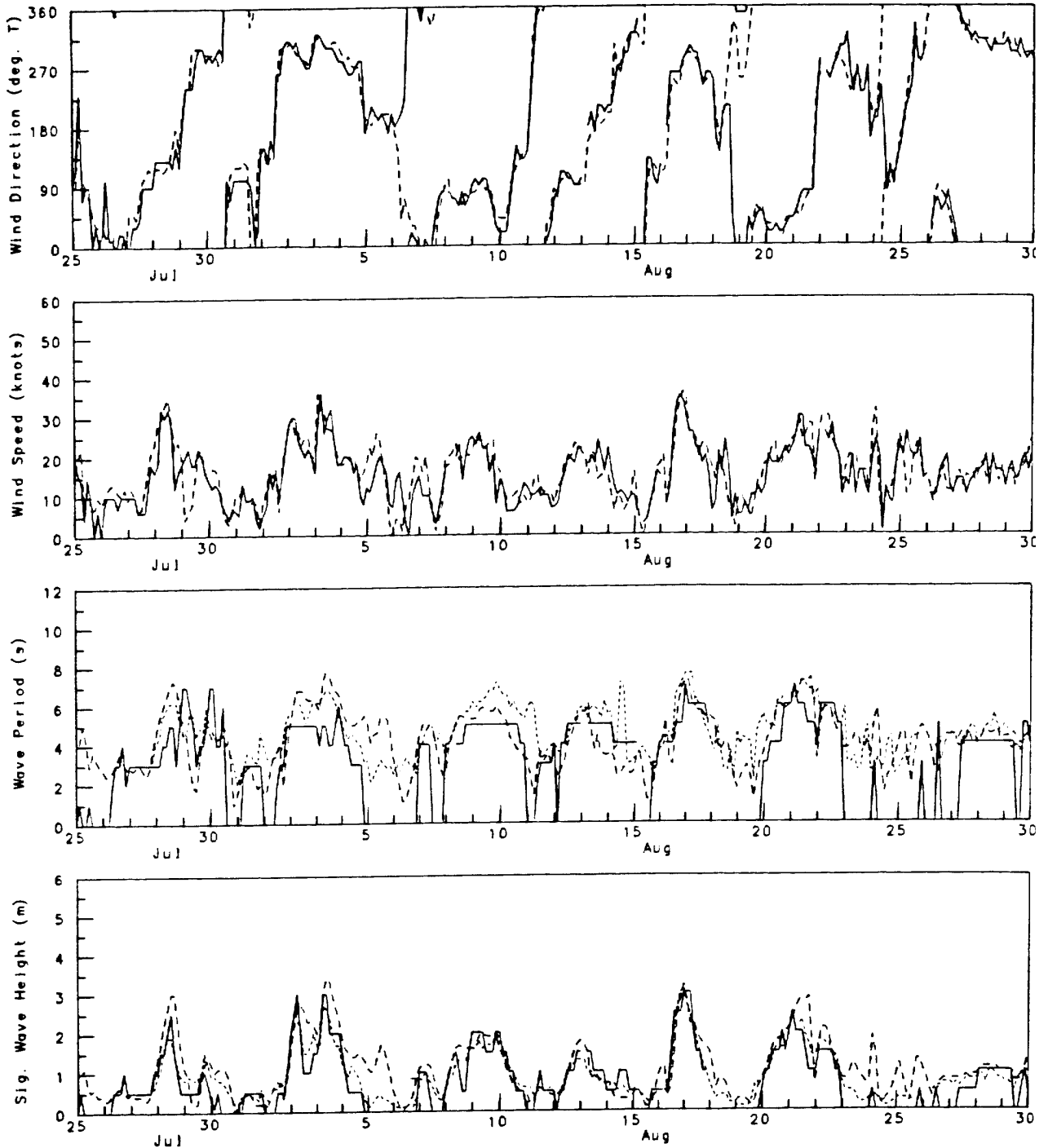


Figure 5.2c: Site 3

### BEAUFORT WAVE MODEL COMPARISON

Site 3 - Issungnak (Explorer II)  
August 30, 1981 to October 5, 1981

..... Waverider  
- - - - - Model Estimates  
————— Observed (Dome)

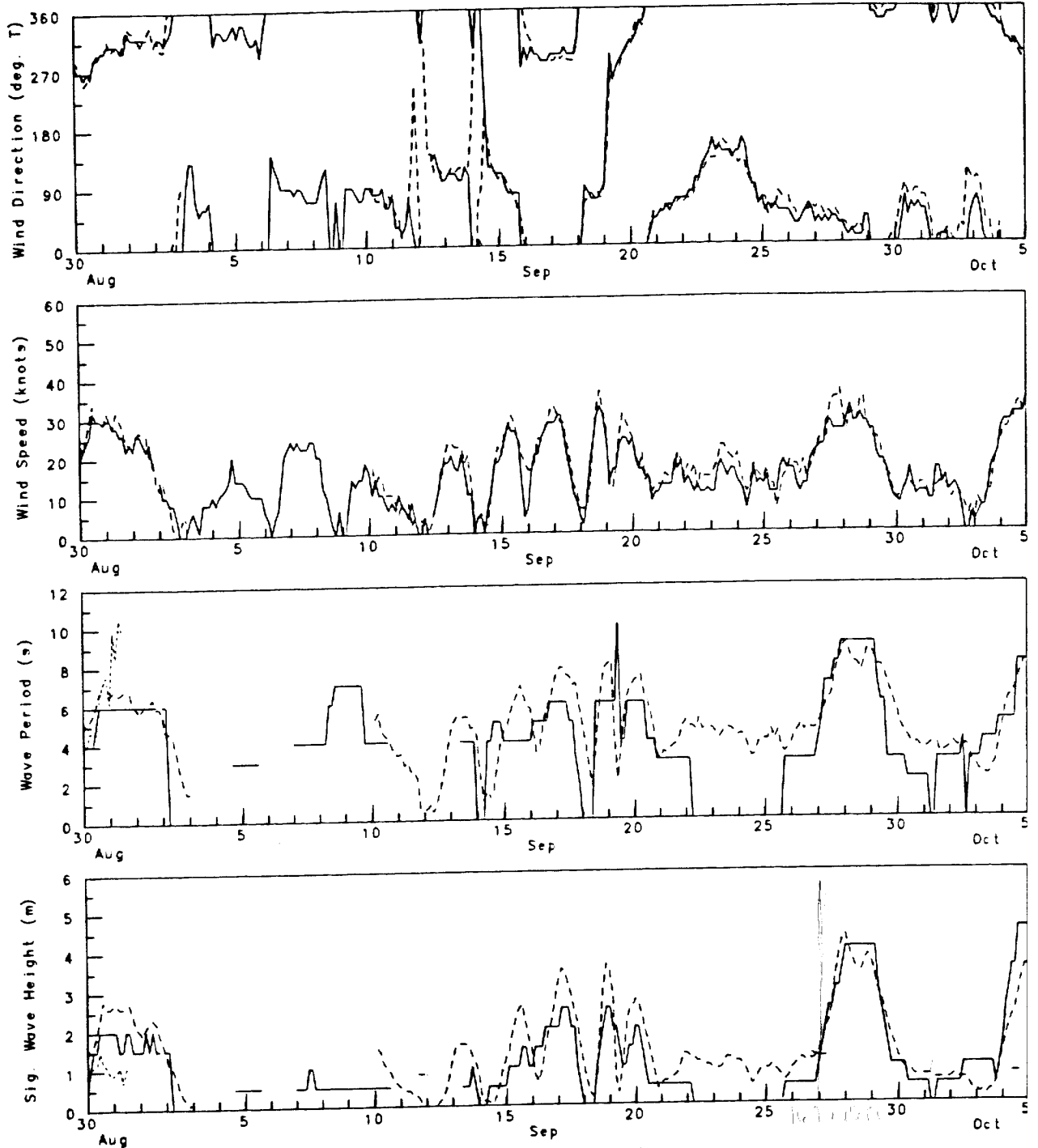


Figure 5.2c (continued)

### BEAUFORT WAVE MODEL COMPARISON

Site 4 - Kookoak (Explorer III)  
July 25, 1981 to August 30, 1981

----- Waverider  
- - - - - Model Estimates  
\_\_\_\_\_ Observed (Dome)

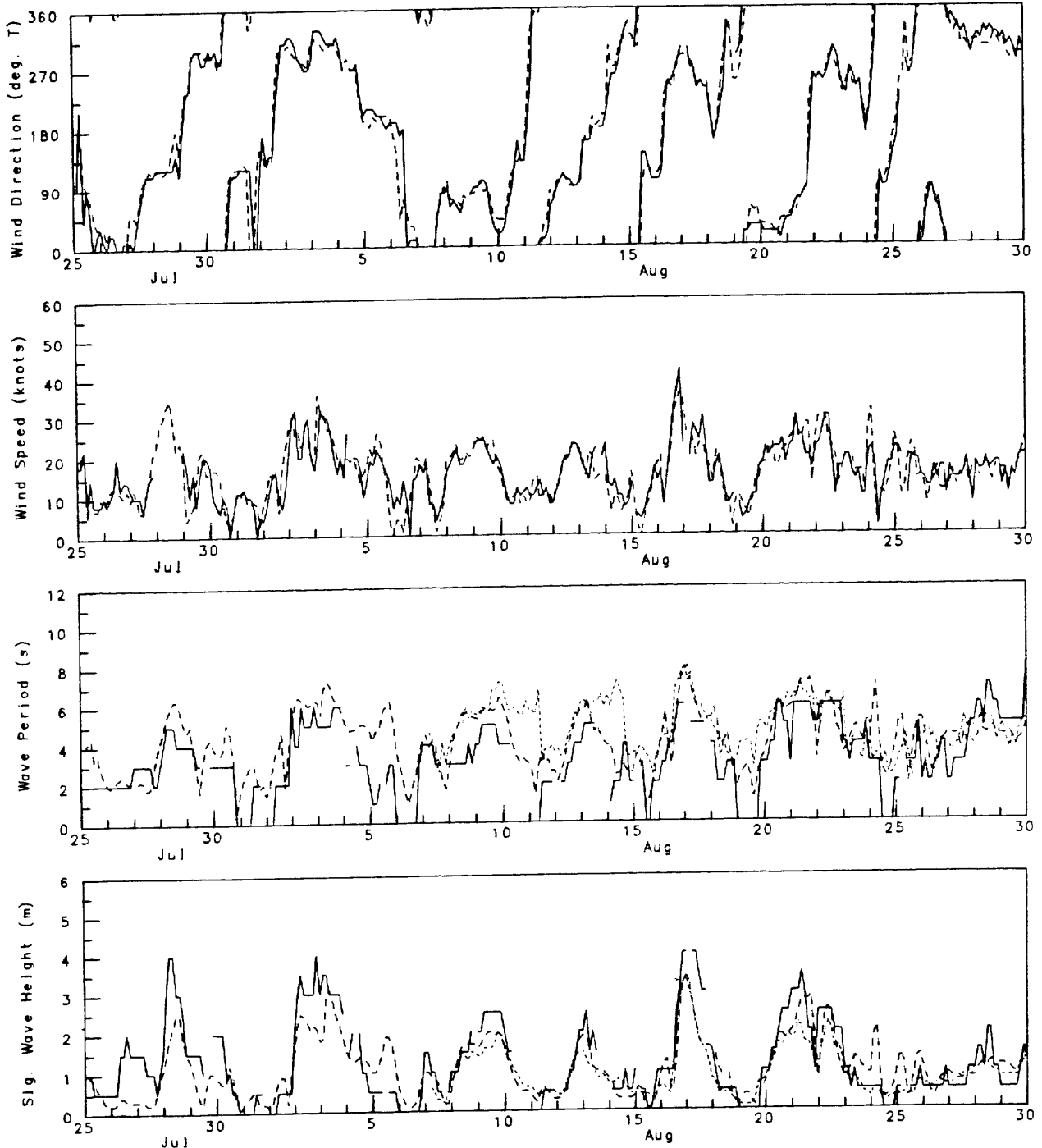


Figure 5.2d: Site 4

### BEAUFORT WAVE MODEL COMPARISON

5-14

Site 4 - Kookoak (Explorer III)  
August 30, 1981 to October 5, 1981

..... Waverider  
- - - - Model Estimates  
———— Observed (Dome)

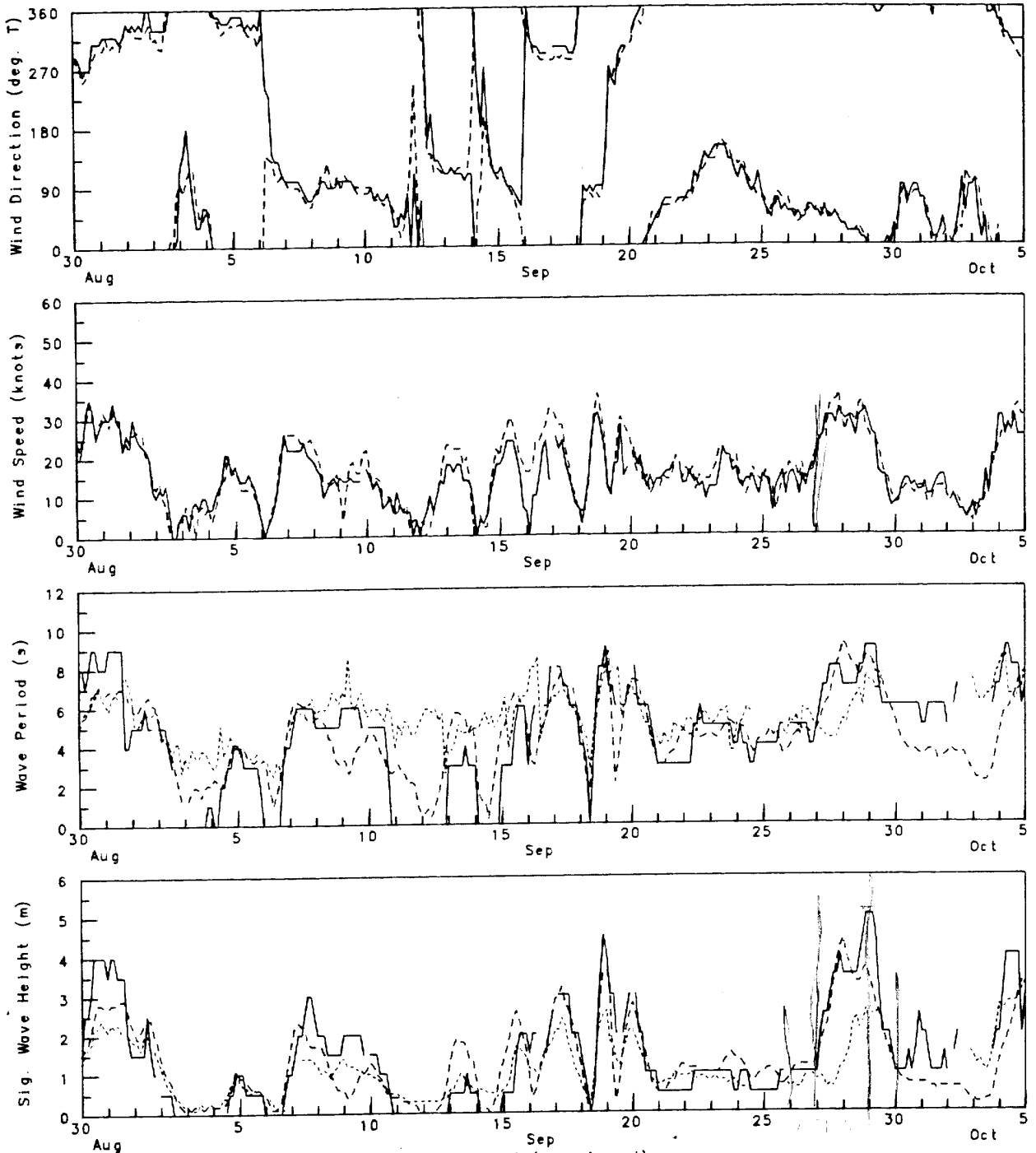


Figure 5.2d (continued)

5-15

BEAUFORT WAVE MODEL COMPARISON

Site 5 - Orvilruk (Explorer IV)  
 August 30, 1981 to October 5, 1981

..... Waverider  
 - - - - - Model Estimates  
 \_\_\_\_\_ Observed (Dome)

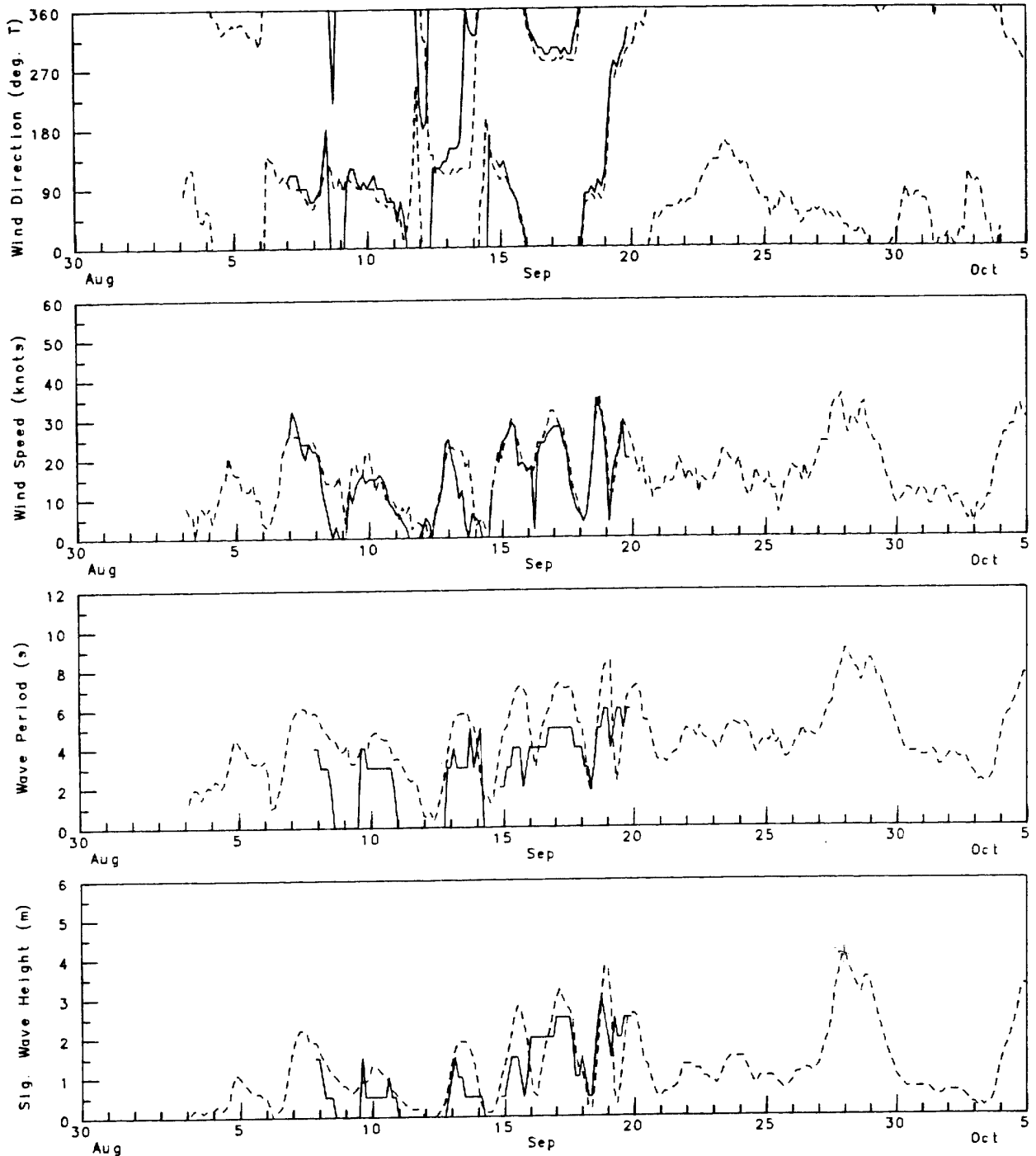


Figure 5.2e: Site 5

BEAUFORT WAVE MODEL COMPARISON

Site 6 - Kenalook (Explorer IV)  
 August 30, 1981 to October 5, 1981

..... Waverider  
 - - - - - Model Estimates  
 \_\_\_\_\_ Observed (Dome)

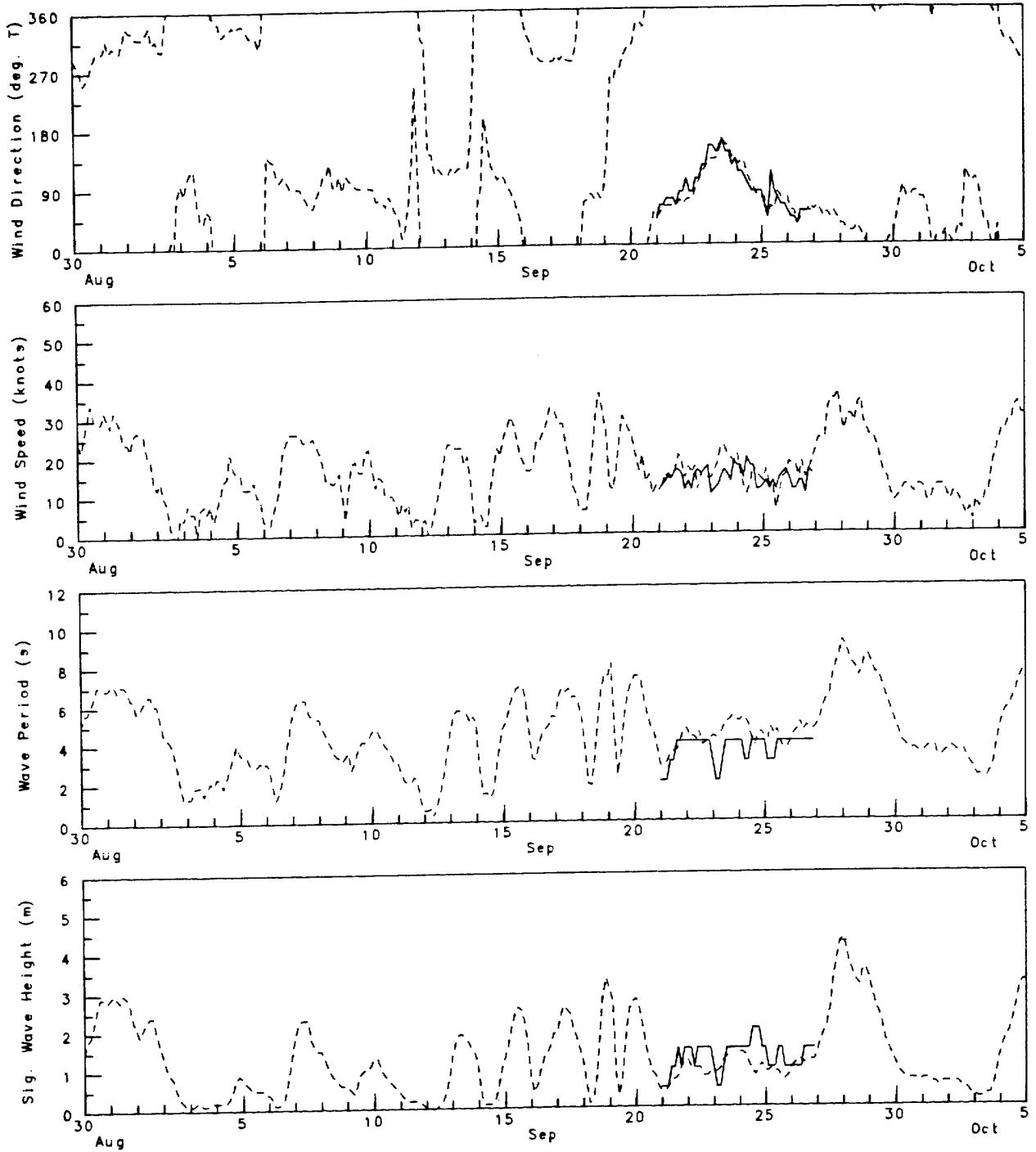


Figure 5.2f: Site 6

### BEAUFORT WAVE MODEL COMPARISON

Site 7 - Irkoluk (Explorer IV)  
August 30, 1981 to October 5, 1981

----- Waverider  
- - - - - Model Estimates  
\_\_\_\_\_ Observed (Dome)

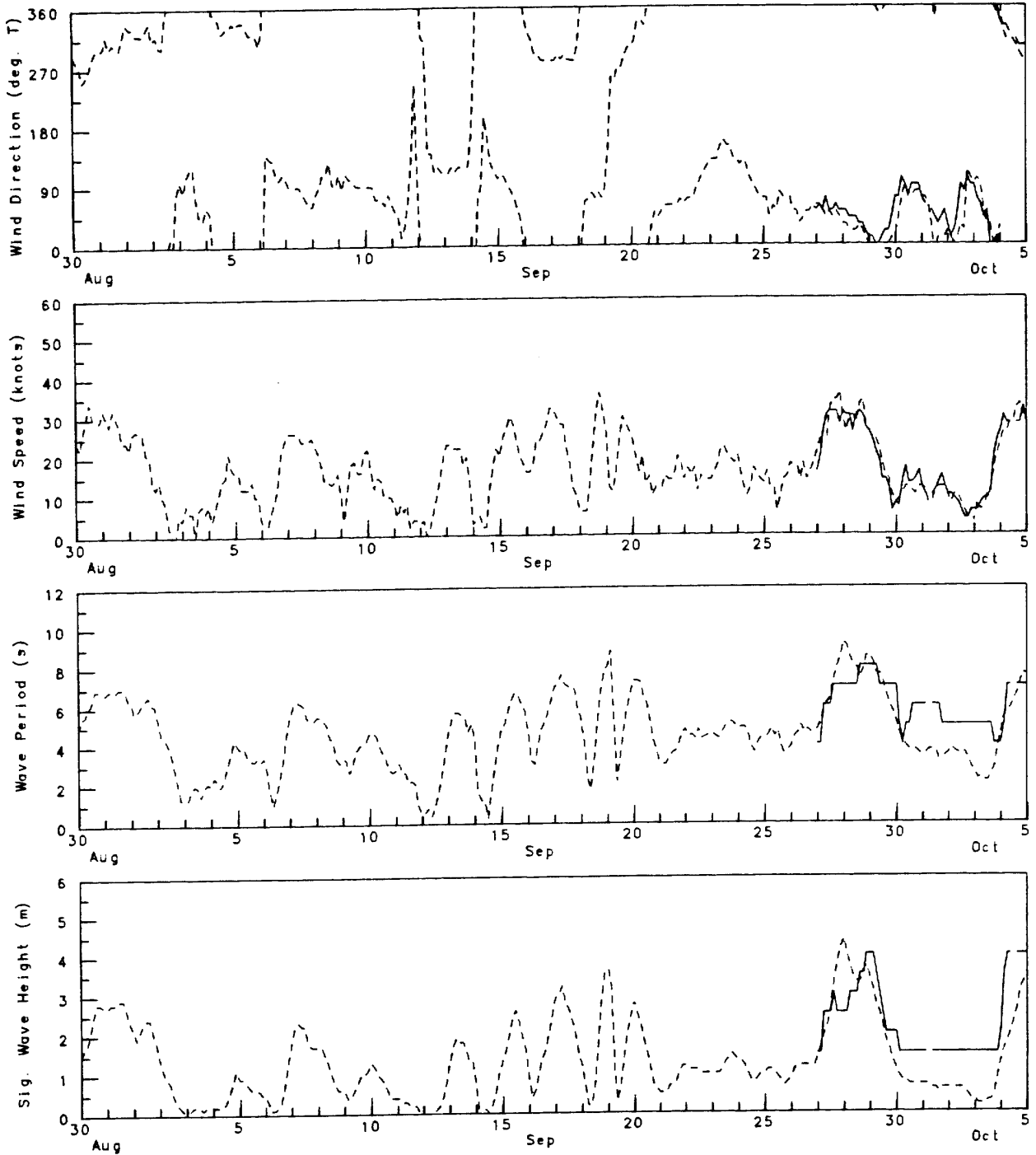


Figure 5.2g: Site 7

BEAUFORT WAVE MODEL - BSWM2

Site 1 - Kilannak (Explorer IV)  
July 25, 1981 to October 5, 1981

Number of Points: 274  
Correlation Coefficient: 0.628

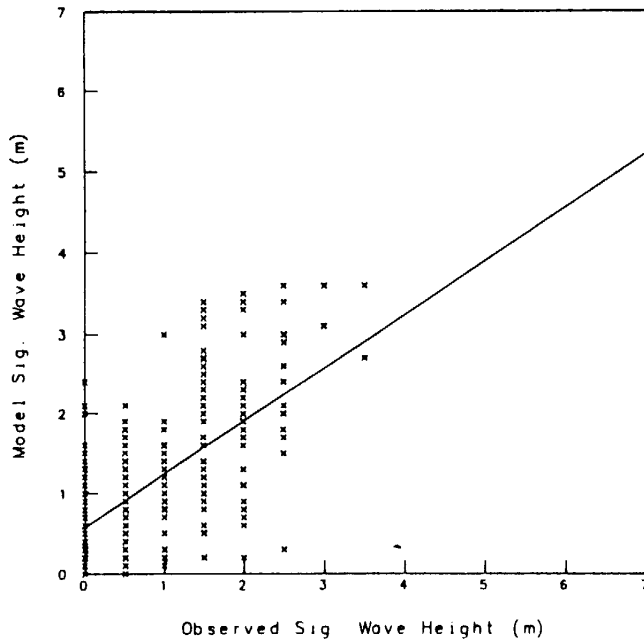


Figure 5.3a : Site 1

BEAUFORT WAVE MODEL - BSWM2

Site 1 - Kilannak (Explorer IV)  
July 25, 1981 to October 5, 1981

Number of Points: 57  
Correlation Coefficient: 0.560

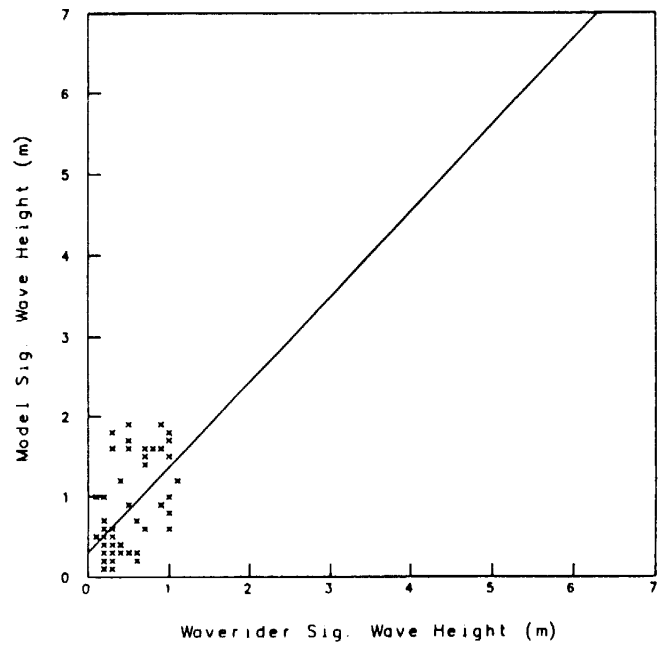
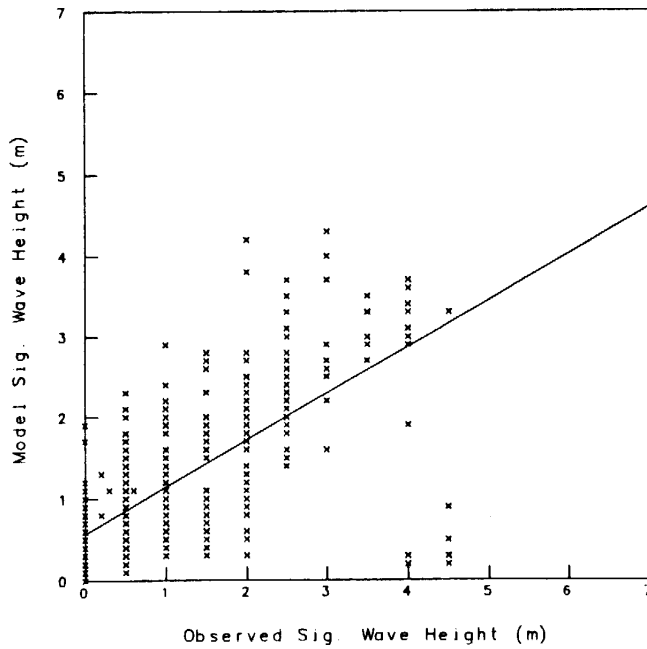


Figure 5.4a : Site 1

BEAUFORT WAVE MODEL – BSWM2

Site 2 – Kopanoar (Explorer I)  
July 25, 1981 to October 5, 1981

Number of Points: 533  
Correlation Coefficient: 0.675



BEAUFORT WAVE MODEL – BSWM2

Site 7 – Irkaluk (Explorer IV)  
July 25, 1981 to October 5, 1981

Number of Points: 63  
Correlation Coefficient: 0.794

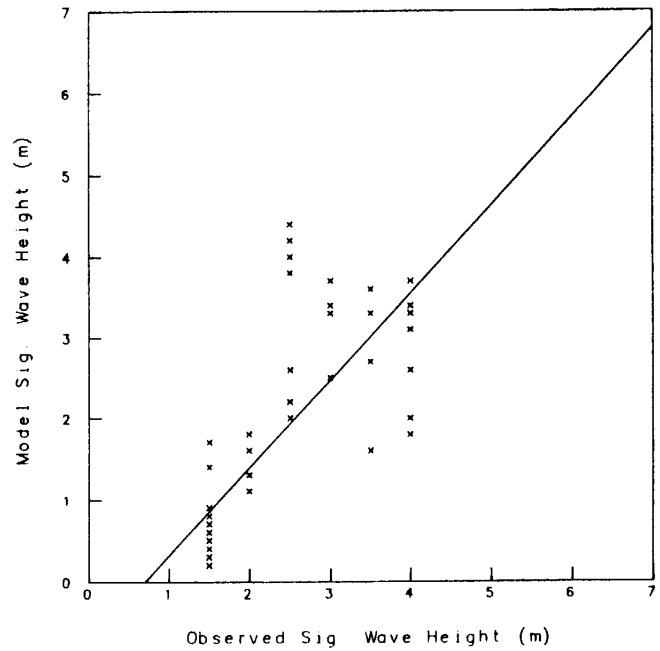


Figure 5.3b: Site 2 and Site 7

BEAUFORT WAVE MODEL - BSWM2

Site 3 - Issungnak (Explorer II)  
July 25, 1981 to October 5, 1981

Number of Points: 494  
Correlation Coefficient: 0.828

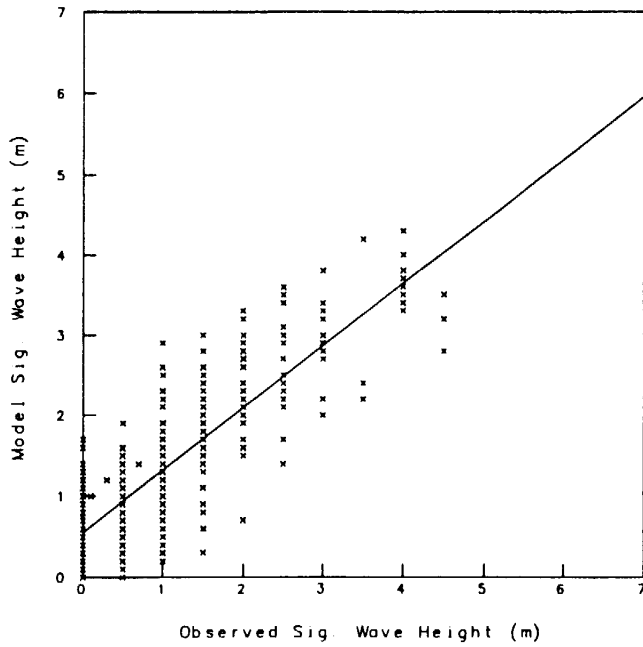


Figure 5.3c : Site 3

BEAUFORT WAVE MODEL - BSWM2

Site 3 - Issungnak (Explorer II)  
July 25, 1981 to October 5, 1981

Number of Points: 267  
Correlation Coefficient: 0.821

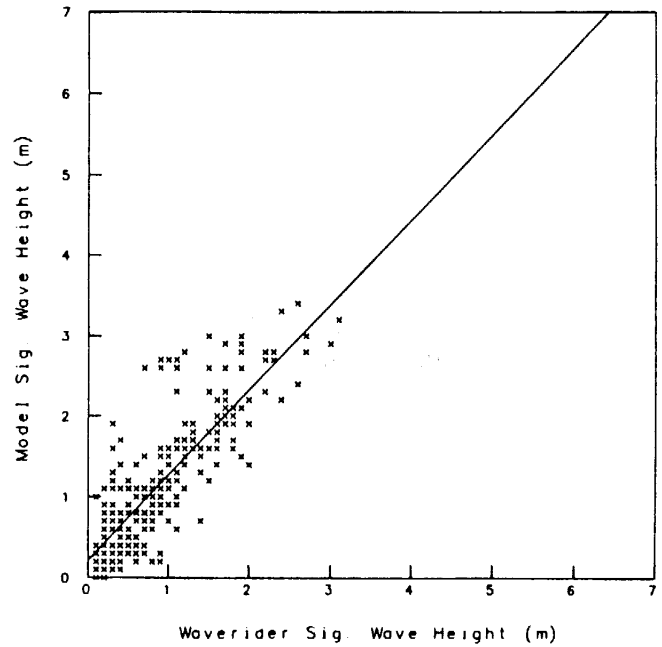


Figure 5.4b : Site 3

BEAUFORT WAVE MODEL - BSWM2

Site 4 - Koakoak (Explorer III)  
July 25, 1981 to October 5, 1981

Number of Points: 529  
Correlation Coefficient: 0.820

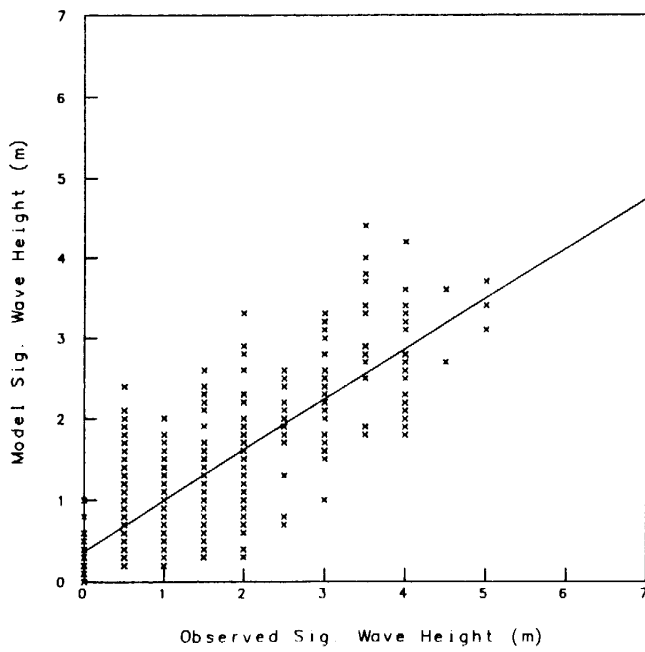


Figure 5.3d : Site 4

BEAUFORT WAVE MODEL - BSWM2

Site 4 - Koakoak (Explorer III)  
July 25, 1981 to October 5, 1981

Number of Points: 433  
Correlation Coefficient: 0.788

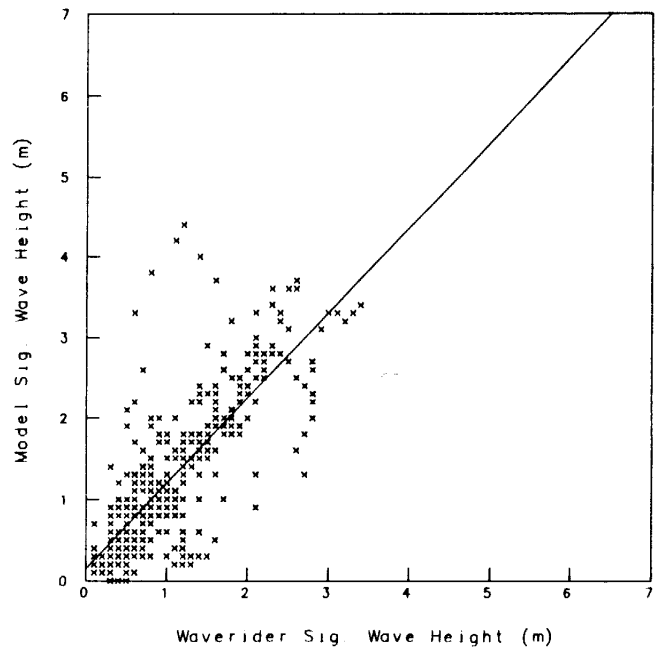


Figure 5.4c : Site 4

BEAUFORT WAVE MODEL - BSWM2  
Site 5 - Orvilruk (Explorer IV)  
July 25, 1981 to October 5, 1981  
Number of Points: 96  
Correlation Coefficient: 0.714

BEAUFORT WAVE MODEL - BSWM2  
Site 6 - Kenalook (Explorer IV)  
July 25, 1981 to October 5, 1981  
Number of Points: 48  
Correlation Coefficient: 0.432

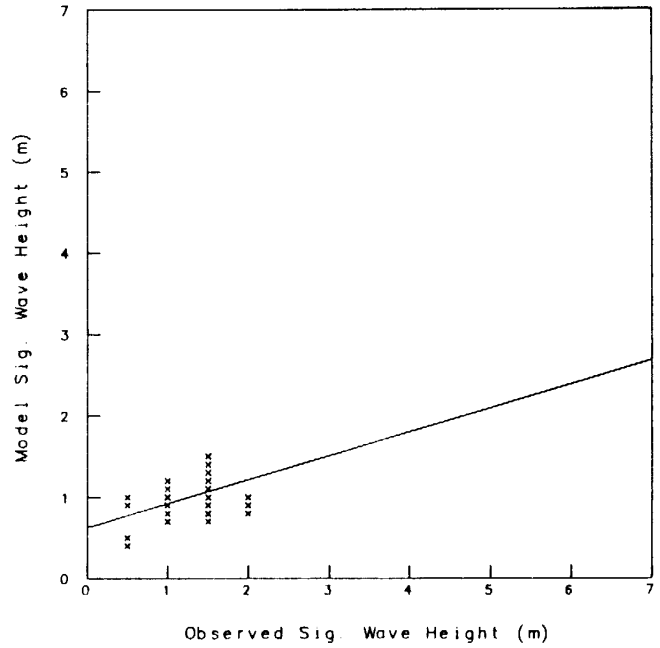
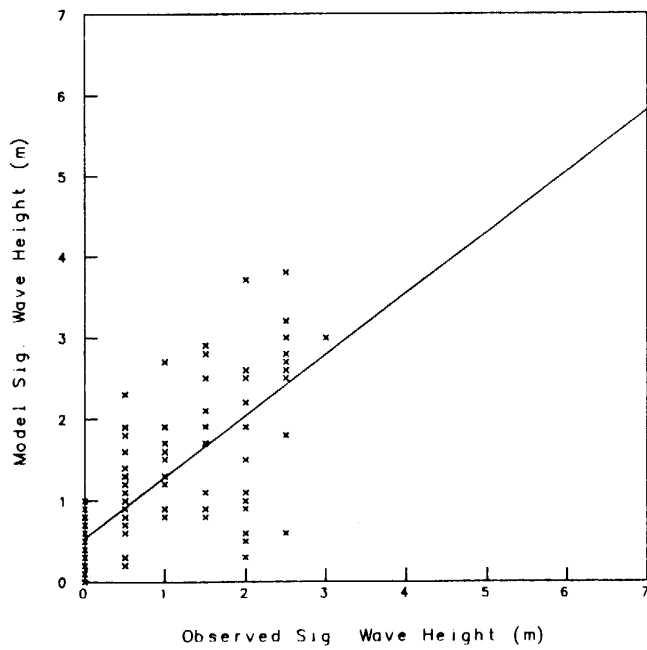


Figure 5.3e: Site 5 and Site 6

### 5.1.2 1981 Storm Events

Four storm events for selected from the 1981 data sets as follows:

Storm 1; July 31 to August 5, 1981

Storm 2; August 14 to August 19, 1981

Storm 3; August 28 to September 3, 1981

Storm 4; September 25 to October 1, 1981

The Figures 5.2 a-g illustrate that in general the storm events are predicted quite well in terms of both magnitude and time of occurrence of the peak values. The exception of course is at Site 1 where a time lag is apparent as previously discussed. The storm events will be briefly discussed below with error statistics for the storm periods presented for Sites 2, 3 and 4. Model results are compared with waverider buoy data unless otherwise indicated.

#### Storm 1, July 31 to August 5, 1981

Storm 1 rapidly developed from a situation of relatively calm easterly winds into a strong but variable westerly flow. The rapid increase in wind speed is correspondingly seen in the rapid increase in wave variables. The statistics calculated for this period are given in Table 5.2 which shows that wave field was modelled extremely well.

**Table 5.2 Evaluation Statistics; Storm 1**

#### a) Significant Wave Height

Site	Error Statistics			Regression Parameters			# of Points	$\sigma_x$ (m)	$\sigma_y$ (m)
	Bias (m)	RMSE (m)	SI %	Intercept Slope (m)		r			
2*	-0.10	0.58	40	0.65	0.40	0.90	39	1.24	0.90
3	0.33	0.54	48	1.24	0.05	0.92	39	0.74	1.00
4*	-0.25	0.67	41	0.61	0.38	0.93	38	1.34	0.88

#### b) Wave Period

Site	Error Statistics			Regression Parameters			# of Points	$\sigma_x$ (s)	$\sigma_y$ (s)
	Bias (s)	RMSE (s)	SI %	Intercept Slope (s)		r			
2*	1.45	1.82	59	0.78	2.13	0.82	39	1.85	1.77
3	0.07	1.14	24	1.15	-0.65	0.82	39	1.36	1.93
4*	1.39	1.70	53	0.75	2.18	0.88	38	2.05	1.75

\*Indicates Dome observed wave data used.

### Storm 2; August 14 to August 19, 1981

Storm 2 is very similar in its development as Storm 1 was. However, Storm 2 was shorter in duration lasting only about one day. Again the model is able to reproduce the storm event accurately, statistics are presented in Table 5.3 .

**Table 5.3 Evaluation Statistics; Storm 2**

a) Significant Wave Height

Site	Error Statistics			Regression Parameters			# of Points	$\sigma_x$ (m)	$\sigma_y$ (m)
	Bias (m)	RMSE (m)	SI %	Intercept Slope (m)		r			
2*	0.21	0.56	67	0.67	0.48	0.90	39	1.13	0.84
3	0.08	0.33	36	0.93	0.14	0.93	41	0.84	0.84
4	0.04	0.37	36	0.93	0.11	0.92	41	0.89	0.91

b) Wave Period

Site	Error Statistics			Regression Parameters			# of Points	$\sigma_x$ (s)	$\sigma_y$ (s)
	Bias (s)	RMSE (s)	SI %	Intercept Slope (s)		r			
2*	1.59	2.24	90	0.53	2.77	0.72	39	2.27	1.65
3	-0.63	1.50	33	0.68	0.85	0.64	41	1.57	1.65
4	-0.82	1.64	33	0.71	0.60	0.65	41	1.61	1.75

\*Indicates Dome observed wave data used.

The reduced correlations in wave period are attributable to the last part of the storm where model periods dropped off rapidly.

### Storm 3; August 28 to September 3, 1981

Storm 3 was also characterized by westerly winds. The direction was relatively constant during the entire storm period. Wind speed was moderate prior to the storm then rose rapidly with peak measured speeds about 25 knots. The wave model has again reproduced the wave field well as shown in the statistics in Table 5.4 .

**Table 5.4 Evaluation Statistics; Storm 3**

a) Significant Wave Height

Site	Error Statistics			Regression Parameters			# of points	$\sigma_x$ (m)	$\sigma_y$ (m)
	Bias (m)	RMSE (m)	SI %	Intercept Slope (m)		r			
2*	0.23	0.43	35	0.83	0.44	0.89	48	0.80	0.74

3*	0.41	0.55	48	1.02	0.39	0.89	47	0.67	0.77
4	0.25	0.34	26	1.28	-0.13	0.98	48	0.63	0.82
b)	Wave Period								
	(s)	(s)		(s)				(s)	(s)
2*	0.58	1.00	23	0.68	1.96	0.89	49	1.74	1.32
3*	0.86	1.58	37	0.49	3.03	0.80	47	2.11	1.29
4	-0-17	0.74	14	1.16	-1.02	0.87	48	1.09	1.45

\*Indicates Dome observed wave data used

#### **Storm 4; September 25 to October 1, 1981**

Storm 4 differs from the previous 3 events in that the wind is generally northerly. Error statistics, all based on Dome observations, for this event, given in Table 5.5, again indicate good agreement between model and observed wave variables.

**Table 5.5 Evaluation Statistics; Storm 4**

#### a) Significant Wave Height

Site	Error Statistics			Regression Parameters			# of points	$\sigma_x$ (m)	$\sigma_y$ (m)
	Bias (m)	RMSE (m)	SI %	Intercept Slope (m)		r			
2*	0.09	0.64	36	0.85	0.36	0.86	49	1.20	1.18
3*	0.25	0.51	31	0.79	0.60	0.97	49	1.47	1.21
4*	-0.23	0.69	32	0.74	0.33	0.88	48	1.39	1.17

#### b) Wave Period

	(s)	(s)		(s)				(s)	(s)
2*	0.71	1.62	32	0.62	2.59	0.77	49	2.28	1.84
3*	1.15	2.02	44	0.53	3.28	0.90	49	3.10	1.84
4*	-0-36	1.18	19	0.94	-0.01	0.78	48	1.48	1.79

\*Indicates Dome observed wave data used

A partial waverider record is available for Site 4 and it shows a definite lag in development behind the model and observed variables. An explanation for this discrepancy is not obvious as yet. Another concern on the data quality for this period is seen in comparing the Dome observed data for Sites 2, 3 and 4. The wave height observations at Sites 2 and 4 are consistently higher than at Site 3 for the storm events. This may suggest a bias exists between different observers.

The storm specific error statistics have indicated that the model performs accurately during high wind events. The enhanced ability

to reproduce the wave field during the storms may in part be due to the fact that winds are better resolved for higher wind events.

## 5.2 1982 Storm Events

The data availability for the 1982 drilling season is illustrated in Table 3.1b with site locations defined in Figure 3.3b . (Note: there are 2 observation stations located near Site 2, Tarsiut Island and Kiggavik H-32). Although the spatial coverage is small, the temporal coverage is quite good. The forcing for the model is provided by assuming a homogeneous wind field, a consequence of the proximity of the data sites. Site 4 winds were selected based on several factors including quality of data, length of the record, few gaps and also its central location. The wind was measured at an anemometer height of 65 metres. Unfortunately, the temperature record was incomplete so neutralizing the wind was not performed for Storm 5. The boundary layer effects were considered for Storms 6, 7 and 8 with the winds transformed to their effective 10 m value. The model was spun-up from rest. Care was taken to provide sufficient time prior to the storm event so that initial spin-up is achieved. The storm events are defined as follows:

Storm 5; July 27 - August 1, 1982

Storm 6; August 12 - 17, 1982

Storm 7; August 18 - 23, 1982

Storm 8; September 18 - 23, 1982

and will be discussed below.

### Storm 5; July 27 to August 1, 1982

Storm 5 is characterized by a rapid rise in wind speed from 10 to 40 knots in about 6 hrs, followed by a gradual decline in speeds for the next 2 days. The winds were westerly for the storm event then shifting to easterly.

The time series plots for the sites at which wave data was available are illustrated in Figures 5.5 a-c. Unfortunately, the observations over this period are quite sparse. Site 6 waverider data provides the best information for comparison. As is obvious, the model overpredicts the peak wave heights, a consequence of not reducing the winds to the 10 m level. The wave period is also overestimated, however, not as much as wave height. The statistics, calculated only for Site 6. of waverider versus model results are listed in Table 5.6 and the scatter plot of wave heights is shown in Figure 5.6 .

**Table 5.6 Evaluation Statistics; Storm 5**

a) Significant Wave Height

Site	Error Statistics			Regression Parameters			# of Points	$\sigma_x$ (m)	$\sigma_y$ (m)
	Bias (m)	RMSE (m)	SI %	Intercept Slope (m)		r			
6	0.84	1.25	90	2.05	-0.62	0.95	39	0.73	1.59

b) Wave Period

Site	Error Statistics			Regression Parameters			# of Points	$\sigma_x$ (s)	$\sigma_y$ (s)
	Bias (s)	RMSE (s)	SI %	Intercept Slope (s)		r			
6	0.80	1.39	24	1.41	-1.50	0.89	36	1.39	2.19

The correlations are remarkably high, however, the model is overpredicting consistently.

A reduction in predicted wave parameters would undoubtedly occur had the winds been converted to 10 m neutral values. Nevertheless, the high correlation suggests that the boundary layer effects would not alter the time series of wind speed radically. The similarity of the winds at each measurement site implies that for this storm, event the assumption of spatial homogeneity of the wind field is acceptable.

**Storm 6; August 12 to August 17, 1982**

A constant easterly wind (measured at about 20 knots) prevailed at the onset of Storm 2. The winds then increased in magnitude to about 30 knots while the wind direction rotated in a clockwise fashion.

The results of the Storm 6 simulations is illustrated in Figures 5.7 a-e. Temperature data was available for this period and the effective neutral 10 m wind was determined. The reduction in wind speeds is dramatic, which is the case for stable atmospheric conditions, peak speeds are reduced by about 40%. The data coverage is much better for this period and error statistics for Sites 2, 3 and 6, having complete waverider records is shown in Table 5.7 .

**Table 5.7 Evaluation Statistics; Storm 6**

a) Significant Wave Height

Site	Error Statistics			Regression Parameters			# of Points	$\sigma_x$ (m)	$\sigma_y$ (m)
	Bias (m)	RMSE (m)	SI %	Intercept Slope (m)		r			
2	0.01	0.53	68	1.61	-0.47	0.78	40	0.37	0.77

3	-0.08	0.59	73	1.40	-0.14	0.56	39	0.28	0.70
6	-0.01	0.48	57	1.63	-0.55	0.86	38	0.41	0.78

## b) Wave Period

								(s)	(s)
2	-1.34	2.48	52	0.08	3.06	0.04	40	1.08	1.83
3	-1.27	2.22	49	0.31	1.86	0.18	39	0.96	1.72
6	-1.13	2.05	44	0.82	-0.28	0.37	38	0.84	1.84

The scatter plots illustrating wave height comparisons for these sites is shown in Figures 5.8 a-c. The wave heights are marginally correlated while the wave periods are apparently uncorrelated. The lack of correlation may result from several factors. The reduction of the wind appears to be too severe, at least at the beginning of the storm. The underestimation of both wave height and period during this time significantly affects the statistics. It is interesting to note that there is little structure in the waverider period estimates for the first 3 days. As well, the waverider heights show little variation for the entire storm period. The answer may lie in the fact that during the storm, when the wind speeds are largest, the wind direction was changing continuously. Therefore, the wave field could not develop fully. Another potential explanation for the initially constant measured wave periods is that this represents swell persisting from a previous storm. In fact, on August 11, 1982, a small storm did occur with wind speeds measured at 20 knots. The model, at present, does not include swell as a distinct component. The comparisons performed in the evaluation of the model suggested that swell was a negligible factor and in no way affected the wave field for more than several hours.

As mentioned previously the model was spun-up from rest. Therefore, depending on the wind conditions, the initial period of the simulation represents spin-up. For this case, the winds are so low that spin-up is achieved rapidly and no errors induced by the spin-up process are negligible. In fact, this case was run again, but starting about 12 hours earlier and no significant changes in the wave variables occurred.

An explanation for the poor performance of the model during this storm event is not apparent.

The measured winds are quite similar at all sites. However, a comparison of Site 2 and Site 4 measured winds suggests that Site 4 winds lag those at Site 2 by about 6 hours. This phase shift is perceptible in the wave height record of Site 2 where the Modelled values show such a lag behind the observations. Again, this phase shifting can degrade the statistics. The assumption of

spatial homogeneity for this storm event is poor based on these observations.

### Storm 7; August 18 to August 23, 1982

Storm 7 is dominated by westerly winds with peak measured speeds on the order of 40 knots. The time series for this storm, are illustrated in Figures 5.9 a-e. Visually the model provides very good results. Statistics for sites 3, 4, 5 and 6 are given in Table 5.8 . The statistics for Sites 5 and 6 are based on the Dome observed wave data. The scatterplots of wave heights for these sites is shown in Figures 5.10 a-d.

**Table 5.8 Evaluation Statistics; Storm 7**

a) Significant Wave Height

Site	Error Statistics			Regression Parameters			# of Points	$\sigma_x$ (m)	$\sigma_y$ (m)
	Bias (m)	RMSE (m)	SI %	Slope	Intercept (m)	r			
3	0.35	0.47	37	1.10	0.22	0.92	35	0.65	0.78
4	0.45	0.80	68	1.24	0.17	0.54	30	0.34	0.77
5*	0.21	0.54	42	0.77	0.50	0.78	39	0.75	0.75
6*	0.21	0.48	34	0.86	0.40	0.87	40	0.87	0.86

b) Wave Period

Site	Error Statistics			Regression Parameters			# of Points	$\sigma_x$ (s)	$\sigma_y$ (s)
	Bias (s)	RMSE (s)	SI %	Slope	Intercept (s)	r			
3	0.35	0.66	13	0.94	0.65	0.90	35	1.23	1.28
4	0.49	1.16	24	0.99	0.53	0.57	30	0.74	1.29
5*	0.20	1.27	26	0.68	1.79	0.40	39	0.80	1.34
6*	0.91	1.41	32	1.17	0.13	0.69	40	0.87	1.47

\*Dome observed wave information used.

The correlations indicate that this storm was generally well reproduced. The reduced correlations at Site 4 is largely a result of the deviations on August 21. The drop in the waverider variables at this time is not evident at any of the other sites. The development of the wave field as a function of fetch is easily seen in the model results (i.e. wave heights increasing from Sites 2 to 6 corresponding to the fetch defined by the westerly winds). The measured wave field correspondingly shows this tendency resulting from the relatively constant forcing. There is no significant evidence to indicate that the assumption of a homogeneous wind field is poor given the similarity of measured winds at each site.

**Storm 8; September 18 to September 23, 1982**

Storm 8 is characterized by a two day period of generally easterly winds with speeds of about 30 knots. The constancy of the forcing effectively fixes the fetch length for each station. The results of this simulation is illustrated in Figures 5.11 a-e. The development of the model wave field is almost identical for Sites 1 to 5. The observations, although highly correlated with the model results, vary in magnitude from site to site. The error statistics for Storm 8 are given in Table 5.9 which quantifies the accuracy of the predicted wave field.

**Table 5.9 Evaluation Statistics; Storm 8**

## a) Significant Wave Height

Site	Error Statistics			Regression Parameters			# of Points	$\sigma_x$ (m)	$\sigma_y$ (m)
	Bias (m)	RMSE (m)	SI %	Slope	Intercept (m)	r			
1	0.35	0.83	50	1.73	-0.87	0.93	38	0.76	1.41
2	0.50	0.98	64	1.97	-0.97	0.92	40	0.65	1.39
3	0.69	1.12	87	2.45	-1.18	0.94	40	0.52	1.35
4	0.50	0.90	58	1.82	-0.77	0.95	40	0.73	1.41
5*	0.49	0.68	41	1.20	0.16	0.96	38	1.12	1.40

## b) Wave Period

Site	Error Statistics			Regression Parameters			# of Points	$\sigma_x$ (s)	$\sigma_y$ (s)
	Bias (s)	RMSE (s)	SI %	Slope	Intercept (s)	r			
1	-0.42	1.68	27	1.27	-2.11	0.70	38	1.23	2.25
2	-0.20	1.61	26	1.22	-1.55	0.70	40	1.25	2.19
3	0.04	1.65	29	1.11	-0.59	0.63	40	1.21	2.12
4	-0.07	1.92	32	1.02	-0.21	0.50	40	1.07	2.21
5*	1.04	1.85	37	1.41	-1.04	0.74	38	1.14	2.17

\*Indicated Dome observed data used

In this case the model consistently overpredicted the event's peak wave height as well as the peak period at all sites with the largest overprediction at sites 1, 2 and 3. This is also reflected in observed variance values and the regression slopes as expected. The scatterplots for these sites are illustrated in Figures 5.12 a-e, The changes in the measured wave field do not appear to be a result of wind variations since the measured wind speeds are virtually identical. However, there is an apparent counter-clockwise deviation in measured wind directions at sites 1, 2 and 5 (as shown in Figures 5.11 a, b and c), i.e. the

model wind directions are more easterly, therefore, larger fetch, than actual observed and hence overprediction of wave parameters. Of course, variation in boundary layer effects may result in substantial changes to the winds from site to site. Other potential causes may be topographic influences or measurement variability or effect of ice boundaries and the existence of local ice patches.

BEAUFORT WAVE MODEL COMPARISON

Storm 5 - Site 4 Irkaluk B-35 (Explorer II)  
July 27, 1982 to August 1, 1982

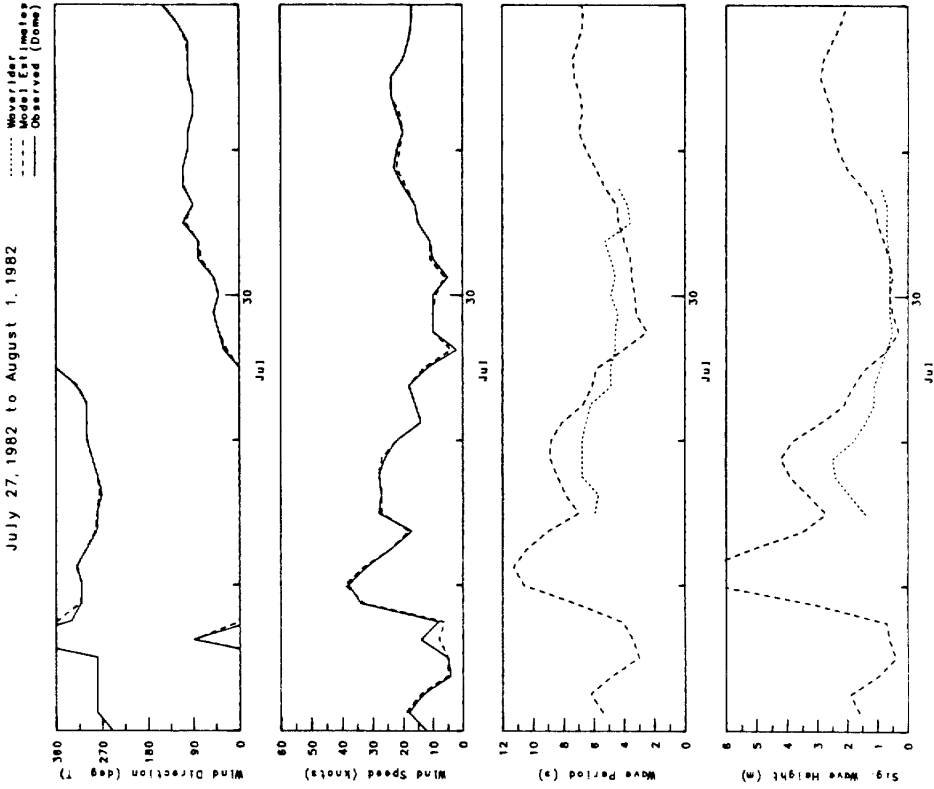


Figure 5.5b

BEAUFORT WAVE MODEL COMPARISON

Storm 5 - Site 2 Kiggavik H-32 (Explorer I)  
July 27, 1982 to August 1, 1982

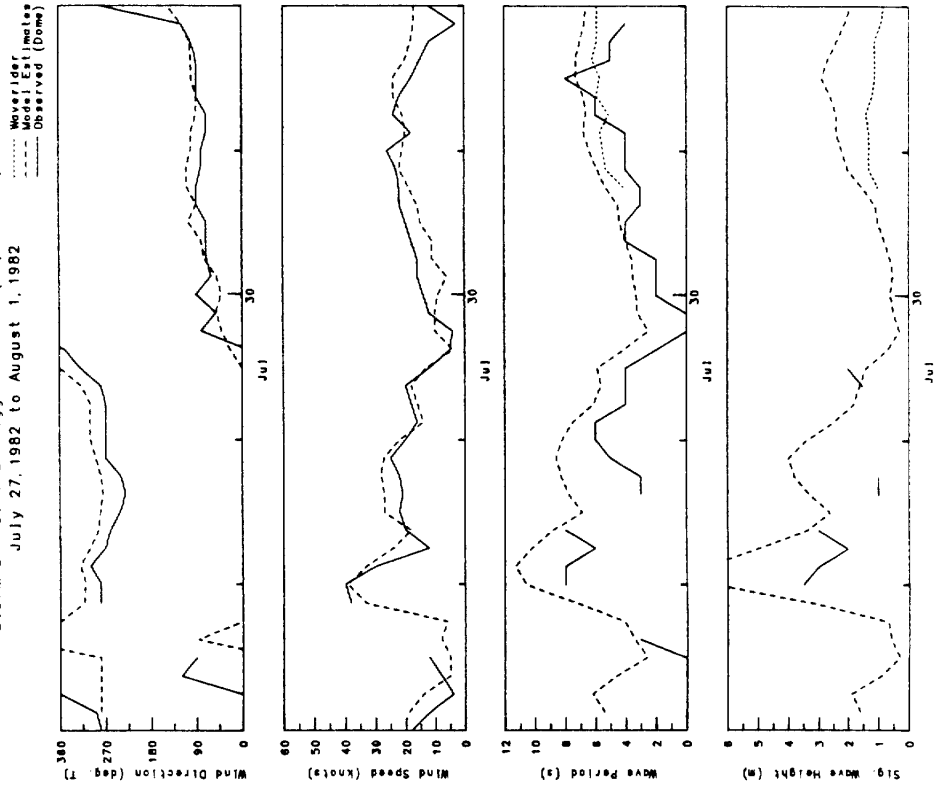


Figure 5.5a

BEAUFORT WAVE MODEL COMPARISON

Storm 5 - Site 6 Nerlerk M-98 (Explorer III)  
July 27, 1982 to August 1, 1982

Waverider  
Model Estimate  
Observed (Dome)

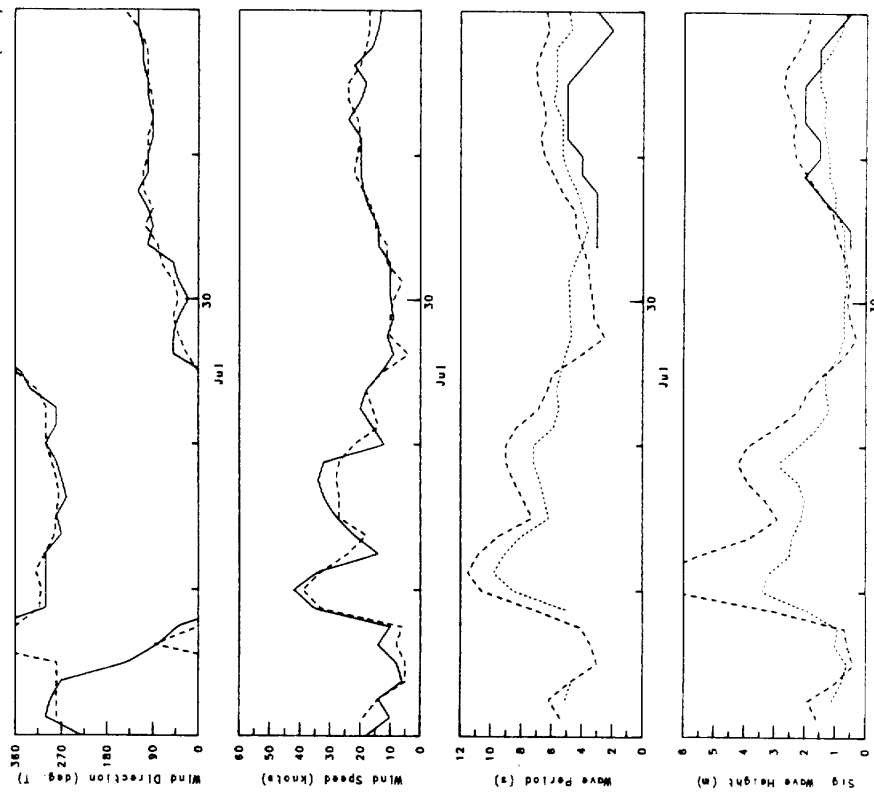


Figure 5.5c

BEAUFORT WAVE MODEL - BSWM2

Storm 5 - Site 6 Nerlerk M-98 (Explorer III)  
July 27, 1982 to August 1, 1982

Number of Points: 39  
Correlation Coefficient: 0.948

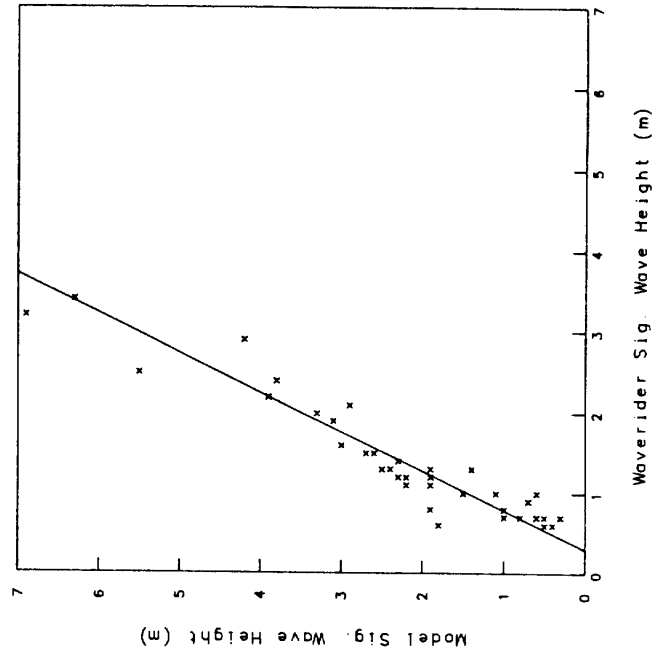
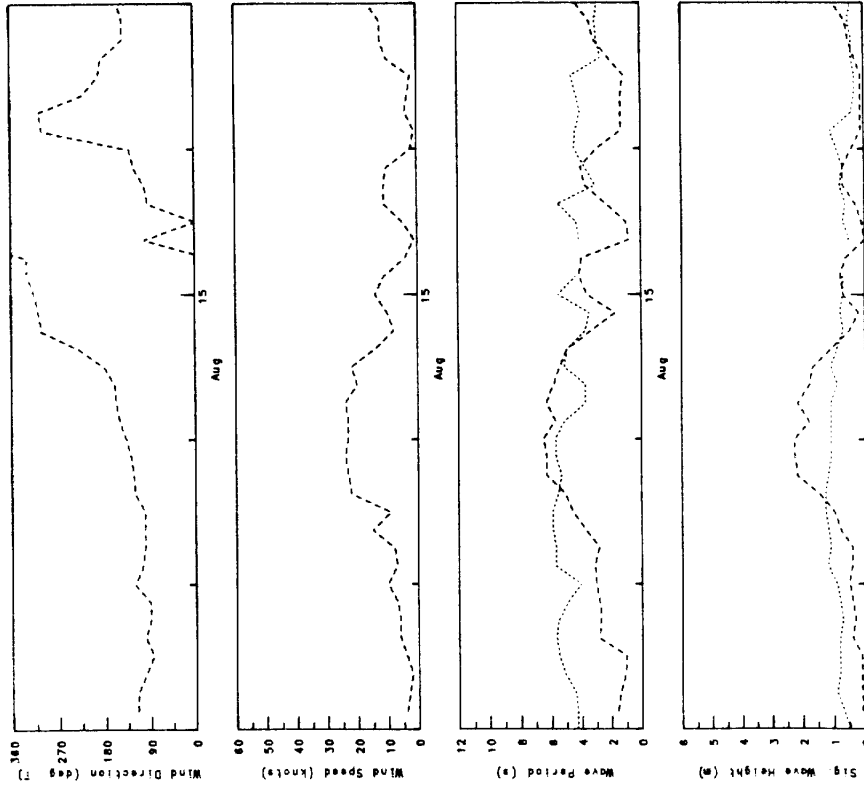


Figure 5.6

BEAUFORT WAVE MODEL COMPARISON

Storm 6 - Site 3 Itiyok Island (Esso)  
August 12, 1982 to August 17, 1982

Waverider  
Model Estimates  
Observed



5-36

Figure 5.7b

BEAUFORT WAVE MODEL COMPARISON

Storm 6 - Site 2 Kiggovik H-32 (Explorer I)  
August 12, 1982 to August 17, 1982

Waverider  
Model Estimates  
Observed (Dime)

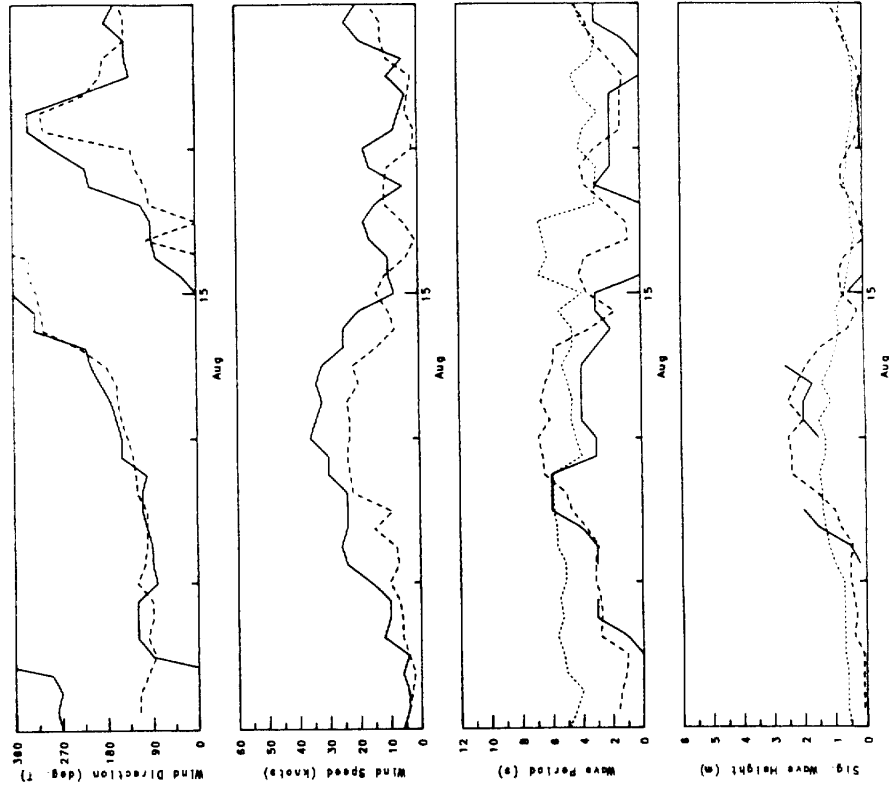
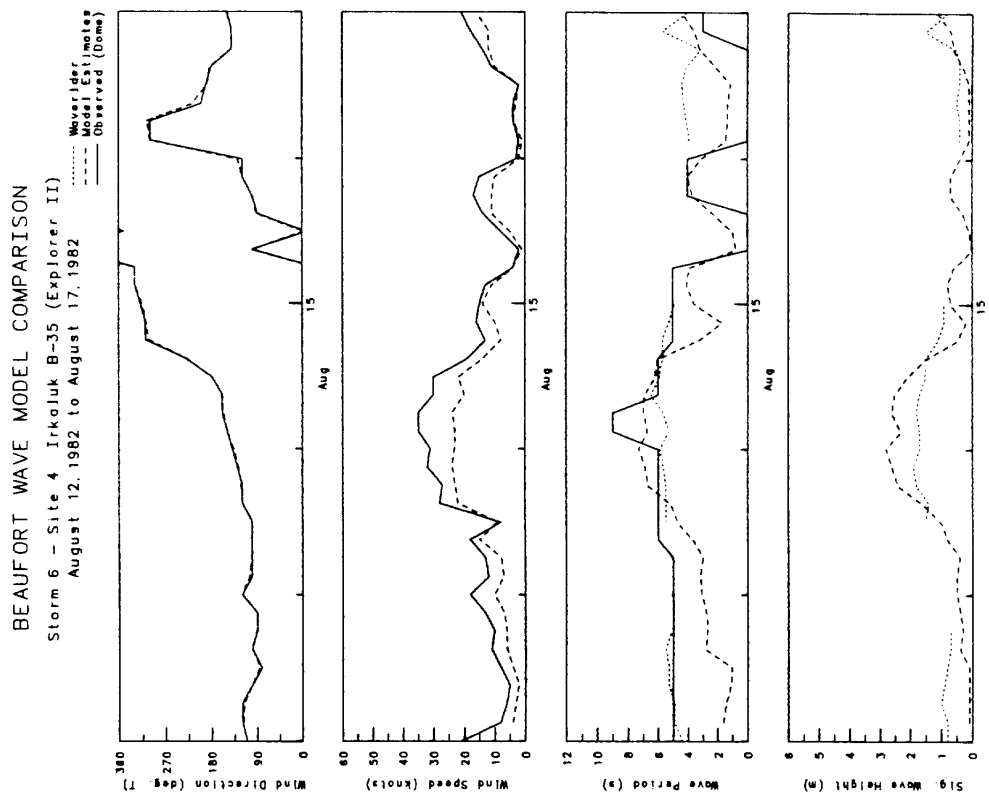
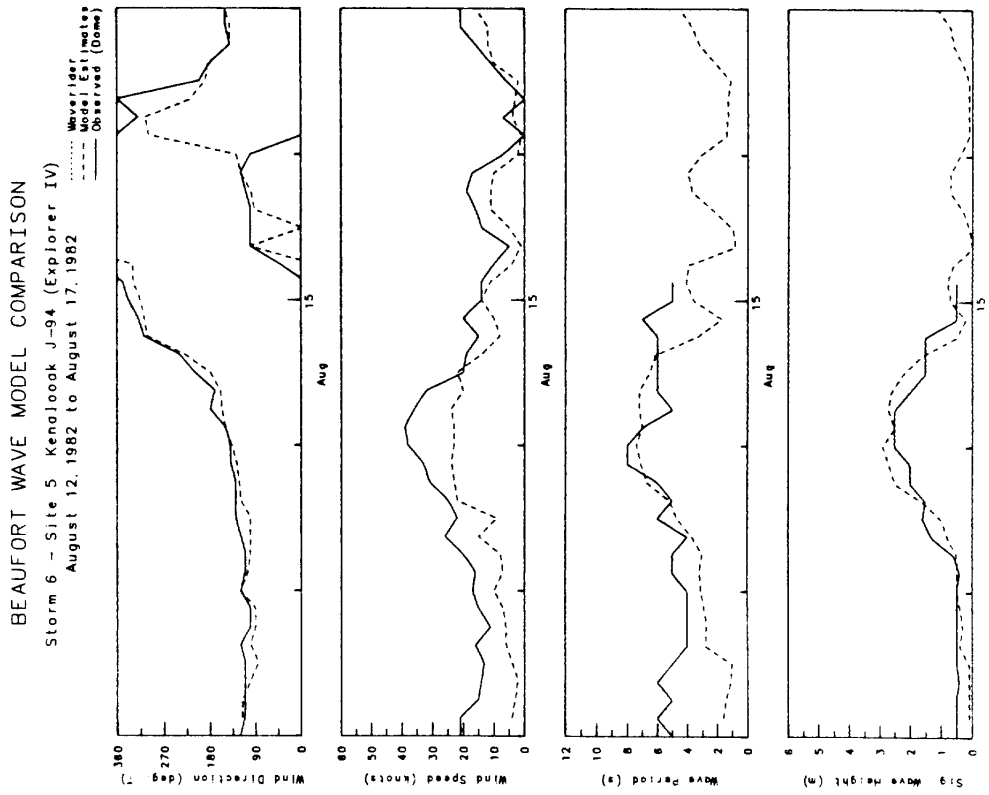


Figure 5.7a



5-37

Figure 5.7d

Figure 5.7c

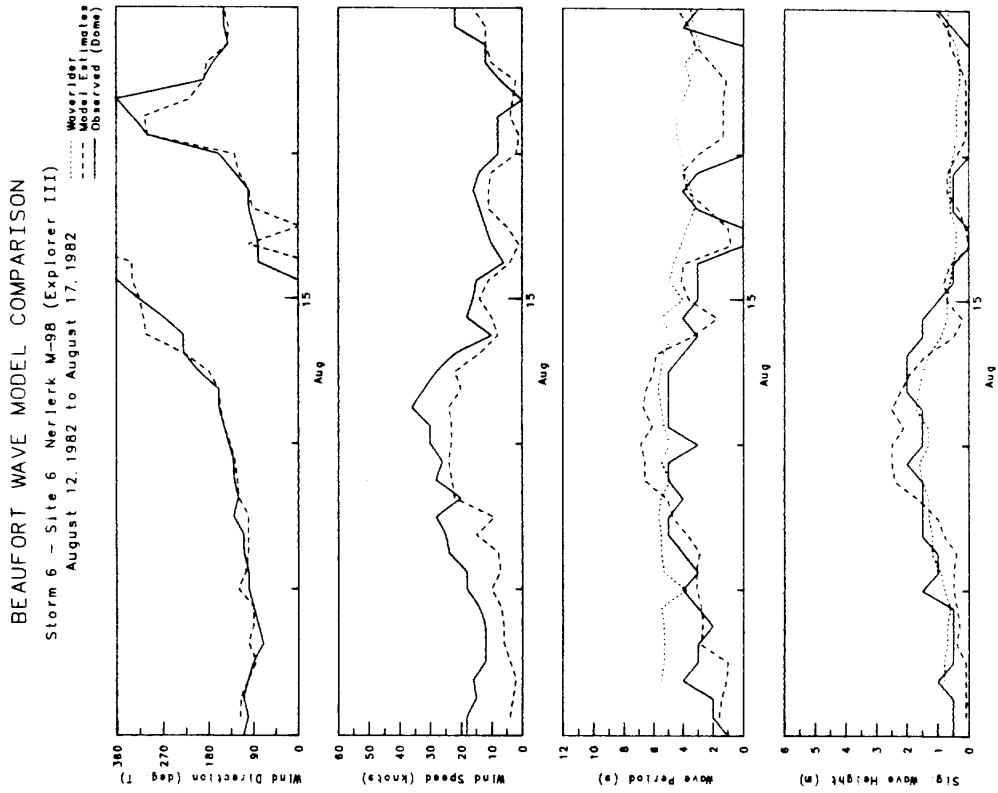


Figure 5.7c

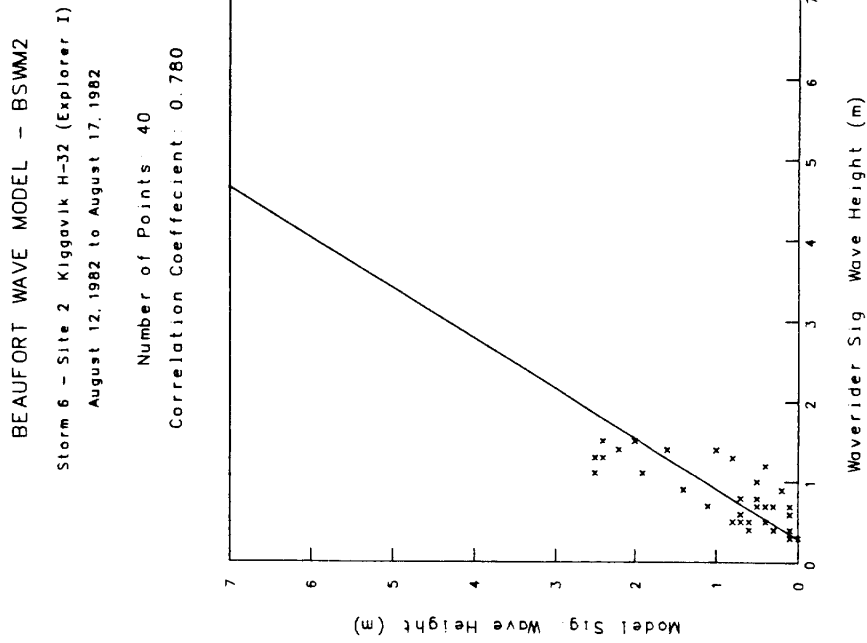


Figure 5.8a

BEAUFORT WAVE MODEL - BSWM2  
 Storm 6 - Site 6 Nerlerk M-98 (Explorer III)  
 August 12, 1982 to August 17, 1982  
 Number of Points: 38  
 Correlation Coefficient: 0.860

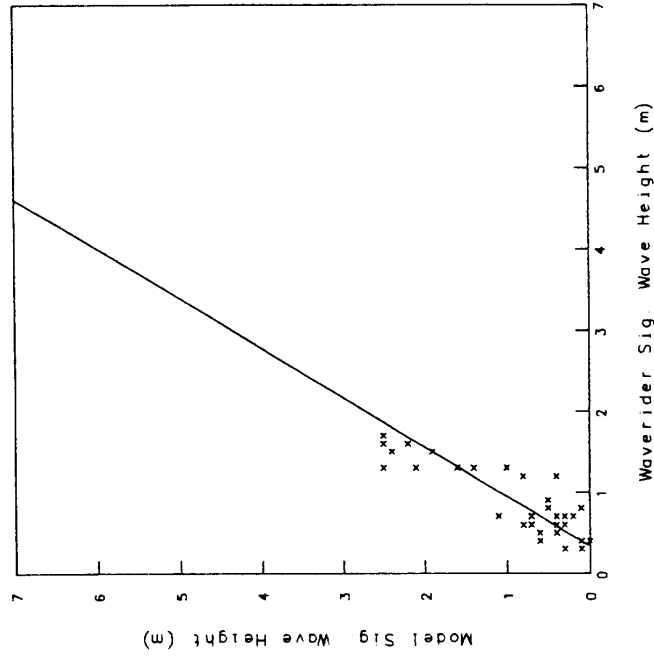


Figure 5.8c

BEAUFORT WAVE MODEL - BSWM2  
 Storm 6 - Site 3 Itijok Island (Esso)  
 August 12, 1982 to August 17, 1982  
 Number of Points: 39  
 Correlation Coefficient: 0.563

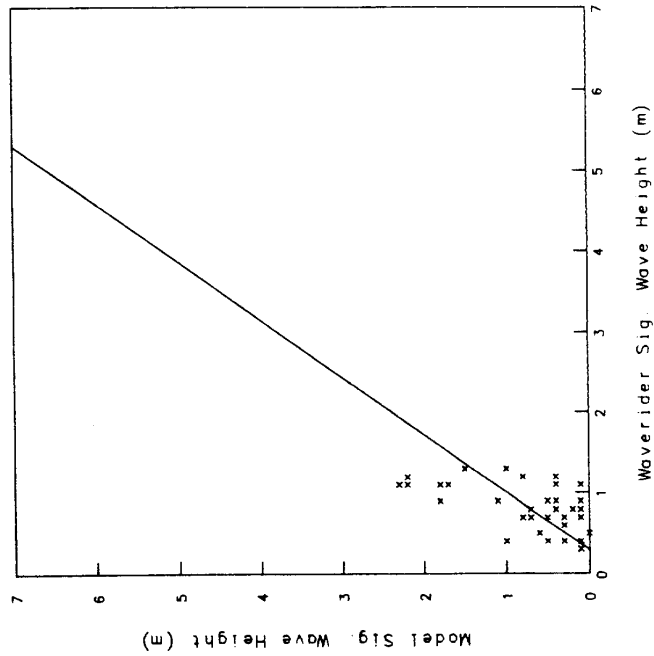
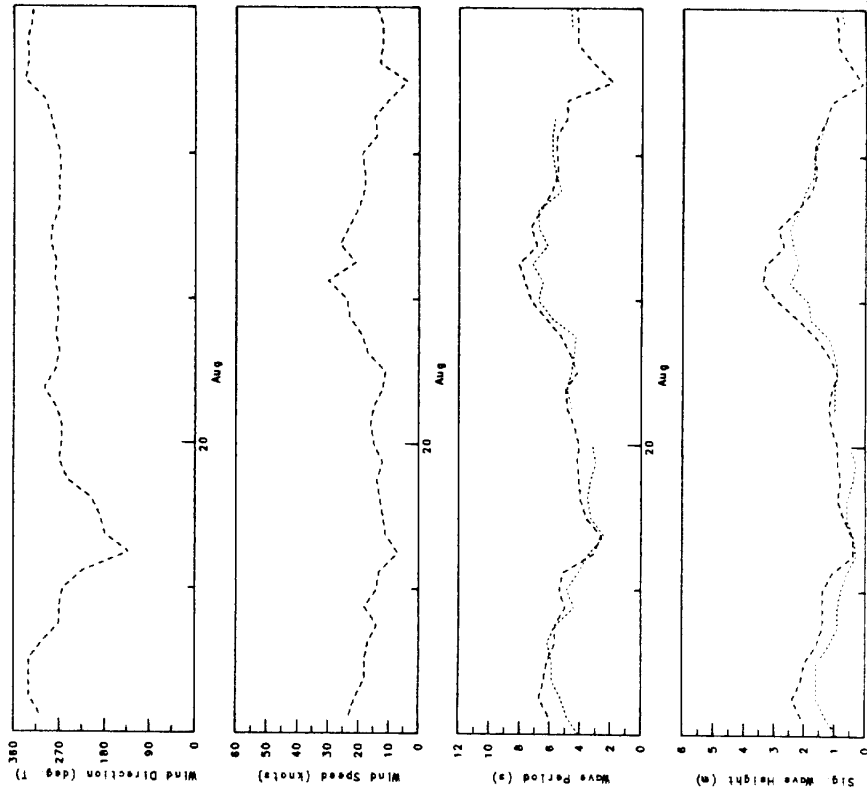


Figure 5.8b

BEAUFORT WAVE MODEL COMPARISON

Storm 7 - Site 3 Itiyok Island (Esso)  
August 18, 1982 to August 23, 1982

Waverider  
Model Estimates  
Observed



5-40

Figure 5.9b

BEAUFORT WAVE MODEL COMPARISON

Storm 7 - Site 2 Kiggavik H-32 (Explorer I)  
August 18, 1982 to August 23, 1982

Waverider  
Model Estimates  
Observed

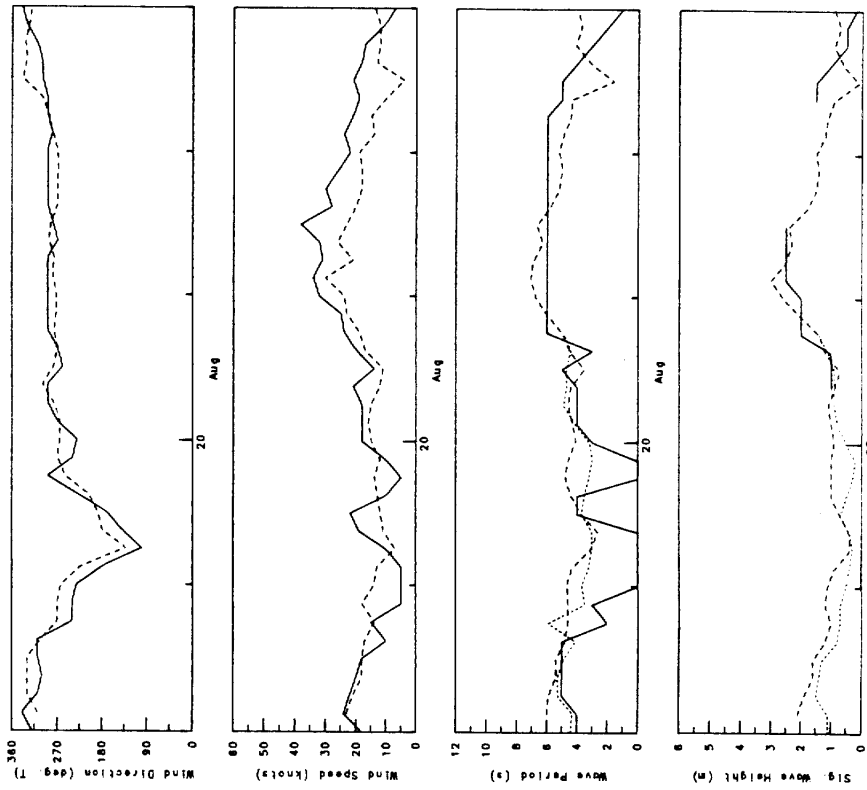


Figure 5.9a

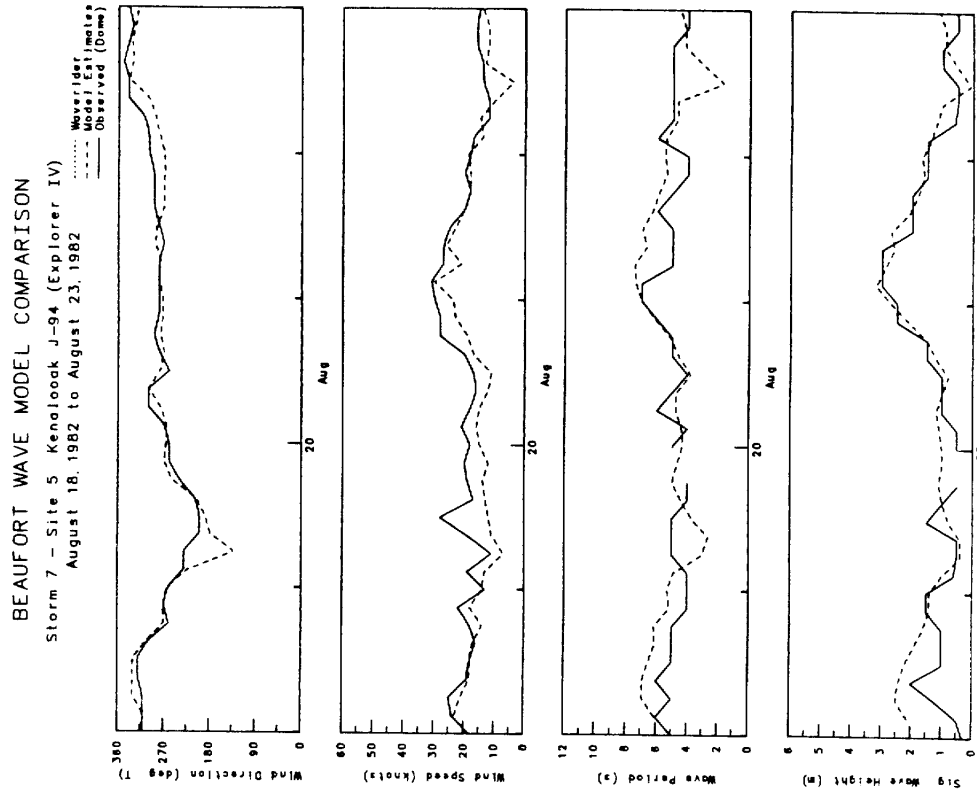


Figure 5.9d

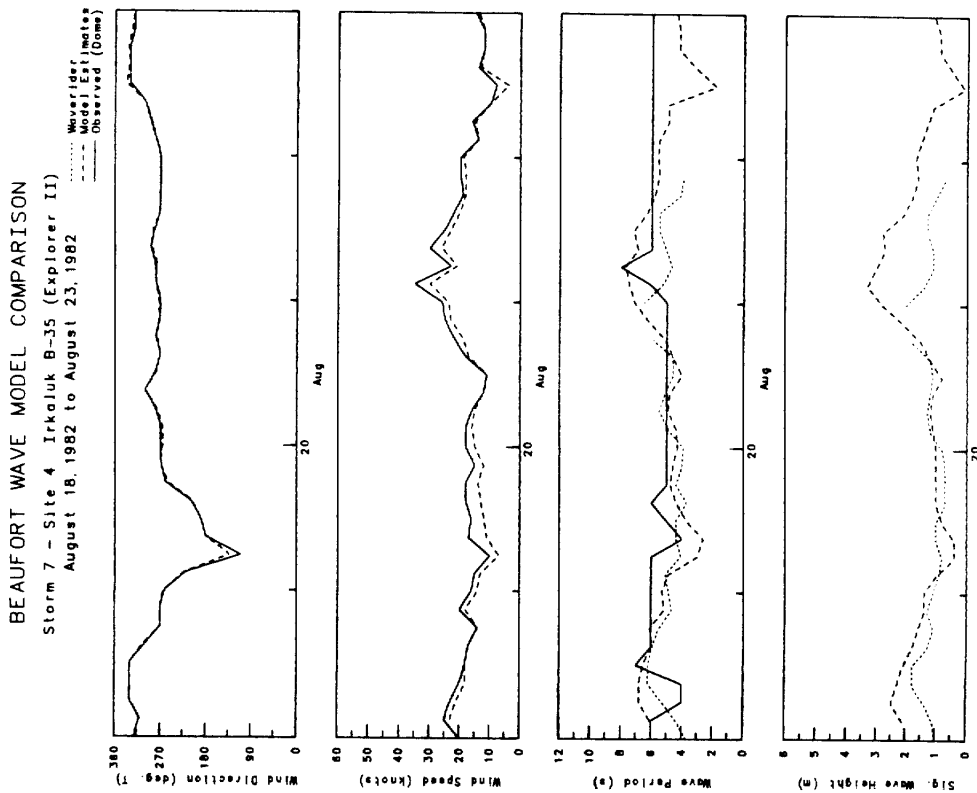


Figure 5.9c

### BEAUFORT WAVE MODEL COMPARISON

Storm 7 - Site 6 Nerlerk M-98 (Explorer III)  
August 18, 1982 to August 23, 1982

..... Waverider  
- - - - Model Estimates  
———— Observed (Dome)

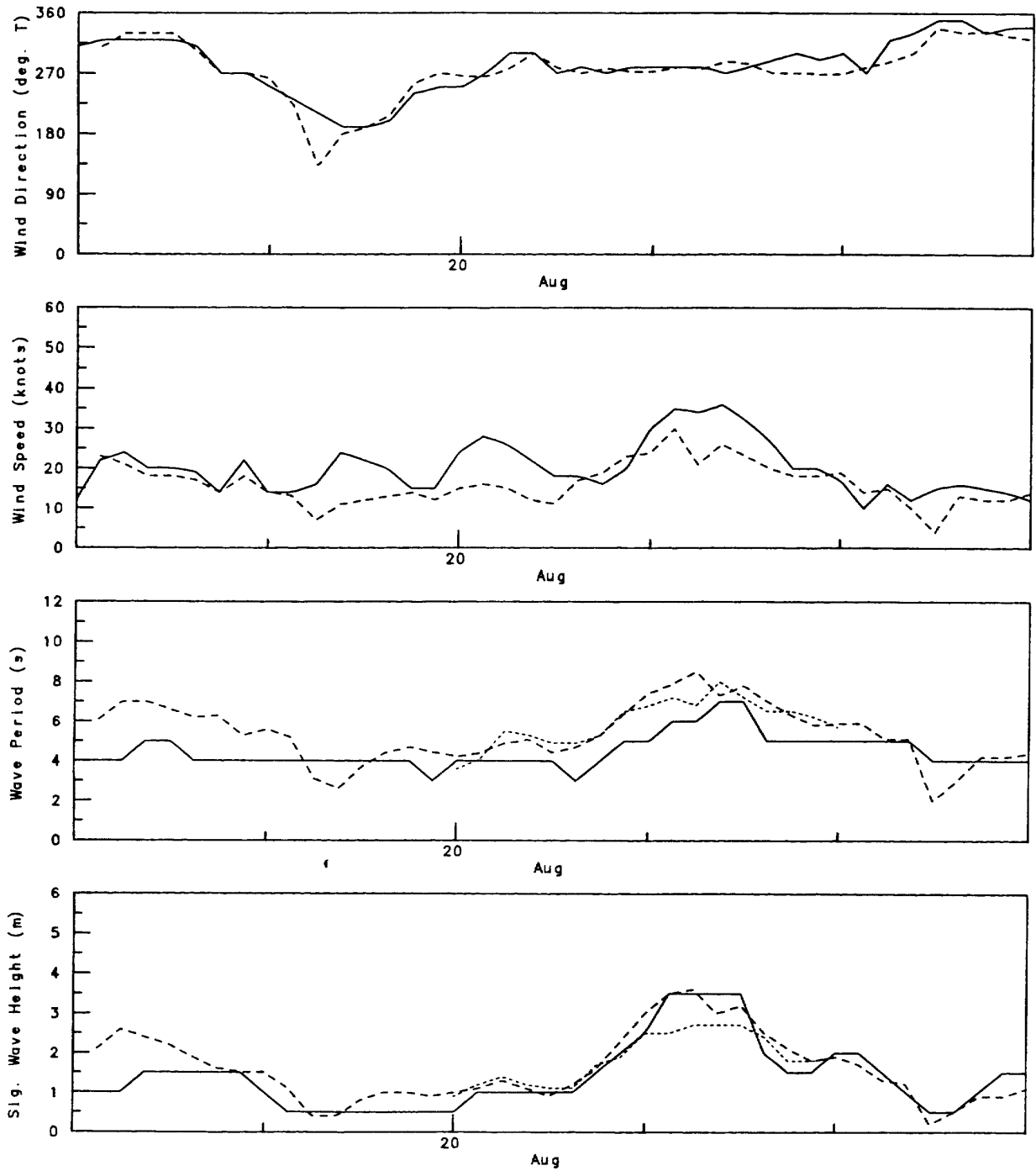


Figure 5.9e

BEAUFORT WAVE MODEL - BSWM2  
 Storm 7 - Site 4 Irkoluk 8-35 (Explorer II)  
 August 18, 1982 to August 23, 1982  
 Number of Points: 30  
 Correlation Coefficient: 0.543

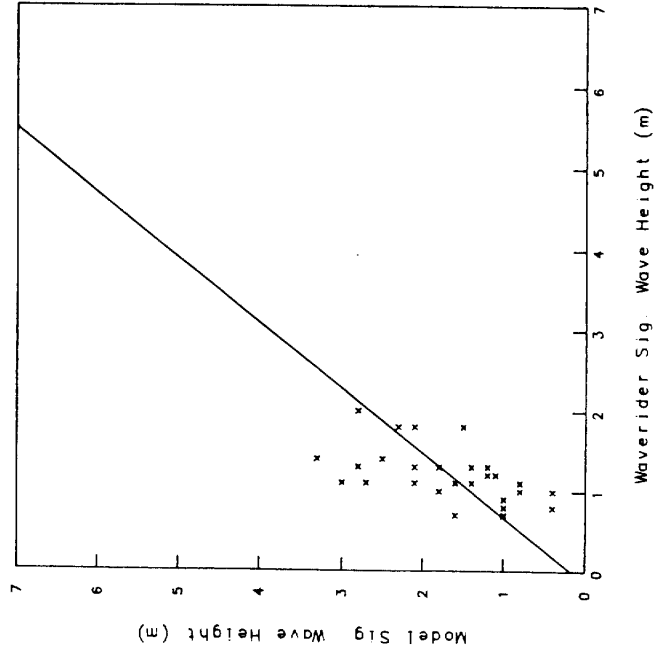


Figure 5.10b

BEAUFORT WAVE MODEL - BSWM2  
 Storm 7 - Site 3 Itliyok Island (Esso)  
 August 18, 1982 to August 23, 1982  
 Number of Points: 35  
 Correlation Coefficient: 0.922

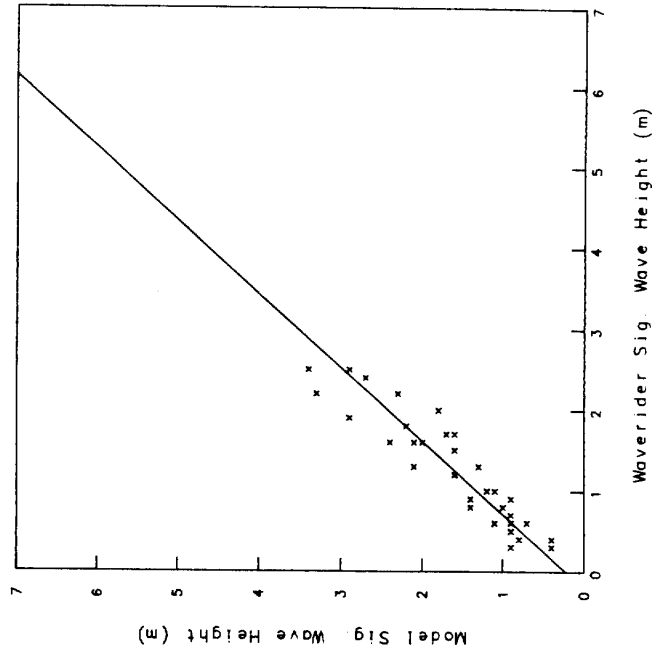


Figure 5.10a

BEAUFORT WAVE MODEL - BSWM2  
 Storm 7 - Site 6 Nerlerk M-98 (Explorer III)  
 August 18, 1982 to August 23, 1982

Number of Points: 40  
 Correlation Coefficient: 0.874

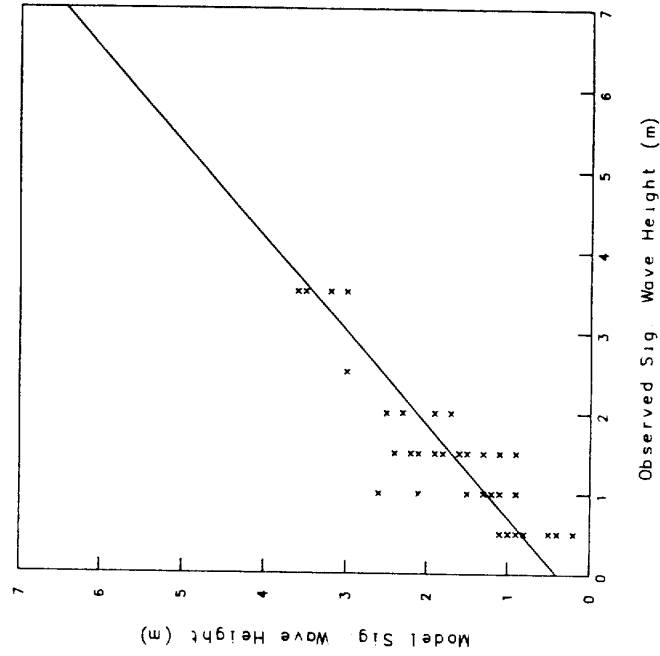


Figure 5.10d

BEAUFORT WAVE MODEL - BSWM2  
 Storm 7 - Site 5 Kenelook J-94 (Explorer IV)  
 August 18, 1982 to August 23, 1982

Number of Points: 39  
 Correlation Coefficient: 0.778

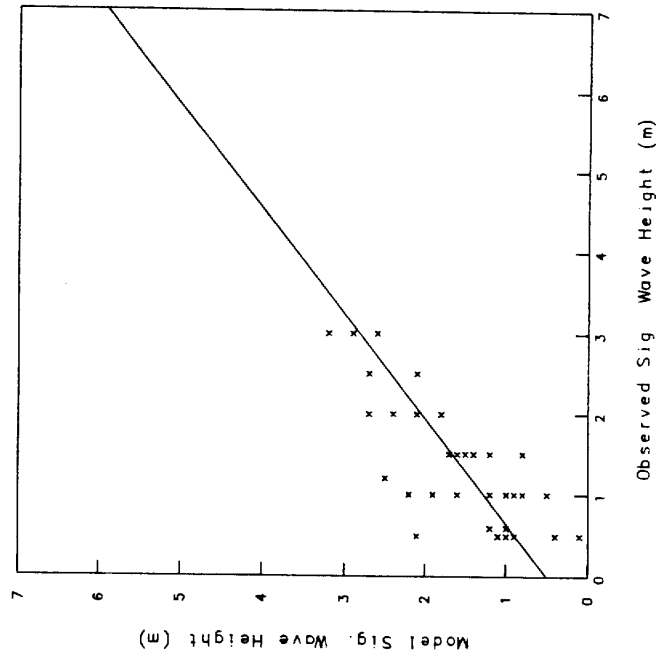
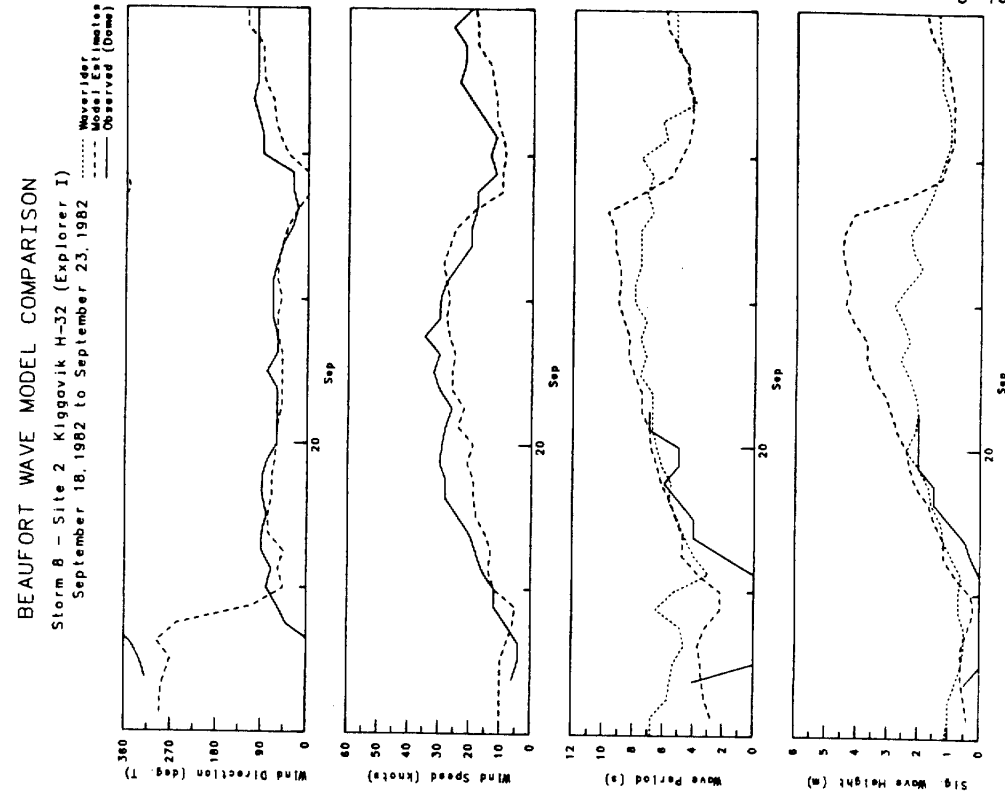


Figure 5.10c



5-45

Figure 5.11b

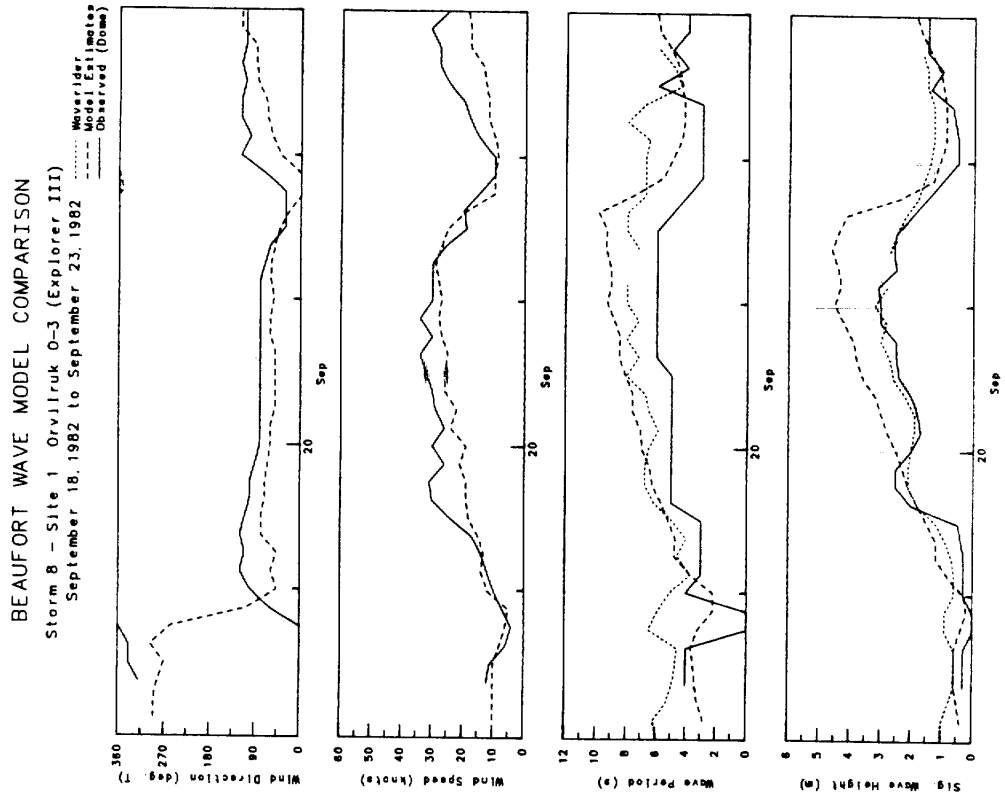
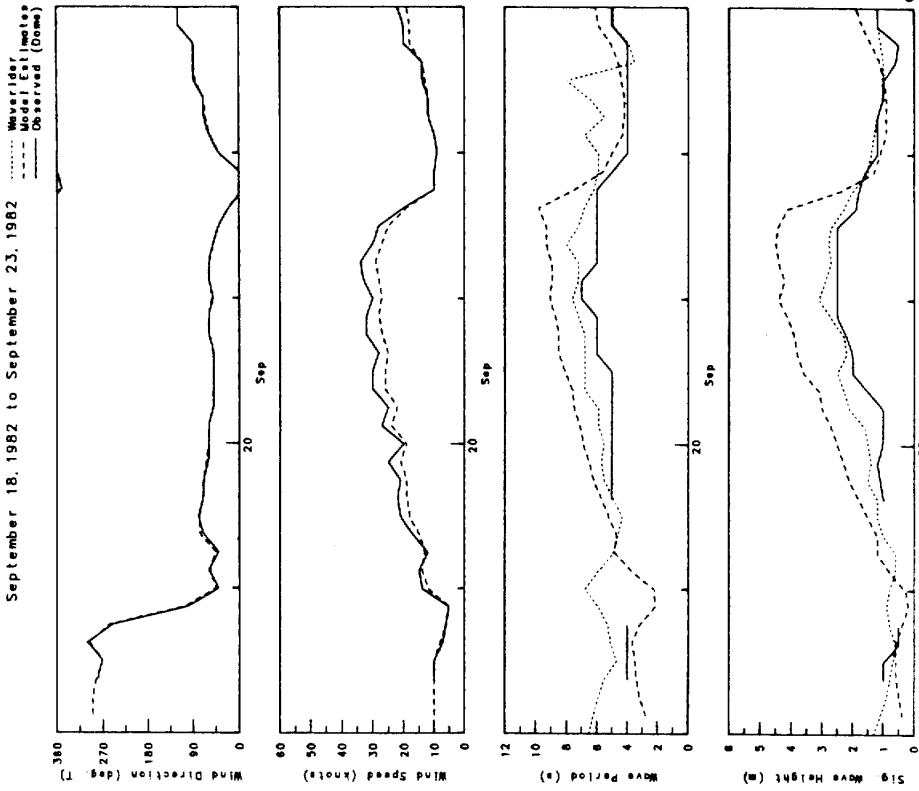


Figure 5.11a

BEAUFORT WAVE MODEL COMPARISON

Storm 8 - Site 4 Irkaluk B-35 (Explorer II)  
September 18, 1982 to September 23, 1982



5-46

Figure 5.11d

BEAUFORT WAVE MODEL COMPARISON

Storm 8 - Site 3 Itiyok Island (Esso)  
September 18, 1982 to September 23, 1982

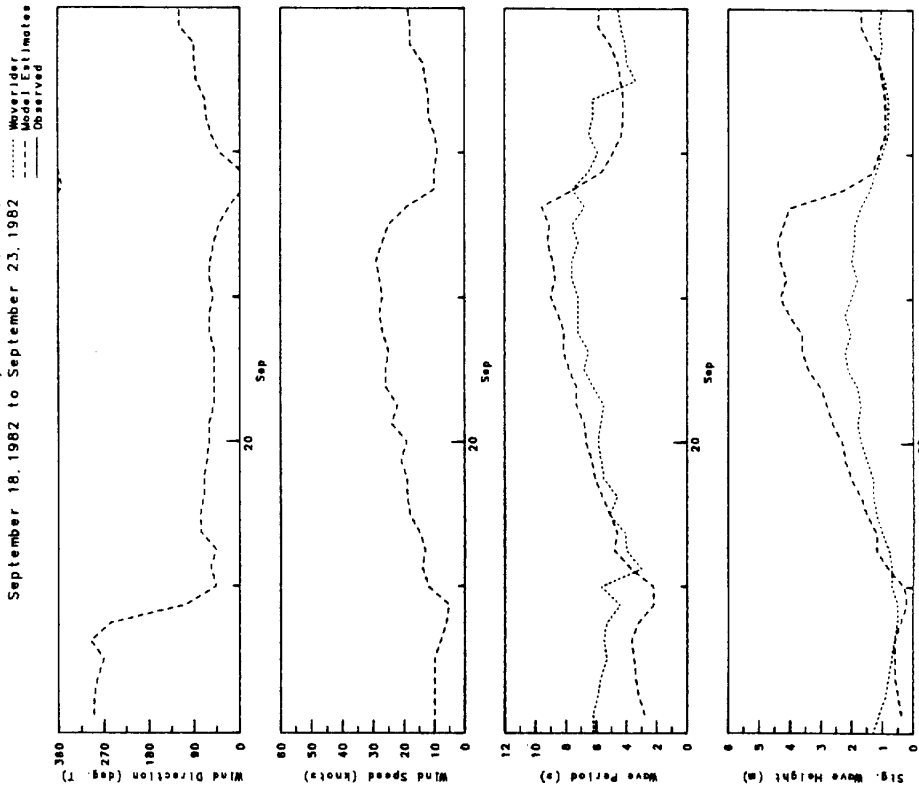


Figure 5.11c

BEAUFORT WAVE MODEL COMPARISON

Storm 8 - Site 5 Kenalook J-94 (Explorer IV)  
September 18, 1982 to September 23, 1982

Waverider  
Model Estimates  
Observed (Dome)

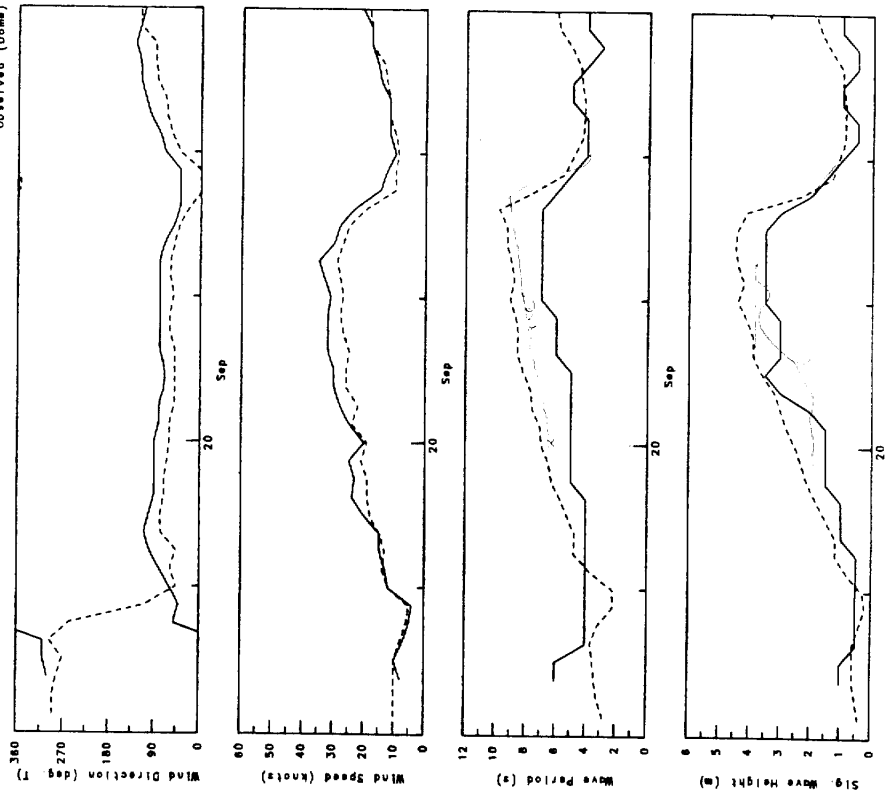


Figure 5.11e

BEAUFORT WAVE MODEL - BSWM2

Storm 8 - Site 1 Orvilruk 0-3 (Explorer III)  
September 18, 1982 to September 23, 1982

Number of Points: 38

Correlation Coefficient: 0.932

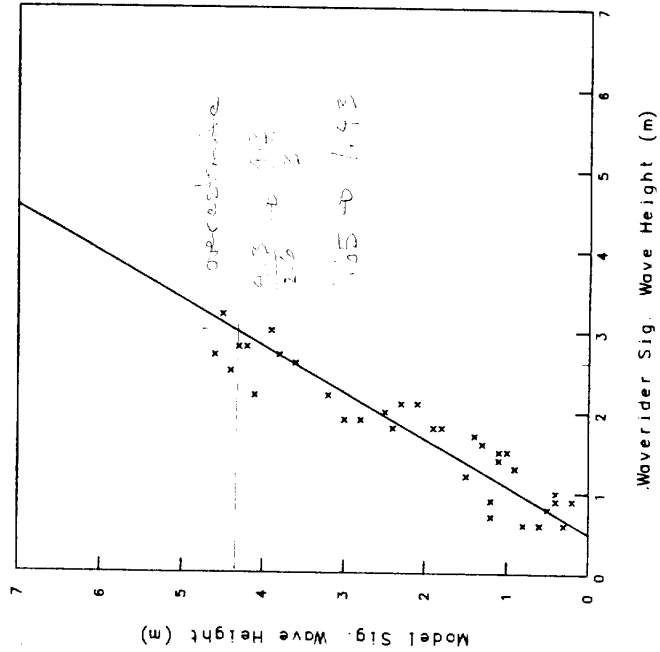
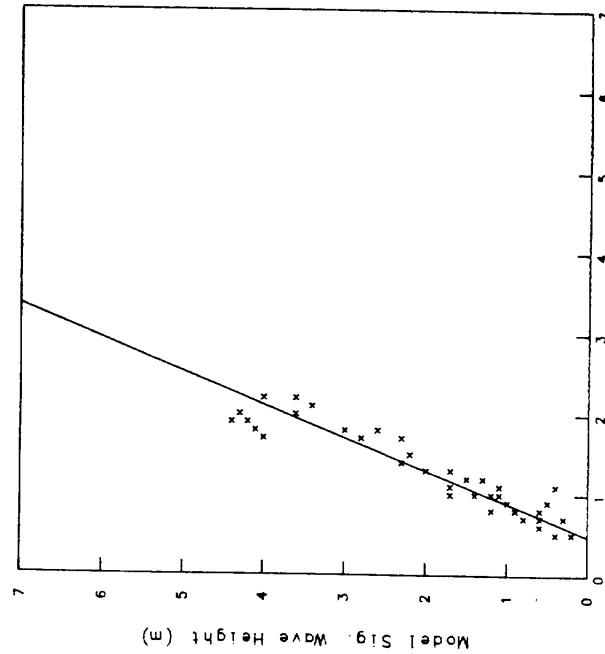


Figure 5.12a

BEAUFORT WAVE MODEL - BSWM2

Storm 8 - Site 3 Itiyok Island (Esso)  
September 18, 1982 to September 23, 1982

Number of Points: 40  
Correlation Coefficient: 0.939



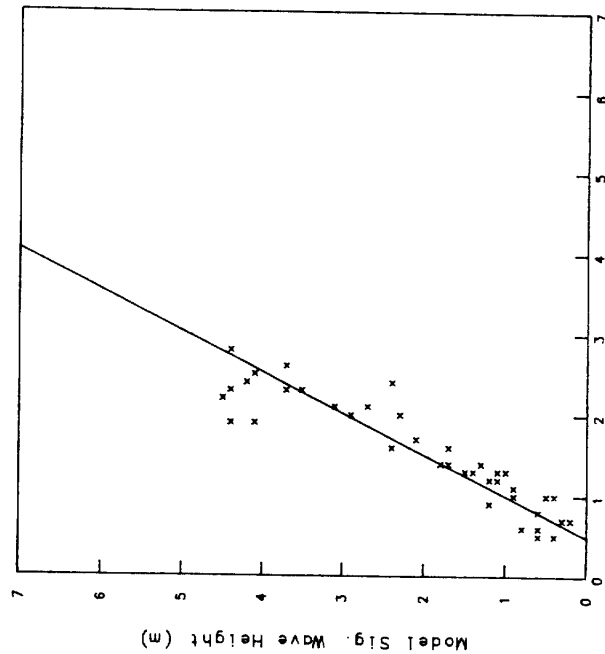
Waverider Sig. Wave Height (m)

Figure 5.12c

BEAUFORT WAVE MODEL - BSWM2

Storm 8 - Site 2 Kiggavik H-32 (Explorer I)  
September 18, 1982 to September 23, 1982

Number of Points: 40  
Correlation Coefficient: 0.915



Waverider Sig. Wave Height (m)

Figure 5.12b

BEAUFORT WAVE MODEL - BSWM2  
 Storm 8 - Site 5 Kenalook J-94 (Explorer IV)  
 September 18, 1982 to September 23, 1982  
 Number of Points: 38  
 Correlation Coefficient: 0.955

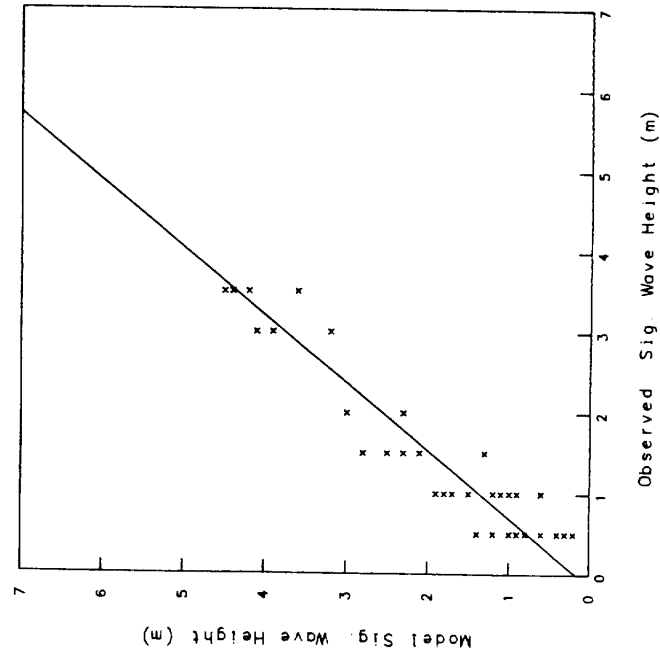


Figure 5.12e

BEAUFORT WAVE MODEL - BSWM2  
 Storm 8 - Site 4 Irkaluk B-35 (Explorer II)  
 September 18, 1982 to September 23, 1982  
 Number of Points: 40  
 Correlation Coefficient: 0.951

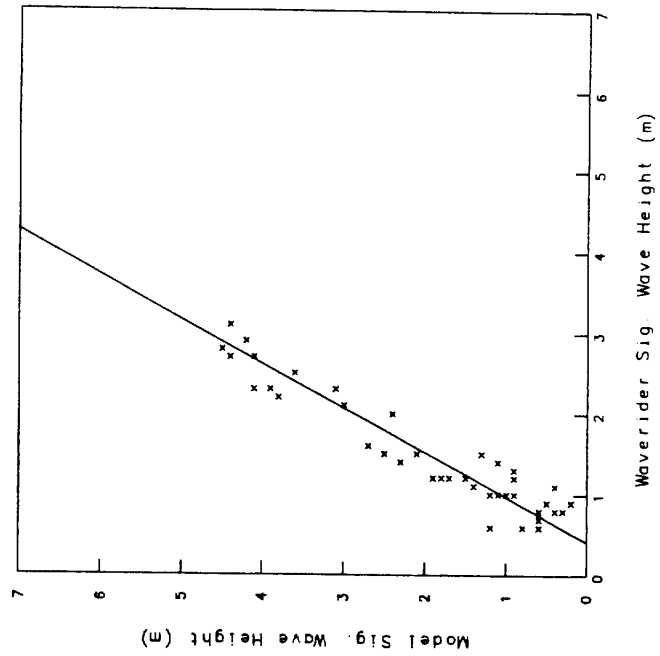


Figure 5.12d

### 5.3 1986 Storm Events

This test was carried out to provide a preliminary evaluation of model results when driven by a gridded wind fields obtained from the CMC NWP model for three storm events in the 1986 open water season.

The data available for the 1986 storm events is illustrated in Table 3.1c with site locations defined in Figure 3.3c . The spatial coverage of the observation sites and available wind data was quite good. Unfortunately, the temporal coverage was poor with many of the observation sites having frequent gaps in their records. The wind input to the model for the 1986 storm cases was the CMC 1000 mb-level winds given at six hourly increments. The CMC wind fields were extracted from the archived model output database at the Dorval Computer Centre in the form of wind components (u,v) given at every sixth grid point as shown in Figure 3.3c . A bilinear interpolation was performed on the given coarse grid CMC wind values to estimate wind data for each model grid point.

The storms under consideration for the 1986 season are defined as:

Storm 9; August 20 to August 25, 1986

Storm 10; September 19 to September 24, 1986

Storm 11; October 3 to October 8, 1986

Due to the limited number of data, no statistical analysis was performed. The results of the model simulations for each storm is briefly described below.

#### Storm 9, August 20 to August 25, 1986

Storm 9 is dominated by westerly winds with wind speeds decreasing prior to the storm then increasing in distinct jumps during the storm event. The time series plots are illustrated in Figures 5.13 a-c for sites with data available. Site 5 at Arnak provides the best wave data for comparison. The model prediction seems to be poorly correlated with both observed wave height and period. For all sites there is reasonable agreement between measured winds in terms of directionality, however, speeds are poorly correlated. Of course a proper comparison of speeds can only be made if the 1000 mb wind is assigned height and boundary layer effects can be estimated. There is a significant difference in model winds from site to site. The bilinear interpolation allows the spatial structure of the CMC winds to be retained. The CMC winds, however show a definite tendency to lag behind the observations. The sparsity of data does not allow a quantitative

assessment of this observation to be made. At each site, the modelled waves are dominated by the forcing wind at the site as illustrated by the high correlation (visual) between model wind speed and the model wave variables. This feature again emphasizes the need to adequately represent the wind field spatially.

Site 5 is only in 7 m of water and it is likely that bottom effects could be important.

#### **Storm 10, September 19 to September 24, 1986**

Relatively calm southerly winds prevailed prior to the onset of Storm 10. A rapid shift in wind direction to westerly was accompanied by an increase in wind speeds of up to 40 knots. The storm event lasted about a day. The time series illustrating this event are shown in figures 5.14 a-c. Again the available observations are poor for this period. Site 4 at Kaubvik has the most information available during this storm. Unfortunately the waverider did not return data for a portion of the storm even. The model determines a peak wave height of about 6 m on September 22 at 00 hrs resulting from an applied 40 Kt wind. The waverider, on the other hand, measured a peak wave Height of 3 m about 15 hrs earlier coincident with an observed wind speed of about 35 knots. The CMC winds appear to lag behind the observations. In fact there is evidence for this at Site 1 as well, where the rise in wind speed of the observations precedes the CMC values. The development of the wave field was again dominated by the local wind forcing and also the fetch conditions. When the wind was southerly, the fetch was short for all sites and the wave heights correspondingly low. As the wind shifted to westerly, the speeds increased, and the fetch also increased for all sites, resulting in large wave heights and periods.

Apart from the apparent timing discrepancy, the modelled wave heights are twice as high as the waverider values. One explanation might be that the CMC winds do not consider boundary layer effects adequately and are thus too large resulting in over estimation of wave heights. On the other hand, Site 4 is only in about 17 m of water such that bottom, effects might be affecting the waves.

#### **Storm 11, October 3 to October 5, 1986**

Storm 11 is characterized by a variable forcing field. Prior to the storm event, the winds are light and rotating in a clockwise fashion. The storm event is bimodal in nature, first an easterly gale occurs, then as the system passes over the area, winds decrease then increase again in a north-westerly gale. The wave field produced at Site 1 by this forcing is illustrated in Figure

5.15 . Unfortunately, no wave data was available for comparison for this period. The bimodal character of the storm winds is reproduced in the wave variables. Again the waves are dominated by the local wind forcing. The variation in wind speeds at each site is reflected in the wave variables. Site 1 recorded some wind measurements and again there is an apparent phase lag of the CMC behind the observations.

Unfortunately the data availability for the 1986 storms was too poor to allow a quantitative evaluation. However several important observations on model performance are evident. First, the model results are dominated by the local wind, supplied at each grid point. It is unfortunate that the finer spatial resolution of the wind field afforded by the CMC data could not be better exploited. However, even though the CMC data provides for increased spatial resolution, uncertainty about its accuracy have been raised. In particular, there are apparent time lags and of course uncertainty about the effects of the boundary layer considered in the CMC 1000 mb wind. Shallow water effects at Site 3 and 5 might be responsible, in part, for the poor correlations between model and observed values there.

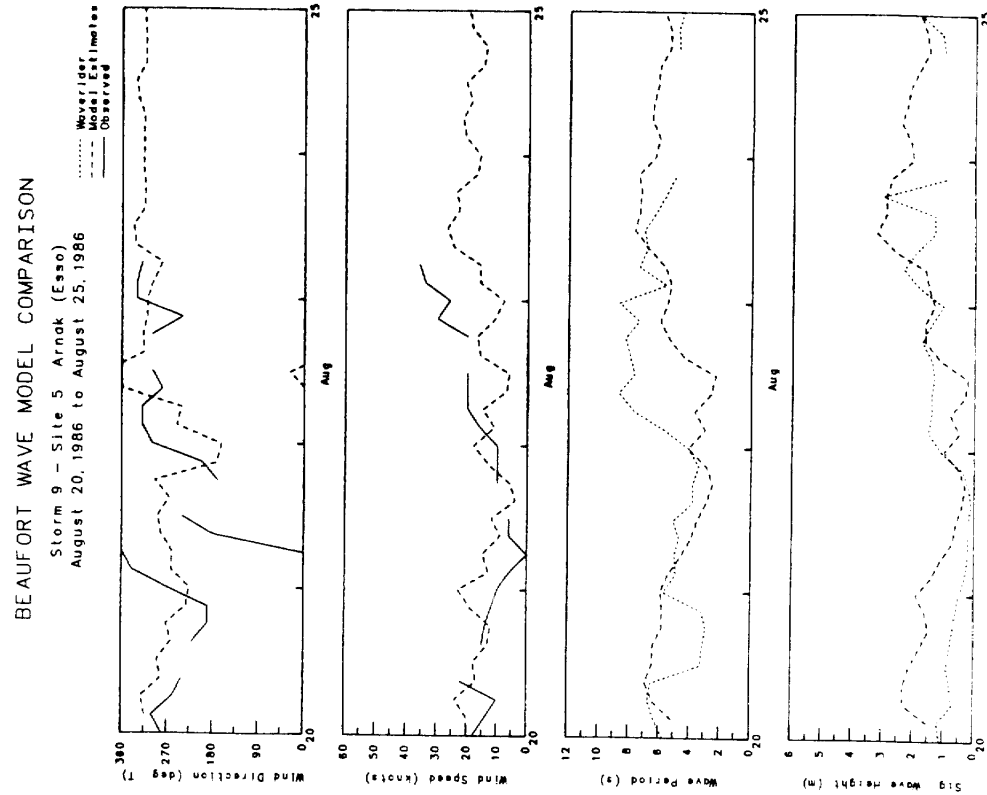


Figure 5.13b

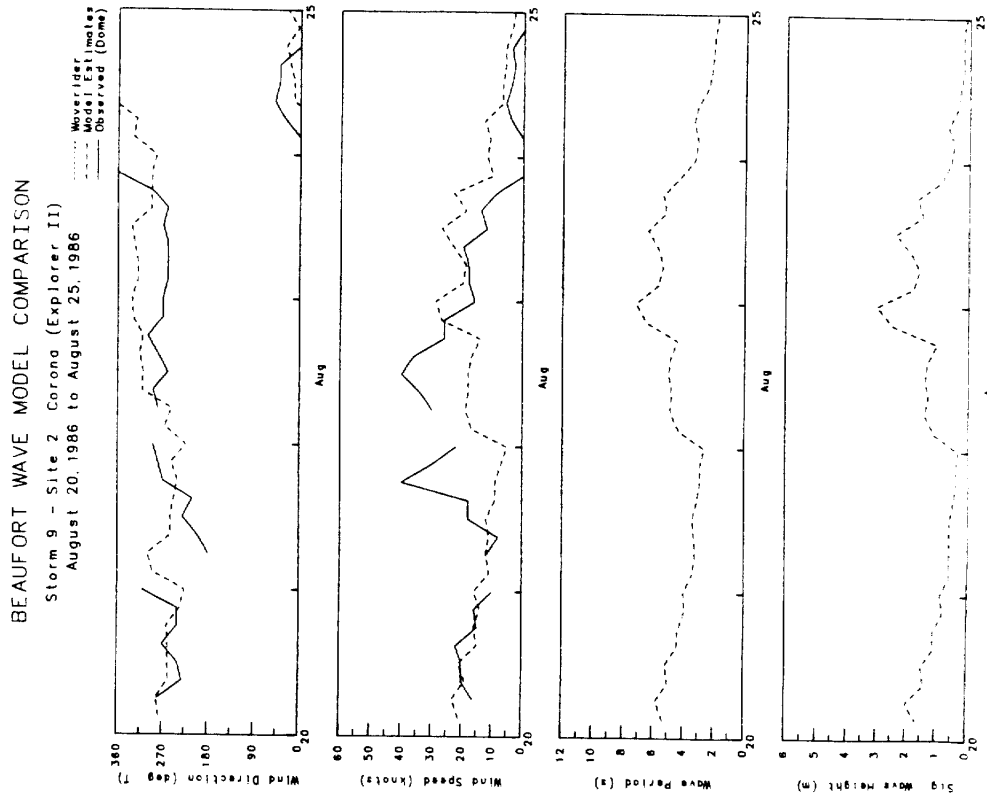


Figure 5.13a

5-54

### BEAUFORT WAVE MODEL COMPARISON

Storm 9 - Site 6 Havik (Explorer I)  
August 20, 1986 to August 25, 1986

..... Waverider  
- - - - - Model Estimates  
————— Observed (Dome)

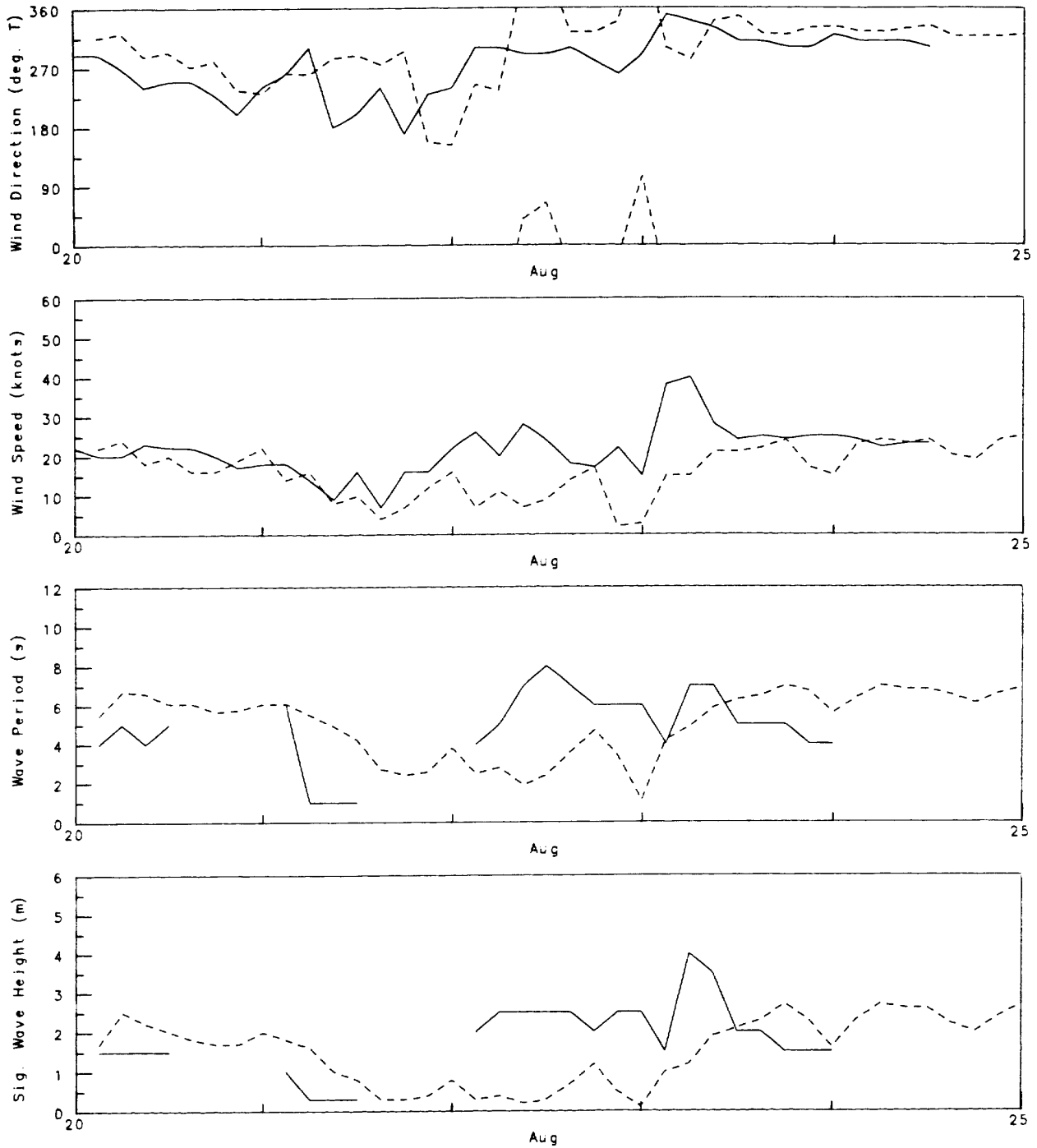
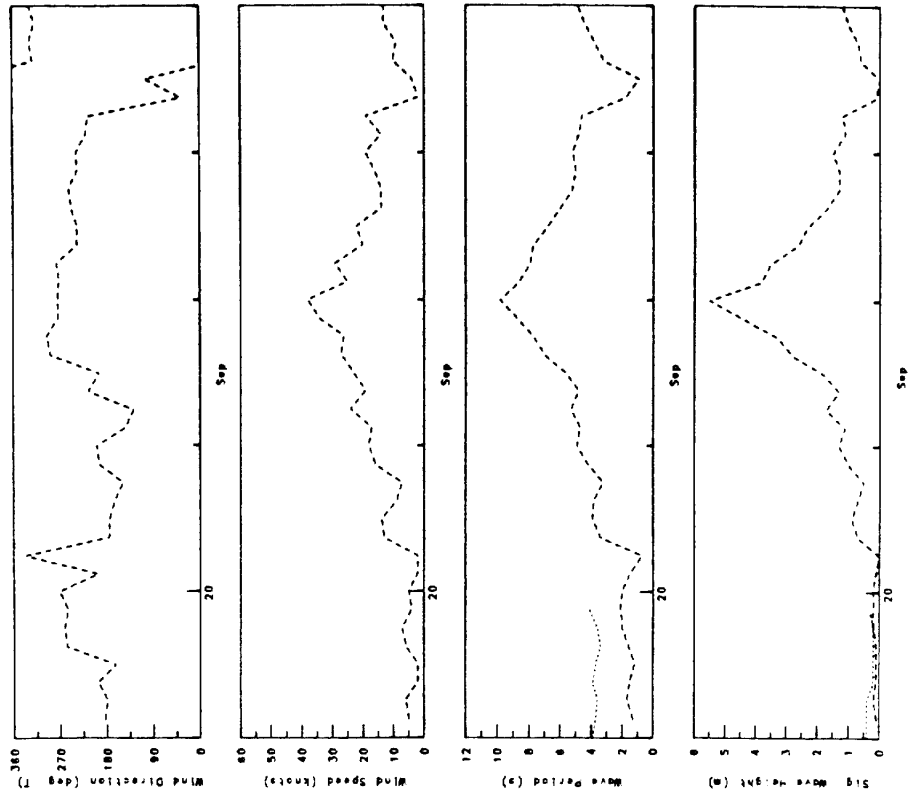


Figure 5.13c

BEAUFORT WAVE MODEL COMPARISON

Storm 10 - Site 3 Minuk (Esso)  
September 19, 1986 to September 24, 1986

Model Identifier  
Model Estimates  
Observed



5-55

Figure 5.14b

BEAUFORT WAVE MODEL COMPARISON

Storm 10 - Site 1 Hammerhead (Explorer II)  
September 19, 1986 to September 24, 1986

Model Identifier  
Model Estimates  
Observed (Dome)

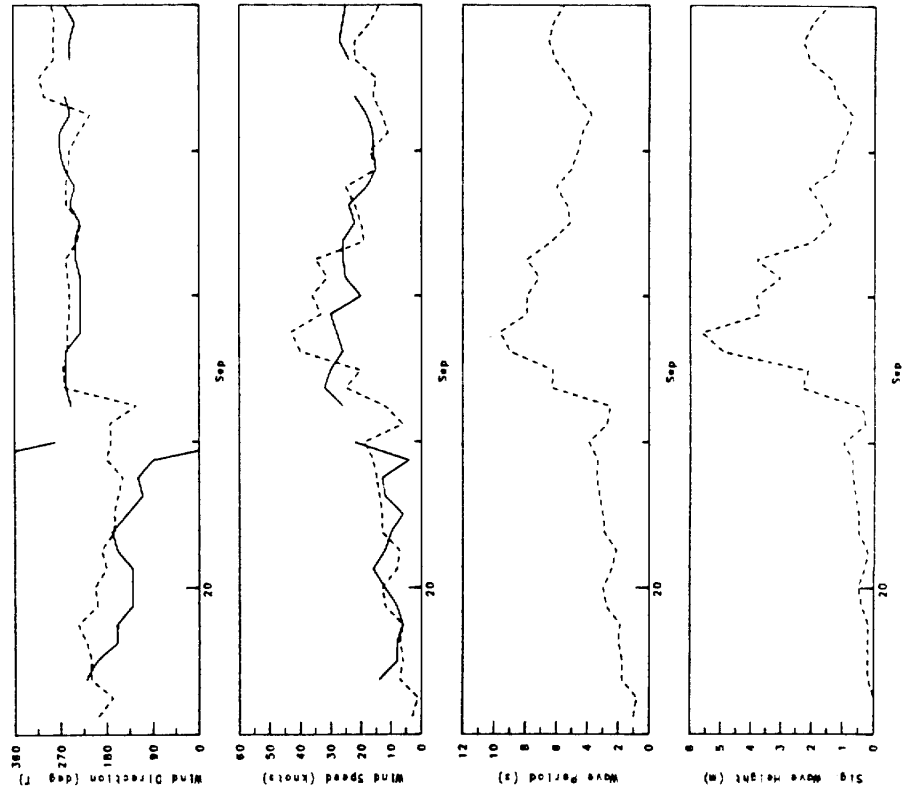


Figure 5.14a

5-56

### BEAUFORT WAVE MODEL COMPARISON

Storm 10 - Site 4 Koubvik (Esso)  
September 19, 1986 to September 24, 1986

..... Waverider  
- - - - Model Estimates  
———— Observed

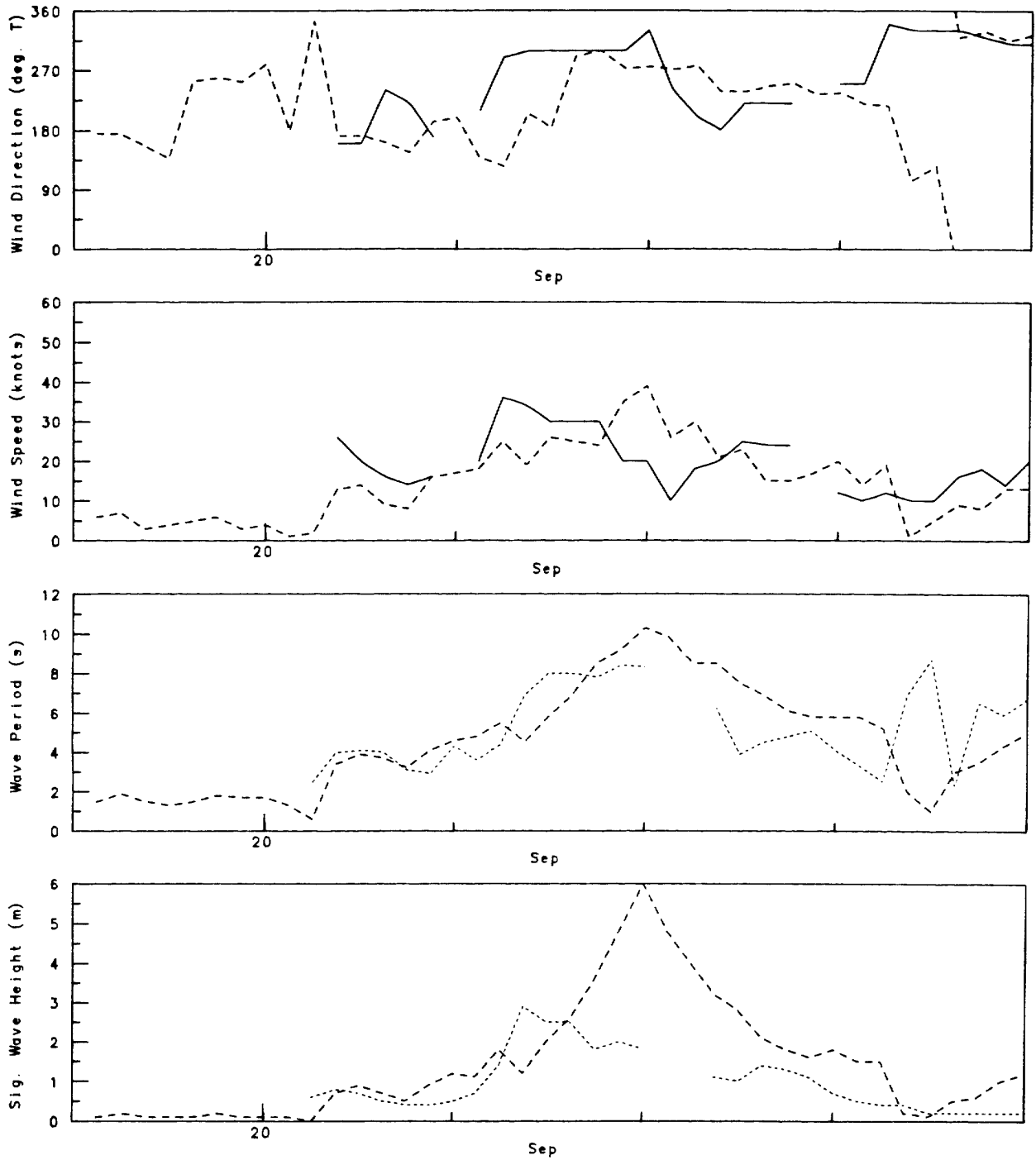


Figure 5.14c

5-57

### BEAUFORT WAVE MODEL COMPARISON

Storm 11 - Site 1 Hammerhead (Explorer II)  
October 3, 1986 to October 8, 1986

..... Waverider  
- - - - - Model Estimates  
————— Observed (Dome)

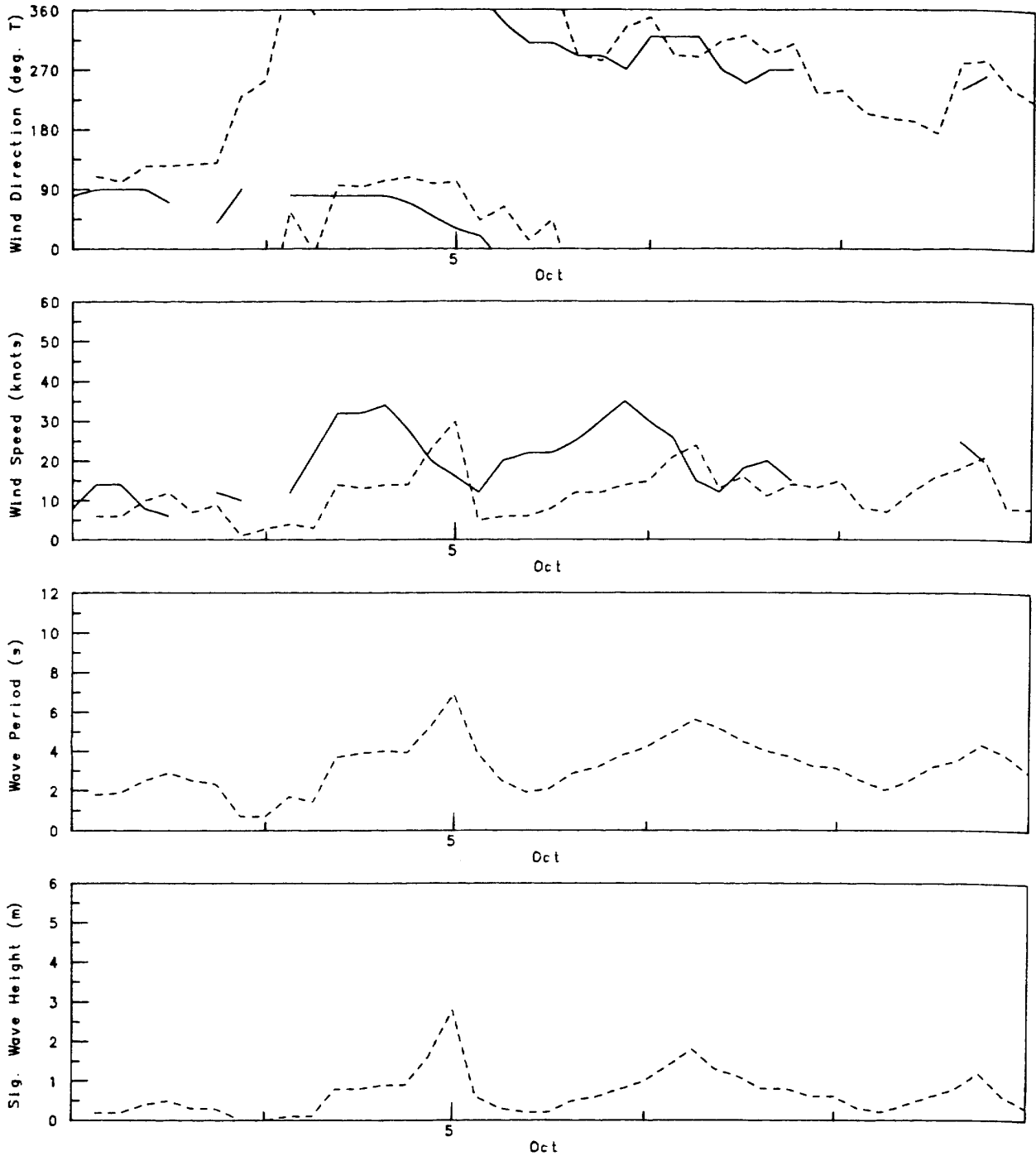


Figure 5.15

## **6.0 SUMMARY, CONCLUSIONS AND RECOMMENDATIONS**

### **6.1 SUMMARY OF WORK DONE**

The primary objective of this study was to develop a model for forecasting wind Generated waves in the Beaufort Sea. This was accomplished by modifying an existing AES lake wave model (GLERL) to work under Beaufort Sea conditions. In particular, modifications were required due to the dynamic nature of the ice edge. During the model development, other refinements were incorporated such as including a spatial smoothing function and modifying the momentum flux terms and allowing for various options in processing the wind input data. The model (BSWM2) developed in this study complements an existing wave model (BSWM) developed for the Beaufort Sea by MacLaren Plansearch Ltd. (1986). Model BSWM2 has several refinements over its predecessor and increased accuracy in hindcasting was achieved. Prior to performing any hindcasts, the model was tested under ideal controlled conditions in order to evaluate model performance and test parameter values. The assembly of a data base for the Beaufort Sea was a major component of the work. Since the data varies in character and availability, several processing options for the wind data were developed. The processing is dependent on considerations on the the spatial coverage of the available data and also the influence of boundary layer effects. The data was acquired, inspected and then formatted for model evaluation purposes. Data for the years 1981, 1982 and 1986 was assembled. The evaluation techniques employed in the study included quantitative statistical analysis as well as qualitative assessments. The model was assessed on its ability to hindcast several storm. events (5 - 7 days) as well as a long period (2 months) simulation. The evaluation was dependent on the type of wind input to the model and improvements in this aspect of the model requirements was stressed. In fact the bulk of the recommendations to be made in the next section are concerned with the suitability of model inputs. This report presents the model BSWM2 in its present state and provides extensive evaluation based on available data. An accompanying report entitled 'Supplementary Data Base Report' provides a complete documentation on the data base assembled for this project.

### **6.2 CONCLUSIONS AND RECOMMENDATIONS**

In the development of a practical wave forecasting system for the Beaufort Sea, it is essential that:

- i) the wave model accurately represents the physics;
- ii) inputs to the model are appropriate;
- iii) adequate wave information is available in order to properly evaluate the model.

The first two requirements must be met if any confidence in the results of the modelling exercise is to be expected. In order to achieve this confidence, one then must ensure that the third requirement is also satisfied. Each requirement will be briefly discussed below.

i) Wave Model Physics.

The GLERL model has proven successful for use in the Great Lakes (Schwab et al. (1986)). The evolution of the GLERL model from Donelan's (1977) original formulation has been scrutinized carefully and model functions tested repeatedly (Clodman (1983, 1983a), Schwab et al. (1984)). The conditions in the Beaufort Sea environment are different, first because the domain is much larger and secondly due to the dynamic nature of the ice edges. The model has been thoroughly tested and found to perform satisfactorily in the Beaufort Sea context. However, some modifications were required. A spatial smoothing function was included because it was found that under certain conditions oscillations in the wave field could be generated when the ice-edge position was updated. The effect of smoothing is to dampen out the spurious oscillations. Tests on the smoothing function indicated that its effect is the largest in regions of large spatial gradients in the wave field. Also the spatial spreading of wave energy was modified to allow for a variable angle of spreading. In the original GLERL model spreading occurred in a band limited to  $\pm 90^\circ$  from the mean direction of wave propagation. In the present model, the angle was set at  $\pm 45^\circ$  for evaluation but, as it is incorporated as a variable, it can be changed.

The model wave field is dominated by the wind's input of momentum. The provision of a suitable wind estimated at a 10 m height above sea level is of fundamental importance, as the stress formulation is based on this requirement. The model has the capability to provide such an estimate given a suitable set of wind data. The data, of course, must have an adequate spatial and temporal coverage and will be discussed later.

Shallow water effects are not included in the model. The effects of bottom topography may play a significant role, especially since many of the evaluation sites are in relatively shallow water ( $\leq 30\text{m}$ ). Except for 1986 data, there was no substantial evidence from the evaluation carried out that topography was important. However, with such a large domain the capability of Generating waves that violate the deep water constraint is possible for several of the site locations. This should be a subject for future model developments.

ii) Input Requirements.

The input to the model consists of ice-edge data, to delineate the model domain, and a wind field to provide the forcing necessary to generate the waves.

The specification of a representative wind field is of utmost importance for the model to provide reliable wave estimates. The data available for use in this project included sets of local observations and CMC 1000 mb model winds. Each will be discussed briefly.

The observations are comprised of a set of measurements made from drilling sites in the Beaufort Sea. The height of the anemometer at the sites varied and it was presumed that the measurements were not affected by local topographic effects. The forcing winds were transformed to their effective value at a 10m height when possible. The stress formulation in the model assumes that winds are prescribed at 10m. As illustrated in several of the case studies, the winds were significantly reduced. However, the structure of the wind remained relatively unchanged. In order to incorporate the boundary layer effects the air and sea temperatures are necessary to account for stability effects. In many cases this data was not available. In one case the wind was not reduced to 10m. The results, in this case, showed overestimation of the wave variables, as expected, however correlations were extremely high. The overestimation can be remedied, in this case, by altering the friction factor, which is certainly dependent on the height of the wind forcing. Due to the poor spatial coverage of the observation sites, a spatially homogeneous wind field was prescribed for all model runs using observed winds for forcing. The wind observation selected to represent wind conditions over the entire domain was based on data quality and central location. The simulations showed that the assumption of spatial homogeneity was poor for some cases and adequate for others. This, of course, is related to the size and propagation characteristics of the weather systems in the area. Indeed, for small intense storms spatial homogeneity is a poor approximation. However, as mentioned previously, the model wave field is dominated by the local wind and, in evaluation of wave data near the forcing site, the correlations were quite good. From the limited observations several features of the wind field were observed. In particular for certain periods the propagation of weather systems was easily identified. In other cases significant spatial variability was encountered over relatively short distances. This could be the result of small scale effects and/or measurement discrepancies. Indeed it is important that the measurements are themselves reliable, although a certain amount

of error is inherent. There is a need for improved spatial coverage of wind observations in the Beaufort Sea if the wave model is to be evaluated properly.

The cases utilizing the CMC 1000 mb winds allowed for improved spatial resolution of the wind field. However, due to poor data coverage, the evaluation was limited to a qualitative assessment. The wave field, as mentioned previously, is dominated by the local wind and this was clearly illustrated in the 1986 test cases. Unfortunately, the adequacy of the CMC wind was suspect since it was found to lag behind the observations consistently. The observed data was too sparse for a proper comparison to be made. The CMC winds, at the 1000 mb level, are not assigned a height above sea level. As a consequence, they are not transformed into their effective value at 10m, as required by the model stress formulation. Further evaluation of the CMC winds is required to assess their adequacy as input to an operational forecasting model.

The ice-edge data supplied to the model is derived from weekly ice charts. As mentioned, it was necessary to provide for a spatial smoothing function to account for oscillations induced by updating the ice-edge weekly. The determination of the ice edge was based on assuming that ice of any concentration would not transmit waves. This assumption has a significant effect in altering effective fetch lengths for certain dates. However varying, the definition of the ice edge was not tested in this project since the effect is predictable to a certain degree. (See MPL (1986) where the effect of changing the ice edge was studied.) Another concern is the existence of transient patches of ice that are unresolved by the weekly charts but might have a significant local effect. Also low concentration ice is not well resolved and so the ice edge may in fact be a diffuse boundary. In order to reduce the potential for these problems to arise requires a finer temporal and spatial resolution of ice information supplied to the model. Prior to any improvements being made in the ice specification, a better understanding is required of actual wave-ice interaction effects, a process largely unstudied to date. This will lead to better criteria being defined for the specification of an effective ice edge.

#### ii) Wave Data and Evaluation.

The evaluation of the model was based on making comparisons of model results with measurements and observations of the wave field at available data sites. Again the evaluation was highly dependent on the quality of the wave data and their availability. Waverider buoy data provided the best comparison data set due to

its compatibility with the model output, (i.e. based on a spectral estimate). The wave observation data provided satisfactory information however, since subjective in nature, it was found to be biased due to perhaps differences between observers. The major drawback of the observations is that they are restricted to 0.5 m resolution.

The model was assessed by compiling error statistics on performance based on a long period ( $\geq 2$  months) and several short period (5 - 7 days) storm event simulations. Again much of the results are highly dependent on the appropriateness of the forcing wind. In general, when the wind was adequate, the model was able to reproduce the storm specific events extremely well. Correlations between model estimates and the data were about 0.9 for wave heights. Wave periods were not as well reproduced with correlation coefficient values of about 0.8. The model was well tuned in that magnitudes of the storm events were matched. As well the timing of the storms was also well reproduced. The long term simulation results were not as good as the storm specific cases. However the model did perform adequately as illustrated by the time series plots in Section 5 . In fact, given the aforementioned inadequacies of the input wind, it is impossible to expect better results. Errors in the wind will be consequently reflected in the model output. Therefore, given the uncertainty in both the input wind and in the observed wave data, it is difficult to properly assess the model, apart from these general comments.

The evaluation techniques employed provided an aid to compare model estimates to the data. The statistics presented must be interpreted with caution and provide only a framework for evaluation. Indeed the evaluation for each case must be treated separately with emphasis placed again on the adequacy of the wind input. In fact, the evaluation technique can itself be improved (e.g. include calculation of lagged correlations).

In summary, the most important condition that must be met, before the model can be used with confidence, is the specification of an appropriate wind field. For the Beaufort Sea, the availability of data is sparse and proper model evaluation is contingent on adequate wind and wave information. Emphasis should be placed on improving the data base for this region. In hindcast mode, one has the ability to select and evaluate the data prior to running the model. In forecast mode, this is not possible and if the model is to be used as an operational tool, its success relies on the wind input. Several improvements to the model physics are envisaged as discussed previously. This includes, for example,

incorporation of shallow water propagation and wave-ice interaction.

Finally, the BSWM2 has provided encouraging results and can be used to provide adequate wave forecast in the Beaufort Sea once the above recommendations have been addressed.

## 7.0 REFERENCES

- Beaufort Weather and Ice Office, 1981 and 1982 Reports. Prepared by AES Western region, Arctic Weather Centre, Edmonton, Alberta.
- Businger, J.A. Wynagaard, J.C, Izumi, U., and Bradley, E.F. (1971), Flux-Profile Relationships in the Atmospheric Surface layer, J. of the Atmospheric Sciences, Vol. 28, pp 181-189.
- Charnock, H., (1955). Wind Stress on a Water Surface, Quart. Journal of Royal Meteorological Society, 81, pp 639-690.
- Clodman, S. (1983). Testing and future application of the Numerical Lakewave Model; Internal Report No. MSRB-83-4, Atmospheric Environment Service, Downsview, Ontario,
- Clodman, S. (1983a). Further study and Testing of the Donelan Lakewave Model. Supplement to Clodman, S. Internal Report No. MSRB-83-4. Atmospheric Environment Service, Downsview, Ontario.
- Clodman, S., (1985) Improving Model Predictions of Great Lakes, Wind Waves. Internal memorandum, Atmospheric Environment Service, Downsview, Ontario. Presented at the 19th Annual Congress of the Canadian Meteorological and Oceanographic Society, June 12-14, Montreal.
- Donelan, M.A., (1975). Are aquatic Micrometeorologists delivering the goods or it is the over-water drag coefficient far from constant? Symposium on Modelling of Transport Mechanisms in Oceans and Lakes, CCIW, Burlington, Ontario, October 1975.
- Donelan, M.A., (1977). A simple numerical model for wave and wind stress prediction, report, National Water Research Institute, CCIW, Burlington, Ontario.
- Donelan M. and Pierson, W.J. (1983). The sampling variability of estimates of spectra of wind-generated gravity waves. Journal of Geophysical Research, Vol. 88, No. C7, pp 4381-4392.
- Dyer, A.M. (1968). An evaluation of eddy flux variation in the atmospheric boundary layer, Journal Applied Meteorology 7, pp. 845-850.
- Hasselmann K., et al. (1973). Measurements of Wind-wave growth and

swell decay during Joint North Sea Wave Project (JONSWAP). Dtsch. Hydrogr. Z. A12, 95 pp., 1973.

Hodson, J. and Donelan M.A., (1978). The computational scheme of a numerical model for wave and wind stress prediction. Applied Research Division and Hydraulics Division, Canada Centre for Inland Waters, Burlington, Ont. 1978.

MacLaren Plansearch Limited, (1986). Forecasting Beaufort Sea Wind Waves by a Momentum Balance Method. Report submitted to Atmospheric Environment Service, Downsview, Ontario.

Schwab, D.J., Bennett, J.R. and Lynn, E.W. (1986). A Two Dimensional Wave Prediction System. Environmental Software, Vol. 1, No. 1, pp 4-9.

Schwab, D.J. Bennett, J.R., Liu, P,C, and Donelan, M.A. (1984). Application of a simple numerical wave prediction model to Lake Erie, Journal of Geophysical Research, Vol. No. 89, No. C3, pp 3586-3592.

Smith, S.D. and Banke, E.G. (1975), Variation of the sea surface drag coefficient with wind speed, Quart. Journal of Royal Meteorological Society, pp 665-673.

APPENDIX A

DESCRIPTION OF MODEL SOFTWARE

## APPENDIX A

## DESCRIPTION OF MODEL SOFTWARE

The adaptation of the GLERL model has resulted in the Beaufort Sea Wave Model Version 2, Model BSWM2, as described in the text. The basic theoretical and numerical procedures of the GLERL model have not been altered except where noted in the text. Most of the modifications are based on the input/output requirements, dependent on data type and ice edge constraints. The model logic is illustrated in the flow chart shown in the following pages. Several comment statements are included in the program coding which was given to the Scientific Authority. This provides a complete description model routines. Reference should also be made to MPL (1986) which includes a description of subroutines identical to those of the present version of the model.

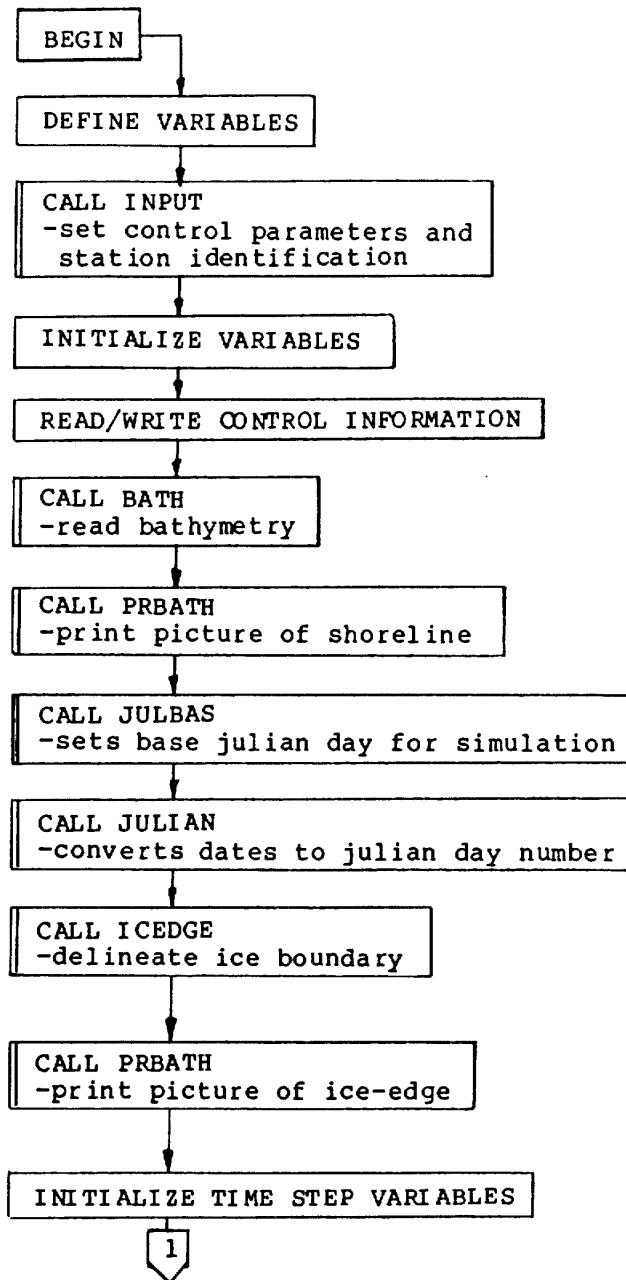


Figure A.1a: Model Flow Chart/Logic Structure.

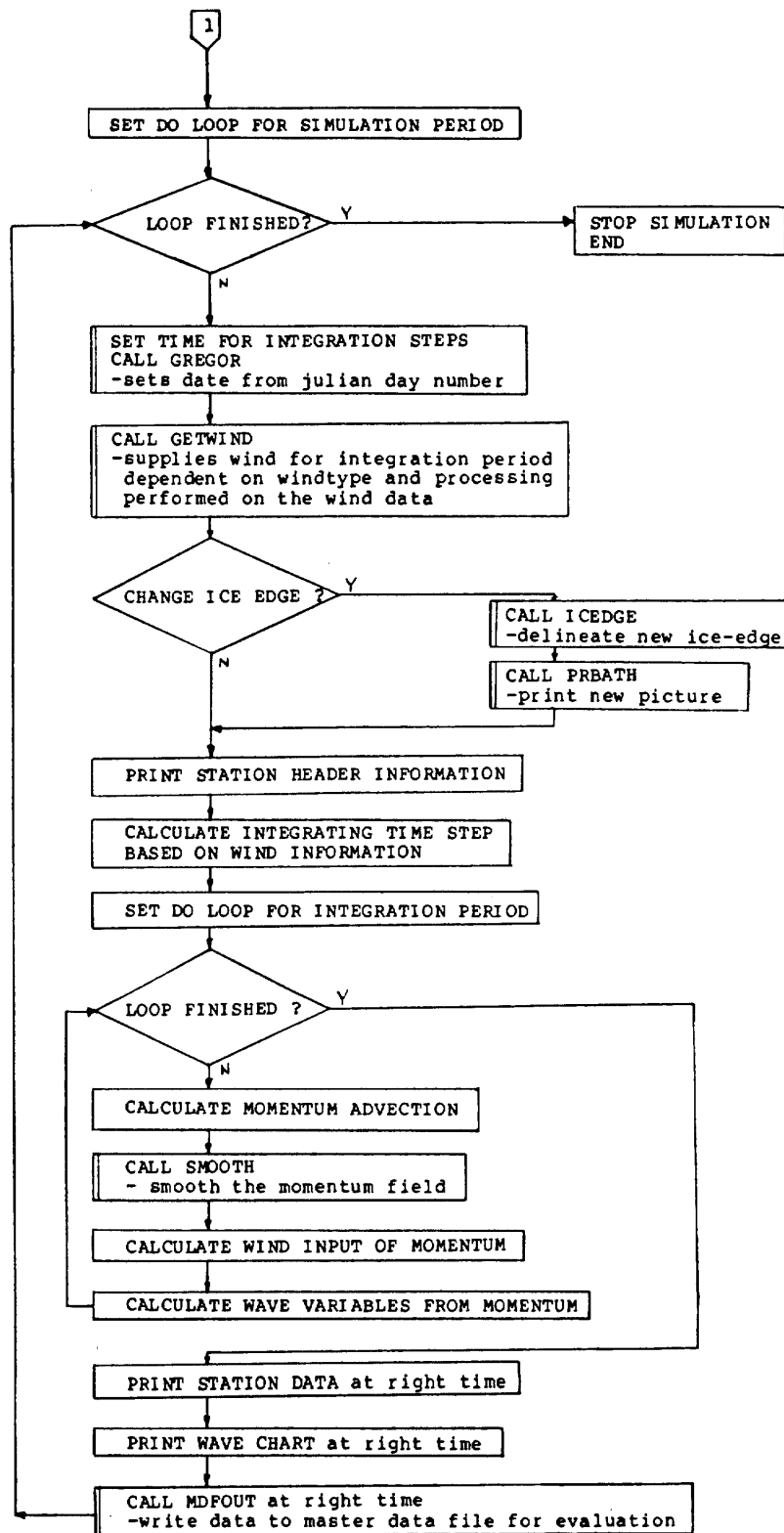


Figure A.1b

APPENDIX B

INPUT DATA FORMAT

LOGICAL UNIT 10 - Bathymetry

This file consists of 67 groups of 5 lines. Each of the 5 lines for Group I has the following format.

LINE	COLUMNS	FORMAT	PARAMETER	DESCRIPTION
I-1	1-80	8F10.2	DEPTH (I,J), J=1,8	Lake depth in meters
I-2	1-80	8F10.2	DEPTH (I,J), J=9,16	for grid point (I,J),
I-3	1-80	8F10.2	DEPTH (I,J), J=17,24	Land and grid boundary
I-4	1-80	8F10.2	DEPTH (I,J), J=25,32	points have the value
I-5	I-10	F10.2	DEPTH (I.33)	zero

LOGICAL UNIT 20 - Input Wind Data

Note several types of winds can be supplied to the model with processing accounted for by parameter WINDTYP designated in Logical Unit 60. At present the model is functional with the specifications listed below, not all the options listed in the text were extended into operational capability. Subroutine GETWND explains the options available (refer to Section 3.4.2 for details).

## a. Observed Wind

WINDTYP "OBS" (Homogeneous WIND FIELD)

\* Given; data from one observation station representative of wind over domain. Each line of this file has the format of the master data file as described in appendix D .

<u>COLUMNS</u>	<u>FORMAT</u>	<u>PARAMETER</u>	<u>DESCRIPTION</u>
1-11	IIX	N/A	N/A
12-13	I2	IY	-Year as e.g. 81 for 1981
14-15	I2	IM	-Month (1-12)
16-17	I2	ID	-Date (1-31)
18-19	I2	IH	-Hour (0,3,6,...,21)
20-32	I3X	N/A	-Not Applicable
33-34	I2	ISPD	-Wind Speed (knots)
35-37	I3	IDIR	-Wind Direction (degrees True from)
38-40	I3	Z	-Anemometer height (metres)
41-44	I4	TW	-Water temperature (tenths of a degree C)
45-48	I4	Ta	-Air temperature (tenths of a degree C)

## b. CMC DATA

i) WINDTYP "CMC" (Weighted Average by Distance)

Given; 7 CMC wind grid points over the Beaufort Sea with U-V components defined by CMC grid,

LOGICAL UNIT 60 - Control Parameters and Identification Information

Free format - ID read as A110 and WNDTYP read as A120; remaining Parameters have format commensurate with standard FORTRAN nomenclature.

Line	Parameter	Description
1	ID	Up to 110 characters of descriptive information
2	WNDTYP	Type: Wind type to determine processing in getwind
3	DS	Grid spacing (meters)
	IDIM	Number of X grid coordinates
	JDIM	Number of Y grid coordinates
	NUMSTN	Number of observation stations (1-10)
	NPRINT	Frequency for printing station data (hours)
4	NSTAT(N)	INTEGER name of observation station N
Thru	DLAT(N)	North latitude of observation station N (deg)
3 +	MLAT(N)	North latitude of observation station N (min)
NUMSTAT	DLONG(N)	West longitude of observation station N (deg)
	MLONG(N)	West longitude of observation station N (min)
	IST(N)	I grid coordinate corresponding to station N
	JST(N)	J grid coordinate corresponding to station N
4 +	NSTEPS	Number of time steps
NUMSTAT	DT	Time step size (minutes)
	CHART1	Frequency to print wave chart (minutes)
	ITMP	Lake shrink factor (1)
	SHOREH	Land grid point identification (-1)
5 +	IYEARW	Start year for wind (1900-1999)
NUMSTAT	MONTHW	Start month for wind (1-12)
	IDATEW	Start day for wind (1-31)
	IHOURLW	Start hour for wind (0,12)
	MINW	Start minute for wind (0 - 23)
	LISTST(1)	Start year for listing station date (1900-1999)
	LISTST(2)	Start month for listing station data (1-12)
	LISTST(3)	Start day for listing station data (1-31)
	LISTST(4)	Start hour for listing station data (0-23)
	LISTST(5)	Start minute for listing station data (0)

FORMAT

Lines 1, 3 and 4 contain information to identify the file. This information is not used in the program.

Line 2 Free format - integer type - 7 CMC grid points:

XW(k), YW(k), k=1,7 Model grid coordinates corresponding to each of the 7 CMC grid point.

Line 5 to end of the file.

COLUMNS	FORMAT	PARAMETER	DESCRIPTION
1-3	I3	IY	-Year as e.g. 81 for 1981
4-6	I3	M	-Month (1-12)
7-9	I3	ID	-Date (1-31)
10-12	I3	IHR	-Hour (- to 12)
13-110	14F7.2	U1(I),U2(I),I=1,7	-Alternate components of U and V for each of the 7 wind stations.

ii) WNDTYP = "CMP" (Planar fit)

Given; as i)

Format as i)

iii) WNDTYP = "CMB" (Bilinear Interpolation)

Given; fine grid of CMC winds coincident with model grid but values given every sixth grid point.

FORMAT

Line 1 5X,4I2 Year, Month, Day and Hour of this data block.

Lines 2,4,...,12 (12F7,2) have U (x axis) wind components of the wind field at specific points.

Lines 3,5,...,13 (12F7.2) have V (Y axis) values.

Lines 1 to 13 are a repeating group for different times.

LOGICAL UNIT 30 - Ice Boundary Data

Each line of the file is free format and each value is integer type.

The format follows:

```

IY   IM   ID   NY   NM   ND
I    J1   J2
.    .    .
.    .    .
.    .    .
68   68   68
IY   IM   ID           NY   NM   ND
I    J1   J2
.    .    .
.    .    .
.    .    .

```

Where:

IY = Chart year of data set (e.g. 1981)  
IM = Chart month of data set (1-12)  
ID = Chart day of data set (1-31)  
NY,NM,ND = Year, month and date of next ice chart  
I = X grid coordinate  
J1 = Y grid coordinate designating start of ice edge  
J2 = Y grid coordinate designating end of ice edge

Notes:

1.  $J1 \leq J2$
2. For a given I, all points J1 through J2 are considered to be ice (or land). Lines with the same I value can be repeated to account for complicated ice edges.
3. I = 68 indicates the end of the current chart.
4. For the last chart, the two dates are identical i.e., IY = NY, IM = NM, ID = ND.

APPENDIX C

OUTPUT DATA FORMAT EXAMPLE

TITLE: 9EAUFORT SEA WAVE MODEL

IDENTIFICATION: INPUT PARAMETERS TO RUN BMS

THIS RUN USES OBSERVED WIND DATA

GRID SPACING IN METRES IS: 18500.0

NUMBER OF X GRID POINTS IS 67

NUMBER OF Y GRID POINTS IS 33

NUMBER OF STATIONS IS 7

PRINT STATIONS EVERY 1 HOURS

STATION 1 IS AT 70 DEG, 46 MIN NORTH LAT. AND 129 DEG, 21 MIN WEST LONG.  
WITH GRID COORDINATES (42,14)

STATION 2 IS AT 70 DEG, 24 MIN NORTH LAT. AND 135 DEG, 12 MIN WEST LONG.  
WITH GRID COORDINATES (31,11)

STATION 3 IS AT 70 DEG, 05 MIN NORTH LAT. AND 134 DEG, 26 MIN WEST LONG.  
WITH GRID COORDINATES (32, 9)

STATION 4 IS AT 70 DEG, 28 MIN NORTH LAT. AND 134 DEG, 06 MIN WEST LONG.  
WITH GRID COORDINATES (33,12)

STATION 5 IS AT 70 DEG, 22 MIN NORTH LAT. AND 136 DEG, 32 MIN WEST LONG.  
WITH GRID COORDINATES (28,11)

STATION 6 IS AT 70 DEG, 42 MIN NORTH LAT. AND 133 DEG, 59 MIN WEST LONG.  
WITH GRID COORDINATES (33,13)

STATION 7 IS AT 70 DEG, 35 MIN NORTH LAT. AND 134 DEG, 14 MIN WEST LONG.  
WITH GRID COORDINATES (33,12)

NO. OF STEPS = 30 THE TIME STEP IS 30.0 MINUTES

SHORE POINTS SET TO DEPTH OF -1.00 METRES

YR/MO/DY/HR/MN

THE WIND STARTS AT 1981/07/25/00/00 AT TIME INTERVALS AS ON THE WIND DATA TAPE

THE LISTING STARTS AT 1981/07/25/00/00 AT INTERVALS OF 1 HOURS

WITH CHARTS OF WAVES EVERY 720. MINUTES

DEEP WATER CALCULATIONS USED

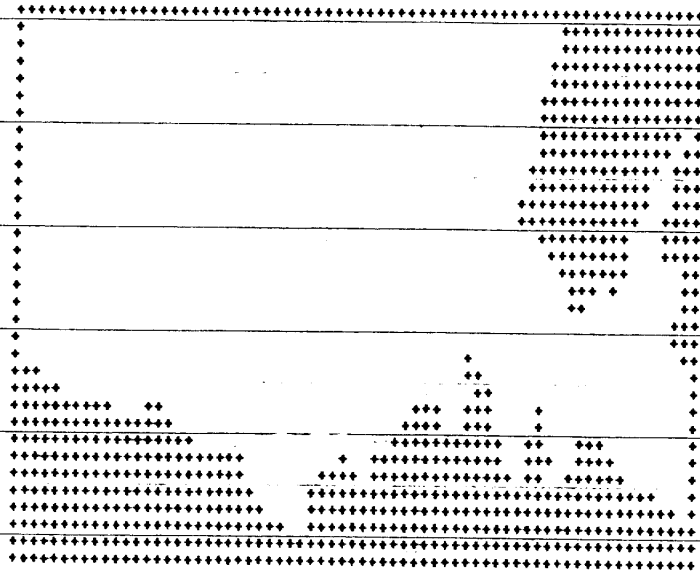
INPUT PARAMETER SPECIFICATION LIST

LAKE DEPTHS IN METRES FOR EACH X COORDINATE

1	0	0	0	0	0	0	0	0	0	0	0	0	0	0	0	0	0	0	0	0						
2	0	0	0	0	0	0	0	0	0	0	0	0	0	0	15	18	33	91	910	2100	2550	2825				
3	3100	3375	3650	3650	3650	3650	3650	3650	3650	3650	3650	3650	3650	0	0	0	0	0	0	0	0					
4	0	0	0	0	0	0	0	0	0	0	0	0	0	16	27	33	73	1370	2275	2650	2925					
5	3200	3475	3650	3650	3650	3650	3650	3650	3650	3650	3650	3650	3650	0	0	0	0	0	0	0	0					
6	0	0	0	0	0	0	0	0	0	0	0	0	0	11	20	35	37	110	2000	2475	2750	3025				
7	3300	3550	3650	3650	3650	3650	3650	3650	3650	3650	3650	3650	3650	0	0	0	0	0	0	0	0					
8	0	0	0	0	0	0	0	0	0	0	0	0	0	9	26	37	44	730	2100	2550	2750	3100				
9	3375	3650	3650	3650	3650	3650	3650	3650	3650	3650	3650	3650	3650	0	0	0	0	0	0	0	0					
10	0	0	0	0	0	0	0	0	0	0	0	0	0	4	13	33	42	49	1370	2275	2650	3025	3200			
11	3475	3650	3650	3650	3650	3650	3650	3650	3650	3650	3650	3650	3650	0	0	0	0	0	0	0	0	0				
12	0	0	0	0	0	0	0	0	0	0	0	0	0	5	20	40	46	53	1925	2375	2650	3025	3375			
13	3550	3650	3650	3650	3650	3650	3650	3650	3650	3650	3650	3650	3650	0	0	0	0	0	0	0	0	0				
14	0	0	0	0	0	0	0	0	0	0	0	0	0	16	33	44	53	180	2000	2550	2750	3100	3375			
15	3475	3475	3475	3475	3600	3650	3650	3650	3650	3650	3650	3650	3650	0	0	0	0	0	0	0	0	0	0			
16	0	0	0	0	0	0	0	0	0	0	0	0	0	24	37	46	91	640	2000	2550	2925	3200	3375			
17	3475	3375	3475	3475	3600	3600	3650	3650	3650	3650	3650	3650	3650	0	0	0	0	0	0	0	0	0	0			
18	0	0	0	0	0	0	0	0	0	0	0	0	0	29	38	51	165	640	2200	2550	3100	3300	3375			
19	3375	3375	3375	3375	3450	3600	3600	3650	3650	3650	3650	3650	3650	0	0	0	0	0	0	0	0	0	0			
20	0	0	0	0	0	0	0	0	0	0	0	0	0	22	31	42	70	400	1000	2250	2600	3050	3175	3300		
21	3375	3375	3375	3375	3400	3550	3600	3600	3650	3650	3650	3650	3650	0	0	0	0	0	0	0	0	0	0			
22	0	0	0	0	0	0	0	0	0	0	0	0	0	24	40	46	90	550	1500	2300	2750	3050	3150	3250		
23	3350	3375	3375	3375	3400	3450	3400	3500	3600	3650	3650	3650	3650	0	0	0	0	0	0	0	0	0	0			
24	0	0	0	0	0	0	0	0	0	0	0	0	0	18	38	48	150	750	1750	2300	2750	3025	3100	3200		
25	3250	3350	3375	3350	3350	3400	3400	3450	3500	3600	3650	3650	3650	0	0	0	0	0	0	0	0	0	0			
26	0	0	0	0	0	0	0	0	0	0	0	0	0	42	63	325	900	2000	2300	2700	3000	3075	3150			
27	3200	3250	3300	3300	3300	3350	3400	3450	3500	3500	3600	3650	3650	0	0	0	0	0	0	0	0	0	0			
28	0	0	0	0	0	0	0	0	0	0	0	0	0	45	66	500	1250	2050	2350	2600	2850	3025	3100			
29	3150	3200	3250	3250	3250	3300	3350	3400	3450	3500	3500	3600	3600	0	0	0	0	0	0	0	0	0	0			
30	0	0	0	0	0	0	0	0	0	0	0	0	0	25	48	100	700	1500	2100	2400	2550	2800	2950	3050		
31	3100	3150	3150	3200	3250	3250	3300	3350	3400	3450	3450	3500	3500	0	0	0	0	0	0	0	0	0	0			
32	0	0	0	0	0	0	0	0	0	0	0	0	0	20	40	52	800	1800	2150	2400	2500	2700	2900	2950		
33	3000	3050	3100	3150	3200	3200	3250	3300	3350	3400	3450	3450	3450	0	0	0	0	0	0	0	0	0	0			
34	0	0	0	0	0	0	0	0	0	0	0	0	0	28	49	60	1000	2000	2200	2400	2500	2650	2800	2900		
35	2950	3000	3050	3100	3150	3200	3250	3250	3300	3350	3400	3450	3450	0	0	0	0	0	0	0	0	0	0			
36	0	0	0	0	0	0	0	0	0	0	0	0	0	31	46	60	500	1300	2100	2200	2400	2450	2550	2700	2800	
37	2900	2950	3050	3050	3100	3150	3200	3250	3300	3350	3400	3400	3400	0	0	0	0	0	0	0	0	0	0	0		
38	0	0	0	0	0	0	0	0	0	0	0	0	0	32	37	46	200	500	1350	2100	2250	2400	2450	2500	2600	2700
39	2800	2900	3000	3050	3100	3150	3200	3200	3250	3300	3350	3350	3350	0	0	0	0	0	0	0	0	0	0	0	0	
40	0	0	0	0	0	0	0	0	0	0	0	0	0	35	50	100	325	600	1350	1950	2100	2250	2350	2450	2550	2650
41	2700	2800	2900	3000	3050	3100	3150	3200	3200	3250	3300	3350	3350	0	0	0	0	0	0	0	0	0	0	0	0	
42	0	0	0	0	0	0	0	0	0	0	0	0	0	35	50	220	475	740	1500	1850	2050	2200	2250	2400	2550	2600
43	2650	2750	2850	3000	3050	3100	3150	3200	3200	3250	3250	3300	3300	0	0	0	0	0	0	0	0	0	0	0	0	
44	0	0	0	0	0	0	0	0	0	0	0	0	0	42	100	245	560	825	1500	1800	2000	2000	2150	2300	2400	2600
45	2600	2700	2800	2950	3050	3050	3100	3150	3150	3200	3250	3250	3250	0	0	0	0	0	0	0	0	0	0	0	0	
46	0	0	0	0	0	22	75	180	275	375	550	750	1300	0	0	0	0	0	0	0	0	0	0	0	0	
47	2500	2650	2750	2900	3000	3050	3050	3100	3150	3150	3200	3250	3250	0	0	0	0	0	0	0	0	0	0	0	0	
48	0	0	0	0	0	37	84	137	184	200	265	400	800	1350	1600	1650	1700	1900	2050	2250	2500	2500	2500	2500	2500	
49	2500	2600	2700	2800	2950	3000	3050	3050	3100	3150	3150	3200	3200	0	0	0	0	0	0	0	0	0	0	0	0	
50	0	0	0	0	0	27	38	50	69	80	90	85	250	775	1350	1550	1500	1600	1750	1950	2250	2400	2400	2400	2400	
51	2400	2500	2650	2750	2850	2950	3000	3050	3050	3100	3150	3150	3150	0	0	0	0	0	0	0	0	0	0	0	0	
52	0	0	0	0	0	6	24	38	45	48	50	48	160	870	1300	1450	1350	1450	1600	2050	2250	2250	2250	2250	2250	
53	2350	2500	2550	2700	2800	2900	2950	3000	3050	3100	3100	3100	3150	0	0	0	0	0	0	0	0	0	0	0	0	
54	0	0	0	0	0	2	5	11	17	23	32	39	59	575	1000	1200	1200	1300	1500	1950	2150	2200	2200	2200	2200	
55	2250	2400	2500	2600	2700	2800	2900	3000	3000	3050	3050	3100	3100	0	0	0	0	0	0	0	0	0	0	0	0	
56	0	0	0	0	0	1	1	1	5	10	15	29	42	55	75	590	810	1050	1250	1400	1850	2000	2100	2100	2100	
57	2200	2300	2450	2550	2650	2700	2800	2900	3000	3000	3000	3050	3050	0	0	0	0	0	0	0	0	0	0	0	0	
58	0	0	0	0	0	0	0	0	0	0	0	0	0	0	0	0	0	0	0	0	0	0	0	0	0	
59	2100	2350	2400	2500	2600	2650	2750	2850	2900	3000	3000	3050	3050	0	0	0	0	0	0	0	0	0	0	0	0	
60	0	0	0	0	0	0	0	0	0	0	0	0	0	0	0	0	0	0	0	0	0	0	0	0	0	
61	2050	2210	2250	2400	2500	2600	2700	2750	2850	2900	3000	3050	3050	0	0	0	0	0	0	0	0	0	0	0	0	
62	0	0	0	0	0	0	0	0	0	0	0	0	0	0	0	0	0	0	0	0	0	0	0	0	0	
63	2030	2130	2200	2300	2400	2500	2600	2700	2750	2850	2900	2900	3000	0	0	0	0	0	0	0	0	0	0	0	0	
64	0	0	0	0	0	0	0	0	0	0	0	0	0	0	0	0	0	0	0	0	0	0	0	0	0	
65	1875	2000	2100	2200	2350	2450	2550	2650	2700	2750	2850	2900	2900	0	0	0	0	0	0	0	0	0	0	0	0	

PARTIAL BATHYMETRY RECORD

ORIGINAL COASTLINE AS DEFINED BY BATHYMETRY:



LAND (+) AND ICE (\*) COASTLINES AS OF 1981/07/25:



LAND BOUNDARY AND EXAMPLE OF ICE CHART

STN	TIME STEP	HOUR	MIN	DA	MO	AV-CD X1000	AVWND (M/S)	SIG-WT (M)	PERIOD (SEC)	WIND-SPD (M/S)	WAVE-DIR (DEG)	WIND-DIR (DEG)
1	2	01	00	25	07							
							OBSERVATION STATION ON THE ICE AT THIS TIME					
2	2	01	00	25	07	2.23	7.83	0.58	3.06	7.83	287	105
3	2	01	00	25	07	2.23	7.83	0.58	3.05	7.83	287	105
4	2	01	00	25	07	2.23	7.83	0.58	3.04	7.83	287	105
5	2	01	00	25	07	2.23	7.83	0.58	3.06	7.83	287	105
6	2	01	00	25	07							
							OBSERVATION STATION ON THE ICE AT THIS TIME					
7	2	01	00	25	07	2.23	7.83	0.58	3.04	7.83	287	105
1	4	02	00	25	07							
							OBSERVATION STATION ON THE ICE AT THIS TIME					
2	4	02	00	25	07	1.52	7.56	0.80	3.73	7.56	286	099
3	4	02	00	25	07	1.53	7.56	0.80	3.72	7.56	286	099
4	4	02	00	25	07	1.54	7.56	0.77	3.64	7.56	286	099
5	4	02	00	25	07	1.52	7.56	0.80	3.73	7.56	286	099
6	4	02	00	25	07							
							OBSERVATION STATION ON THE ICE AT THIS TIME					
7	4	02	00	25	07	1.54	7.56	0.77	3.64	7.56	286	099
1	6	03	00	25	07							
							OBSERVATION STATION ON THE ICE AT THIS TIME					
2	6	03	00	25	07	1.21	7.40	0.92	4.07	7.40	284	092
3	6	03	00	25	07	1.22	7.40	0.91	4.05	7.40	284	092
4	6	03	00	25	07	1.29	7.40	0.83	3.84	7.40	284	092
5	6	03	00	25	07	1.21	7.40	0.92	4.08	7.40	284	092
6	6	03	00	25	07							
							OBSERVATION STATION ON THE ICE AT THIS TIME					
7	6	03	00	25	07	1.29	7.40	0.83	3.84	7.40	284	092
1	8	04	00	25	07							
							OBSERVATION STATION ON THE ICE AT THIS TIME					
2	8	04	00	25	07	0.68	5.20	0.97	4.50	5.20	284	113
3	8	04	00	25	07	0.69	5.20	0.95	4.45	5.20	284	113
4	8	04	00	25	07	0.70	5.20	0.80	4.02	5.20	285	113
5	8	04	00	25	07	0.68	5.20	0.98	4.53	5.20	284	113
6	8	04	00	25	07							
							OBSERVATION STATION ON THE ICE AT THIS TIME					
7	8	04	00	25	07	0.70	5.20	0.80	4.02	5.20	285	113
1	10	05	00	25	07							
							OBSERVATION STATION ON THE ICE AT THIS TIME					
2	10	05	00	25	07	1.40	4.96	0.90	4.65	4.96	286	164
3	10	05	00	25	07	1.40	4.96	0.87	4.58	4.96	285	164
4	10	05	00	25	07	0.98	4.96	0.70	4.10	4.96	288	164
5	10	05	00	25	07	1.48	4.96	0.93	4.73	4.96	285	164
6	10	05	00	25	07							
							OBSERVATION STATION ON THE ICE AT THIS TIME					
7	10	05	00	25	07	0.98	4.96	0.70	4.10	4.96	288	164
1	12	06	00	25	07							
							OBSERVATION STATION ON THE ICE AT THIS TIME					
2	12	06	00	25	07	1.92	7.80	0.70	4.00	7.80	313	196
3	12	06	00	25	07	1.91	7.80	0.66	3.82	7.80	313	196
4	12	06	00	25	07	1.73	7.80	0.57	3.33	7.80	323	196
5	12	06	00	25	07	1.98	7.80	0.74	4.20	7.80	310	196
6	12	06	00	25	07							
							OBSERVATION STATION ON THE ICE AT THIS TIME					
7	12	06	00	25	07	1.73	7.80	0.57	3.33	7.80	323	196
1	14	07	00	25	07							
							OBSERVATION STATION ON THE ICE AT THIS TIME					
2	14	07	00	25	07	1.24	6.38	0.74	3.94	6.38	331	198
3	14	07	00	25	07	1.26	6.38	0.68	3.69	6.38	335	198
4	14	07	00	25	07	1.22	6.38	0.67	3.63	6.38	339	198
5	14	07	00	25	07	1.24	6.38	0.76	4.04	6.38	329	198
6	14	07	00	25	07							
							OBSERVATION STATION ON THE ICE AT THIS TIME					
7	14	07	00	25	07	1.22	6.38	0.67	3.63	6.38	339	198
1	16	08	00	25	07							
							OBSERVATION STATION ON THE ICE AT THIS TIME					
2	16	08	00	25	07	1.30	3.32	0.70	4.09	3.32	332	189
3	16	08	00	25	07	0.59	3.32	0.63	3.88	3.32	339	189
4	16	08	00	25	07	0.67	3.32	0.67	4.01	3.32	338	189
5	16	08	00	25	07	1.59	3.32	0.71	4.13	3.32	330	189
6	16	08	00	25	07							
							OBSERVATION STATION ON THE ICE AT THIS TIME					
7	16	08	00	25	07	0.67	3.32	0.67	4.01	3.32	338	189

HOURLY STATION OUTPUT



APPENDIX D

MASTER DATA FILE FORMAT

Card Image of Record on the Final Data Tape "FDT"

S <sub>1</sub>	Location				Date Time				S <sub>2</sub>	Waves		Wind <sub>1</sub>		Wind <sub>2</sub>		Additional Information if Necessary	
	N Lat dg   m.	W Lat dg   m.	Yr	Mo	Dy	Hr	S <sub>3</sub>	Hs		Pp	SPD	DIR	SPD	DIR	Z		
XX	XX	XX	XX	XXX	XX	XX	XX	XX	XX	XXX	XXX	XX	XXX	XX	XXX	XXX	

Field  
No. 1 2 3 4 5 6 7 8 9 10 11 12 13 14 15

Field Number Column No. Element

01	01-02	Site Code Number
02	03-06	Latitude (N; degrees and minutes)
03	07-11	Longitude (W; degrees and minutes)
04	12-13	Year (e.g. 83, 84, etc.)
05	14-15	Month
06	16-17	Day
07	18-19	Hour
08	20	Data Source code (e.g. 1, 2 or 3)
	21	Blank
09	22-24	Significant Wave Height (Hs, in decimeter)
10	25-27	Wave Peak Period(Pp. in tenths of seconds)
11	28-29	Wind speed at standard (model) height
12	30-32	Wind direction at standard (model) height
13	33-34	Wind speed measured at actual anemometer height
14	35-37	Wind direction measured at actual anemometer height
15	38-40	Actual anemometer height above sea level (metres)
16	41-80	Additional data (may vary depending on source type, available data, etc.) as described above.

NOTE

1) Wind<sub>1</sub> means wind data measured, analyzed or computed at a specified height above the sea level.

Wind<sub>2</sub> is the actual winds "measured" at the anemometer level (Z).

2) All missing data should be replaced by -9 or -99 or -999, etc, depending on the number of data fields.

3) All data are in INTEGER form as described previously.

DATABASE STRUCTURETape Data Field

1. SITE, (2 fields): 01 is Site 1, 02 is Site 2, etc.

2. LOCATION (9 fields): Latitude (4 field) and Longitude (5 field) of a given location (i.e. measuring site or model grid point).

3. DATE (8 fields): YMMDDHH (HH in GMT unless otherwise specified)

4. DATA SOURCE, S<sub>2</sub>S<sub>3</sub>, (2 fields):

- First field; S<sub>2</sub> = 1 = measured data  
2 = wave model output  
3 = CMC winds

- Second field; S<sub>3</sub> is left blank

5. RECORDS

a) Waves (measured or predicted)

/H<sub>s</sub>H<sub>s</sub>H<sub>s</sub>/P<sub>p</sub>P<sub>p</sub>P<sub>p</sub>/ (6 fields)

where H<sub>s</sub>H<sub>s</sub>H<sub>s</sub> = significant wave height (H<sub>s</sub>) in decimetres (e.g. 3.7m = 037)

P<sub>p</sub>P<sub>p</sub>P<sub>p</sub> = Wave "Peak" period in tenths of a second (e.g. 10.5s =; 8.7 = 087)

b) Winds (measured or modeled)

/ffddd/ffddd/ZZZ/

where ff = wind speed in knots (2 fields)

ddd = wind direction in degrees (true) (3 fields: 0-360)

ZZZ = Anemometer height above MWL in metres (e.g. 65m = 065)

Note: The first set of wind speed and direction refers to the effective forcing winds (model winds) and the second set is the measured winds at a given anemometer height (ZZZ).

c) Additional Information Field

Any additional data is recorded following the above data fields. This includes the following:

The water and air temperature is entered (8 field) as follows:

/S<sub>n</sub>T<sub>w</sub>T<sub>w</sub>T<sub>w</sub>/S<sub>n</sub>T<sub>a</sub>T<sub>a</sub>T<sub>a</sub>/

where S<sub>n</sub> = Sign of temp. (zero or blank for temp. above zero and 1 for temp. below zero)

T<sub>w</sub>T<sub>w</sub>T<sub>w</sub> = Sea surface temperature in tenths of degrees Celsius.

T<sub>a</sub>T<sub>a</sub>T<sub>a</sub> = Air temperature in tenths of degrees Celsius (e.g. 15.4 = 154; 0.8 = 008)

For Forecast Mode, this additional field can include e.g. the 24, 48 and 72 hour forecasts (hs. Ppi f and d) in the following format: for example;

/tt/H<sub>s</sub>H<sub>s</sub>H<sub>s</sub>/P<sub>p</sub>P<sub>p</sub>P<sub>p</sub>/ffddd/

where tt = lead time i.e. 24, 48 or 72)

APPENDIX E

ICE BOUNDARY CHARTS

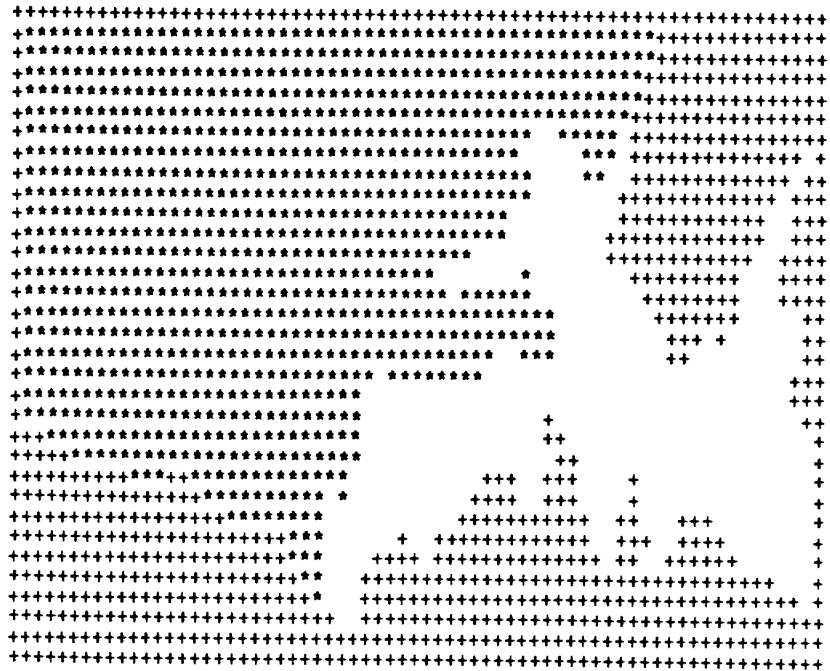
Land (+) and ice (\*) coastlines as of 1981/07/25:



Land (+) and ice (\*) coastlines as of 1981/07/30:



Land (+) and ice (\*) coastlines as of 1981/08/06:



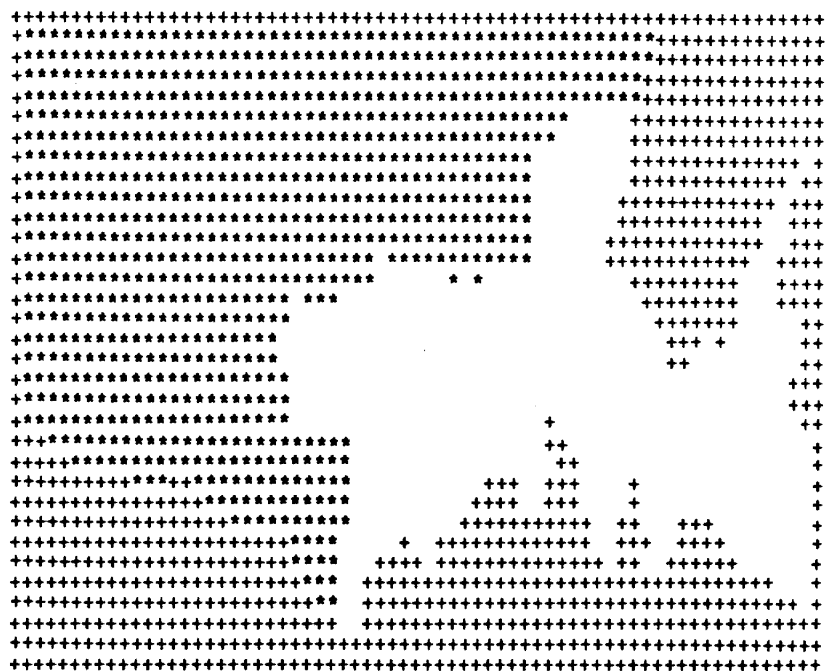
Land (+) and ice (\*) coastlines as of 1981/08/13:



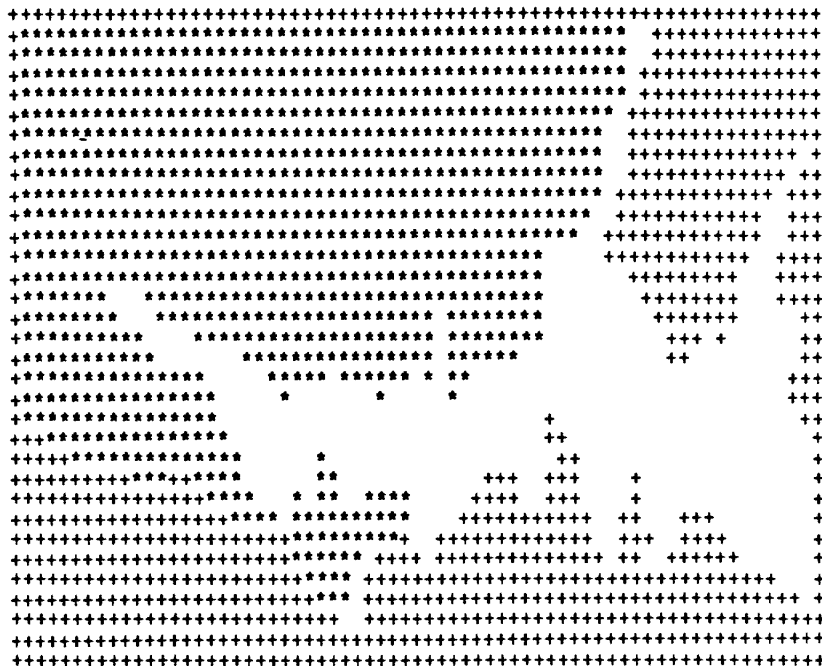
Land (+) and ice (\*) coastlines as of 1981/08/20:



Land (+) and ice (\*) coastlines as of 1981/08/27:



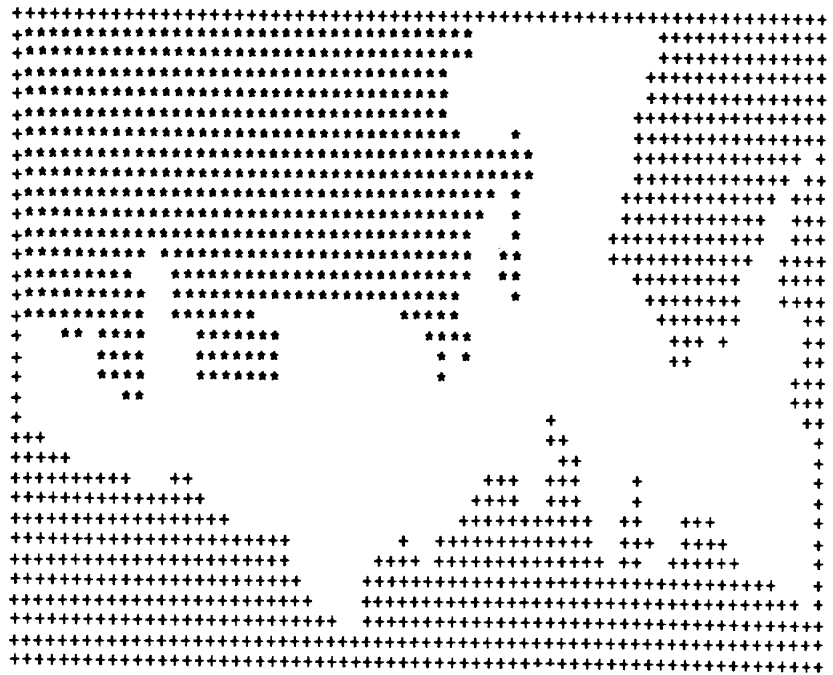
Land (+) and ice (\*) coastlines as of 1981/09/03:



Land (+) and ice (\*) coastlines as of 1981/09/10:



Land (+) and ice (\*) coastlines as of 1981/09/17:



Land (+) and ice (\*) coastlines as of 1981/09/24:



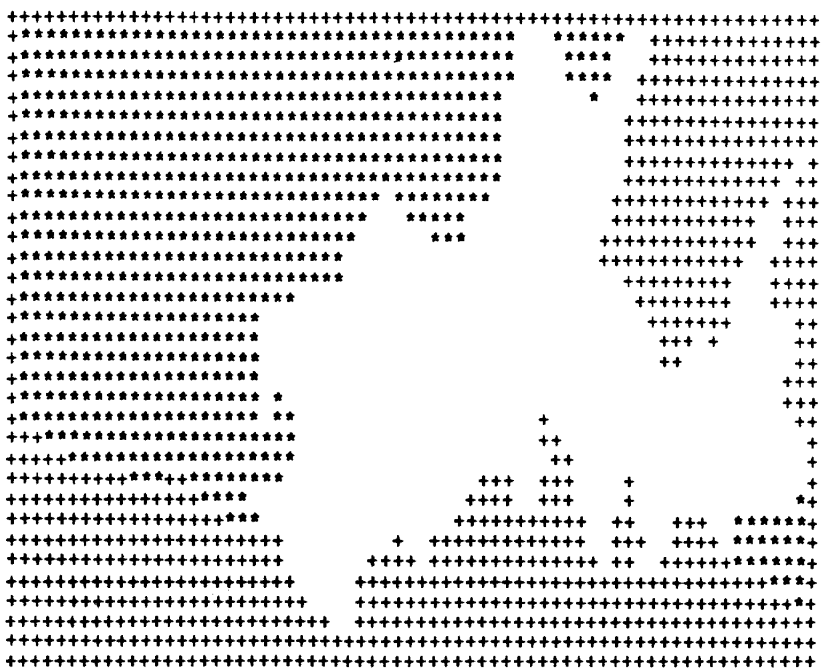
Land (+) and ice (\*) coastlines as of 1981/10/01:



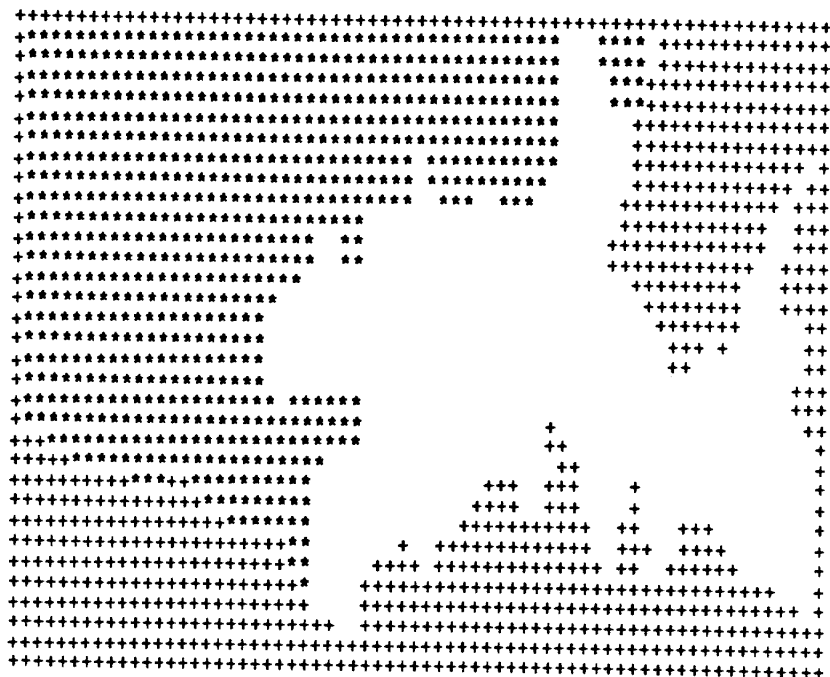
Land (+) and ice (\*) coastlines as of 1982/07/27:



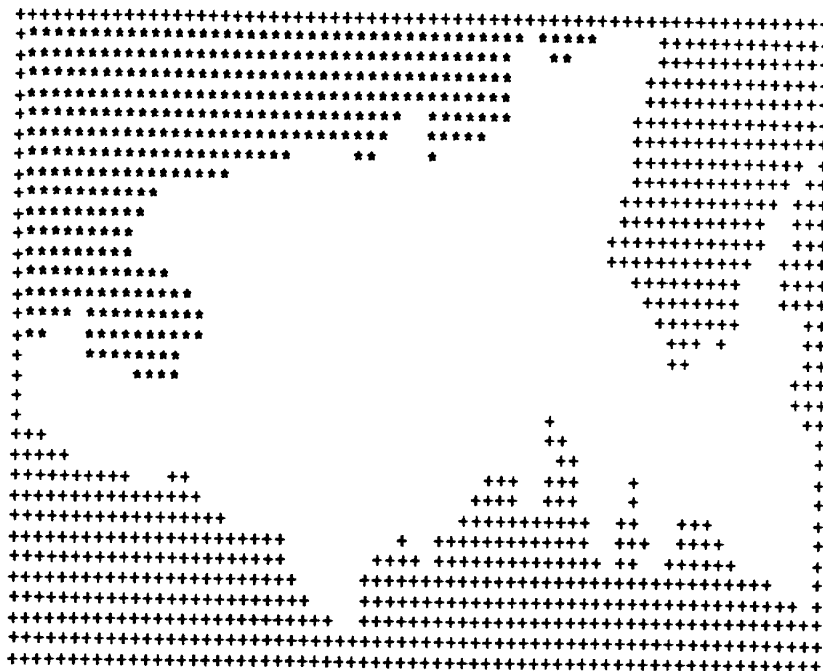
Land (+) and ice (\*) coastlines as of 1982/08/12:



Land (+) and ice (\*) coastlines as of 1982/08/18:



Land (+) and ice (\*) coastlines as of 1982/09/18:



Land (+) and ice (\*) coastlines as of 1986/08/20:



Land (+) and ice (\*) coastlines as of 1986/09/19:



Land (+) and ice (\*) coastlines as of 1986/10/03:

